Small-Scale Shaken Bioreactors for Fed-Batch Cultivation with Parallel Online Monitoring

Geschüttelte Kleinkultur-Bioreaktoren im Fed-Batch-Betrieb mit paralleler Online-Prozessüberwachung

Von der Fakultät für Maschinenwesen der Rheinisch-Westfälischen Technischen Hochschule Aachen zur Erlangung des akademischen Grades eines Doktors der Naturwissenschaften genehmigte Dissertation

vorgelegt von

Tobias Habicher

Berichter: Universitätsprofessor Dr.-Ing. Dr. h. c. (Osaka) Jochen Büchs

Universitätsprofessor Dr. rer. nat. Ulrich Schwaneberg

Tag der mündlichen Prüfung: 06.03.2020

— Für Tilla —

Danksagung

Die vorliegende Arbeit wurde während meiner Tätigkeit als wissenschaftlicher Mitarbeiter am Lehrstuhl für Bioverfahrenstechnik der RWTH Aachen im Rahmen einer Kooperation mit der BASF SE angefertigt.

Mein besonderer Dank gilt Prof. Dr.-Ing. Jochen Büchs für die Möglichkeit zur Promotion am Lehrstuhl für Bioverfahrenstechnik. Ihre Betreuung und Unterstützung haben den Grundstein für diese Arbeit gelegt. Ihre Hingabe zu Forschung und Entwicklung ist beeindruckend. Ich bin dankbar für den intensiven wissenschaftlichen Austausch mit Ihnen und dafür, dass Sie mich auf meiner wissenschaftlichen Laufbahn unterstützt und gefördert haben.

Weiterhin möchte ich mich bei Prof. Ulrich Schwaneberg für die Übernahme des Koreferats und bei Prof. Herbert Olivier für die Übernahme des Prüfungsvorsitzes bedanken.

Meine Arbeit war geprägt von der Kooperation und dem Austausch mit der BASF SE. Hier gilt mein Dank Dr. Andreas Daub und Dr. Tobias Klein für die angenehme und vertrauensvolle Atmosphäre und für die fruchtbare Zusammenarbeit. Auch bei Dr. Kerstin Hage, die das Projekt zu Beginn leitete, möchte ich mich für den angenehmen und strukturierten Einstieg bedanken.

Ein wesentlicher Teil dieser Arbeit beruht auf der Zusammenarbeit mit meinen Studierenden. Deshalb geht mein Dank an Tom Spilker, Arian John, Niklas Scholl, Thomas Frank, Franziska Egidi, Edward Rauls, Aleksandr Lobanov, Dominik Engel und Vroni Czotscher für die engagierte und zuverlässige Unterstützung. Die Zusammenarbeit mit Euch war stets eine Bereicherung, sowohl aus wissenschaftlicher als auch aus persönlicher Sicht.

Als große Bereicherung empfand ich auch das akademische Umfeld und den damit verbundenen wissenschaftlichen Austausch. An dieser Stelle möchte ich mich bei meinen Kolleginnen und Kollegen am Lehrstuhl für Bioverfahrenstechnik der AVT für die angenehme Arbeitsatmosphäre und die wertvollen Diskussionen bedanken. Besonderer Dank gilt denjenigen, die bei der Korrektur der Manuskripte und des Abschlussvortrags beteiligt gewesen sind. Ganz besonders freut es mich auch, dass aus der Promotionszeit schöne Freundschaften hervorgegangen sind.

Ich möchte mich auch bei allen Mitarbeiterinnen und Mitarbeitern des Lehrstuhls bedanken, die im Sekretariat, im Labor und in der Buchhaltung für einen reibungslosen Ablauf gesorgt haben.

Von ganzem Herzen bedanken möchte ich mich bei meiner Familie. Ihr habt mir während Studium und Promotion Rückhalt gegeben und mich immer bedingungslos unterstützt und somit meinen persönlichen als auch beruflichen Werdegang entscheidend beeinflusst.

Zu guter Letzt geht mein Dank and Dich, Alina. Du wurdest in dieser Zeit zu meiner Frau und Mutter unserer wundervollen Tochter Tilla. Vielen Dank für alles und auf eine schöne Zukunft.

“What is now proved was once only imagined”

„Was jetzt bewiesen ist, war einst nur vorstellbar“

William Blake (1757-1827)

Zusammenfassung

Geschüttelte Kleinkultur-Bioreaktoren wie Schüttelkolben und Mikrotiterplatten sind die am häufigsten verwendeten Reaktorsysteme in der initialen Phase der Bioprozessentwicklung. Ursprünglich waren diese Bioreaktoren für den Batch-Betrieb konzipiert. Dies führt jedoch zu unerwünschten Effekten wie Überflussmetabolismus, Substratinhibierung oder Katabolitrepression. Da der Fed-Batch-Betrieb diese Effekte verhindern kann, werden Produktionsprozesse hauptsächlich im Fed-Batch betrieben. Die Umsetzung des Fed-Batch-Betriebs im kleinen Maßstab ist somit essentiell, um physiologische Bedingungen zu erzielen, die mit den Bedingungen in Fed-Batch-Produktionsprozessen vergleichbar sind.

Im Schüttelkolben wurde der Fed-Batch-Betrieb mit den zuvor eingeführten 250 mL membranbasierten Fed-Batch-Schüttelkolben umgesetzt. Im Rahmen dieser Arbeit wurde das System hinsichtlich der Dimensionierung standardisiert und in Design, Handhabung und Robustheit optimiert. Zudem wurde das Funktionsprinzip auf 500 mL Schüttelkolben hochskaliert. Mittels dieser Systeme wurden kohlenstoff- und stickstofflimitierte Fed-Batch-Bedingungen eingeführt. Dadurch wurde die Katabolitrepression und Substratinhibierung in einem Protease-produzierenden *Bacillus licheniformis* Stamm überwunden. In Mikrotiterplatten wurden kohlenstofflimitierte Fed-Batch-Bedingungen mit polymerbasierten Mikrotiterplatten realisiert.

Besonderes Augenmerk galt der Online-Prozessüberwachung der Fed-Batch betriebenen Kleinkultur-Bioreaktoren. Membranbasierte Fed-Batch-Schüttelkolben und polymerbasierte Fed-Batch-Mikrotiterplatten wurden so konzipiert, dass sie mit dem RAMOS- bzw. µRAMOS-Gerät überwachbar sind. Zudem wurde eine Fed-Batch-Mikrotiterplatte mit Polymerringen entwickelt, die die Kulturbrühe optisch zugänglich macht und somit die Online-Prozessüberwachung mit dem etablierten BioLector-Gerät ermöglicht. Zusammenfassend lässt sich sagen, dass die vorgestellten Kleinkultur-Bioreaktoren einen Fed-Batch-Betrieb mit paralleler Online-Prozessüberwachung der wichtigsten Kulturparameter ermöglichen. Dadurch können bereits in der initialen Phase der Bioprozessentwicklung die für die Fed-Batch-Produktionsprozesse relevanten physiologischen Bedingungen nachgebildet werden, was Zeit und Kosten spart und somit die Bioprozessentwicklung beschleunigt.

Abstract

Small-scale shaken bioreactors, such as shake flasks and microtiter plates, are the most frequently used reactor systems during initial bioprocess development. Originally, they were designed to be operated in batch mode. However, batch mode causes adverse effects like overflow metabolism, substrate inhibition or catabolite repression. Fed-batch mode can prevent these effects, and thus, it is predominantly applied in production processes. Consequently, the implementation of fed-batch mode at small scale is crucial to obtain physiological conditions that are comparable to fed-batch production processes.

In shake flasks, fed-batch mode was realized with the previously introduced 250 mL membrane-based fed-batch shake flasks. Within this thesis, the system was standardized regarding its dimensions and optimized in design, handling and robustness. Furthermore, the operating principle was successfully scaled-up to 500 mL shake flasks. The application of membrane-based fed-batch shake flasks allowed to introduce carbon- and nitrogen-limited fed-batch conditions to overcome catabolite repression and substrate inhibition in a protease producing *Bacillus licheniformis* strain. In microtiter plates, carbon-limited fed-batch conditions were realized with polymer-based controlled-release fed-batch microtiter plates.

Special emphasis was paid to the possibilities for online monitoring of the fed-batch operated small-scale shaken bioreactors. Membrane-based fed-batch shake flasks and polymer-based controlled-release fed-batch microtiter plates have been tailored to be compatible with the RAMOS and µRAMOS device, respectively. In order to have access to additional culture parameters, a fed-batch microtiter plate with polymer rings was designed. The polymer rings make the culture broth optically accessible, enabling online monitoring with the established BioLector device. In conclusion, the presented small-scale shaken bioreactors enable fed-batch operation with parallel online monitoring of the most important culture parameters. This allows to mimic the physiological conditions relevant for fed-batch production processes already during initial bioprocess development, which saves time and cost, and accelerates bioprocess development.

Funding, publications and contributions

This work was funded by BASF SE (Ludwigshafen am Rhein, Germany) and funding is gratefully acknowledged.

Parts of this thesis have been published or submitted previously:

- Habicher, T., John, A., Scholl, N., Daub, A., Klein, T., Philip, P., & Büchs, J. (2019). Introducing substrate limitations to overcome catabolite repression in a protease producing *Bacillus licheniformis* strain using membrane-based fed-batch shake flasks. *Biotechnology and Bioengineering*, *116*(6), 1326-1340. [1]
- Habicher, T., Rauls, E. K. A., Egidi, F., Keil, T., Klein, T., Daub, A., & Büchs, J. (2020). Establishing a fed-batch process for protease expression with *Bacillus licheniformis* in polymer-based controlled-release microtiter plates. *Biotechnology Journal*, *15*(2), 1900088. [2]
- Habicher, T., Czotscher, V., Klein, T., Daub, A., Keil, T. & Büchs, J. (2019). Glucose-containing polymer rings enable fed-batch operation in microtiter plates with parallel online measurement of scattered light, fluorescence, dissolved oxygen tension and pH. *Biotechnology and Bioengineering*, *116*(9), 2250-2262. [3]

Contributions to further publications during the preparation of this thesis:

- Philip, P., Kern, D., Goldmanns, J., Seiler, F., Schulte, A., Habicher, T., & Büchs, J. (2018). Parallel substrate supply and pH stabilization for optimal screening of *E. coli* with the membrane-based fed-batch shake flask. *Microbial Cell Factories*, *17*(1), 1–17.
- Keil, T., Dittrich, B., Lattermann, C., Habicher, T., & Büchs, J. (2019). Polymer-based controlled-release fed-batch microtiter plate–diminishing the gap between early process development and production conditions. *Journal of Biological Engineering*, *13*(1), 18.
- Müller, J., Hütterott, A., Habicher, T., Mußmann, N. & Büchs, J. (2019). Validation of the transferability of membrane-based fed-batch shake flask cultivations to stirred-tank reactor using three different protease producing *Bacillus* strains. *Journal of Bioscience and Bioengineering*, *128*(5), 599–605.

[1] Reprinted (adapted) with permission from John Wiley and Sons.
[2] Reprinted (adapted) with permission, Open Access CC BY 4.0, https://creativecommons.org/licenses/by/4.0/.
[3] Reprinted (adapted) with permission from John Wiley and Sons.

Contents

Nomenclature

Abbreviations

Abbreviation	**Description**
CTR	carbon dioxide transfer rate
DOT	dissolved oxygen tension
EcFbFP	*E. coli* codon bias-optimized FbFP
FbFP	flavin-based fluorescent protein
IPTG	isopropyl β-d-1-thiogalactopyranoside
MOPS	3-(N-morpholino)propanesulfonic acid
MTP	microtiter plate
n	number of measurements (sample size)
N-Suc-AAPF-pNA	N-succinyl-alanine-alanine-proline-phenylalanine-p-nitroanilide
OD_{600}	optical density at 600 nm
ODE	ordinary differential equation
OT	accumulated oxygen transfer
OTR	oxygen transfer rate
OTR_{max}	maximum oxygen transfer capacity
RAMOS	Respiration Activity MOnitoring System
rpm	revolutions per minute
RQ	respiratory quotient
TB	terrific broth (medium)

Symbols

Abbreviation	Description	Unit
$\dot{V}$	water flux	$L\ h^{-1}$
μ	specific growth rate	h^{-1}
μ_{max}	maximum specific growth rate	h^{-1}
A	fitting parameter	-
B	fitting parameter	-
C	fitting parameter	-
D	fitting parameter	-
d_0	shaking diameter	mm
$F'_{S_{Glu}}$	volumetric glucose release rate	$g\ L^{-1}\ h^{-1}$
$F_{S_{Glu}}$	accumulated volumetric glucose release	$g\ L^{-1}$
k_La	volumetric mass transfer coefficient	h^{-1}
$K_{S_{Glu}}$	Monod constant related to glucose	$g\ L^{-1}$
L_{O_2}	oxygen solubility	$mol\ L^{-1}\ bar^{-1}$
m_{O_2}	maintenance coefficient related to oxygen	$mol_{O2}\ g_X^{-1}\ h^{-1}$
$m_{S_{Glu}}$	maintenance coefficient related to glucose	$g_{S_{Glu}}\ g_X^{-1}\ h^{-1}$
n	shaking frequency	min^{-1}
O_2	dissolved oxygen concentration	$mol\ L^{-1}$
$O_{2,max}$	maximum dissolved oxygen concentration	$mol\ L^{-1}$
p	pressure	bar
P	product concentration	$g\ L^{-1}$
p_{amb}	ambient pressure	bar
p_{O2}	oxygen partial pressure	bar
q_P	specific production rate	h^{-1}
R_S	substrate release rate	$g\ h^{-1}$
S	substrate concentration	$g\ L^{-1}$
S_{Am}	ammonium concentration	$g\ L^{-1}$
S_{Glu}	glucose concentration	$g\ L^{-1}$
T	temperature	°C
V_{Broth}	volume of the culture broth	mL
V_{Feed}	volume of the feed solution	mL

X	biomass concentration	g L^{-1}
y_{O_2}	mole percent of oxygen within air	%
Y_{P/O_2}	relative protease activity yield per consumed oxygen	L mol^{-1}
$Y_{P/S_{Glu}}$	relative protease activity yield per consumed glucose	g^{-1}
$Y_{P_{FbFP}/S_{Glu}}$	EcFbFP fluorescence yield per consumed glucose	a.u. g^{-1}
Y_{X/O_2}	biomass yield per consumed oxygen	g mol^{-1}
$Y_{X/S}$	biomass yield per consumed substrate	g g^{-1}
$Y_{X/S_{Glu}}$	biomass yield per consumed glucose	g g^{-1}
ε	molar extinction coefficient	M^{-1} cm^{-1}

List of figures and tables

Chapter 1

Introduction

1.1 Advantages of fed-batch mode

Fed-batch mode is characterized by a continuous feed of one or more nutrients resulting in growth limiting conditions. The rate at which nutrients are fed to the culture has a direct impact on the metabolic activity of the cultivated organism (Mears, Stocks, Sin, & Gernaey, 2017; Öztürk, Çalık, & Özdamar, 2016). By choosing an optimal feed rate, adverse metabolic phenomena can be prevented. It was found that glucose-limited fed-batch conditions reduce the formation of the overflow metabolite acetate in *Escherichia coli* cultures, increasing protein production and yield (Eiteman & Altman, 2006; Xu, Jahic, & Enfors, 1999). In pH-uncontrolled *Escherichia coli* cultures, the reduction of the overflow metabolism prevents culture acidification. Since in fed-batch mode nutrients are fed continuously into the reactor, initial substrate concentrations can be kept low. Therefore, potential substrate and osmotic inhibitions are circumvented (Mendoza-Vega, Sabatié, & Brown, 1994; Minihane & Brown, 1986). Furthermore, low initial substrate concentrations avoid oxygen limitation and temperature increase that often occur during unlimited batch growth (Minihane & Brown, 1986).

The most relevant metabolic phenomenon occurring in batch mode is carbon catabolite repression. Since organisms quickly have to react to changing nutritional conditions, promoters of genes related to catabolism are considered to be strong and are thus frequently used for recombinant protein production (Cui et al., 2018; Hubmann, Thevelein, & Nevoigt, 2014;

Kluge, Terfehr, & Kück, 2018; Stöckmann et al., 2009). Industrial processes with *Hansenula polymorpha* rely on promoters derived from the methanol metabolism pathway (Stöckmann et al., 2009). Frequently used promoters in *Pichia pastoris* and *Saccharomyces cerevisiae* are mainly derived from genes involved in the metabolism of alternative carbon sources (Hubmann et al., 2014; Juturu & Wu, 2018). This also applies to promoters used in filamentous fungi (Kluge et al., 2018). The induction or repression of these promoters is catabolite controlled and thus directly coupled with the availability of the preferred carbon source, which most often is glucose. With IPTG-inducible promoters, large quantities of recombinant protein were achieved in *Bacillus subtilis* strains (Chen, Shaw, Chao, Ho, & Yu, 2010; Phan, Nguyen, & Schumann, 2012). As IPTG is expensive and toxic (Liu et al., 2013), these promoters are not suitable for industrial-scale production. Hence, endogenous promoters controlled by catabolite repression are commonly used with *Bacillus* species in industrial applications (Cui et al., 2018; Liu et al., 2013; Schallmey, Singh, & Ward, 2004). Consequently, high glucose concentrations, as they occur in batch mode, have a repressive effect on product formation. Such carbon catabolite regulation is also well known in the production of many secondary metabolites, as for example antibiotics (Ruiz et al., 2010; Sánchez et al., 2010).

1.2 Fed-batch mode in small-scale shaken bioreactors

The above-mentioned metabolic phenomena make fed-batch mode the predominant process mode for large-scale production processes. However, the high number of necessary experiments for screening and bioprocess development make the use of lab-scale reactors time consuming and expensive (Bareither & Pollard, 2011). As a result, small-scale shaken bioreactors, such as shake flasks and microtiter plates (MTP) are most frequently used during strain screening and first steps of bioprocess development (Büchs, 2001). The simple and functional design enables a large number of cost-efficient and parallel experiments (Duetz, 2007; Klöckner & Büchs, 2012). Characterization of the fluid dynamics and maximum oxygen transfer capacities further improved the understanding of shaken bioreactors (Büchs, Lotter, & Milbradt, 2001; Duetz, 2007; Lattermann & Büchs, 2015; Meier et al., 2016). However, these systems were originally designed to be operated in batch mode, and thus, batch mode is still the dominant operation mode for primary screening and initial bioprocess development.

Already in the 1980s, researchers pointed at the importance of adequate screening conditions in order to detect optimal antibiotic producing strains (Iwai & Omura, 1982). Despite the repressing effect of glucose on the biosynthesis of many antibiotics, glucose slowly fed to the investigated cultures was found not to impair biosynthesis (Martin & Demain, 1980). Jeude et al. (2006) used a polymer-based glucose slow-release system, thereby increasing product concentrations up to 420-fold when working with *Hansenula polymorpha*. Based on this release system, Scheidle et al. (2010) realized a glucose feed in microtiter plates. This allowed to screen *Hansenula polymorpha* clones for optimal production capabilities in fed-batch mode. By comparing the fed-batch screening results to those of the batch screening, it was shown that clones were ranked differently in terms of the specific product yield. Therefore, optimal strains found in batch screenings may perform poorly under fed-batch mode in stirred tank reactors during scale-up. Consequently, mimicking large-scale production processes by implementing fed-batch conditions in screenings and early stage bioprocess development is crucial to find optimal production strains and to generate valuable data during initial bioprocess development.

In lab-scale stirred tank reactors, fed-batch mode is realized with peristaltic pumps adding liquid droplets to the culture. A single droplet with an average size of 25 µL corresponds to 0.00125 % of the volume of a reactor operated at 2 liter. The negligible volume change per droplet enables frequent droplet addition, resulting in a continuous feed stream. In shake flasks with a filling volume of 10 mL, a single droplet of 25 µL already corresponds to 0.25 % of the volume. This would need a massive reduction of the droplet addition frequency and is consequently considered as pulse feed rather than continuous feed. The volume change in microtiter plate-based cultivations would even be higher, moving further away from the continuous feed stream design in stirred tank reactors. Consequently, the implementation of simple and versatile shake flask- and microtiter plate-based fed-batch systems with a continuous feed stream design remained challenging (Jeude et al., 2006). In recent years, techniques were developed to enable continuous feeding using microfluidic systems (Funke, Buchenauer, Mokwa, et al., 2010; Funke, Buchenauer, Schnakenberg, et al., 2010), microinjection valves (micro-Matrix, Applikon Biotechnology, Delft, Netherlands), membrane-based systems (Bähr et al., 2012; Philip et al., 2017, 2018), hydrogel-based systems (Wilming, Bähr, Kamerke, & Büchs, 2014), polymer-based systems (Jeude et al., 2006; Keil, Dittrich, Lattermann, Habicher, & Büchs,

2019) and enzymatic release systems (Grimm et al., 2012; Krause et al., 2010; Panula-Perälä et al., 2008, 2014; Toeroek, Cserjan-Puschmann, Bayer, & Striedner, 2015).

Nowadays, several of these release systems are commercially available. The BioLector Pro (m2p-labs, Baesweiler, Germany) represents a microtiter plate-based microfluidic system in which a substrate solution is continuously transferred from a reservoir well into a culture well via micro pumps (Funke, Buchenauer, Mokwa, et al., 2010; Funke, Buchenauer, Schnakenberg, et al., 2010). The micro-Matrix (Applikon Biotechnology, Delft, Netherlands) uses microinjection valves to realize a continuous feed stream in a 24-well microtiter plate. For the BioLector Pro and the micro-Matrix, parallelization for high-throughput screening would require the purchase of additional devices, resulting in substantial investment costs.

Commercially available release systems that are independent of peripheral equipment, such as pumps and valves, are enzymatic release systems. The EnBase system (BioSilta Oy, Oulu, Finland) is based on the enzymatic degradation of glucose polymers (Panula-Perälä et al., 2008). This feature makes them independent of scale, while glucose feeding rates can be easily adjusted via the enzyme concentration. However, many organisms, including *Bacillus* species (Sundarram & Murthy, 2014), secrete amylases and proteases, which leads to uncontrollable glucose release kinetics. Furthermore, it has to be noted that currently only glucose can be released from enzyme-based systems and that release kinetics are influenced by cultivation conditions e.g. pH and temperature (Toeroek et al., 2015). In contrast, the polymer-based controlled-release fed-batch microtiter plate (Feed Plate®, Kuhner Shaker GmbH, Herzogenrath, Germany) uses a silicone matrix with embedded glucose crystals to establish a continuous release of glucose in microtiter plates (Keil et al., 2019). Besides glucose, it is possible to release almost all water-soluble media components with the polymer-based system. Polymer-based release systems can also be applied with shake flasks in the form of beads (FeedBeads, Kuhner Shaker GmbH, Herzogenrath, Germany) (Jeude et al., 2006). An alternative shake flask-based release system, which is not yet commercially available, is the 250 mL membrane-based fed-batch shake flask (Bähr et al., 2012). The diffusion-driven release of one or more components can be individually adjusted, for example by apllying different membranes or feed solutions (Philip et al., 2017, 2018).

1.3 Online monitoring of small-scale shaken bioreactors

In stirred tank reactors, online monitoring of the most important cultivation parameters, such as dissolved oxygen tension and pH, is done with dipping probes. In shake flasks, dipping probes usually alter the liquid flow due to baffling effects (Hansen, Kensy, Käser, & Büchs, 2011). In microtiter plates, dipping probes are usually too large because of the small dimensions of the wells (Ladner, Held, Flitsch, Beckers, & Büchs, 2016). However, to monitor similar process parameters as in lab-scale stirred tank reactors, different measurement techniques were developed for small-scale shaken bioreactors.

A well-known online monitoring device for shake flasks is the Respiration Activity MOnitoring system (RAMOS) (Adolf Kühner AG, Biersfelden, Switzerland or HiTec Zang GmbH, Herzogenrath, Germany). Based on an electrochemical oxygen sensor and differential pressure sensor, which both are connected to the headspace of the measuring flask, the oxygen transfer rate (OTR), carbon dioxide transfer rate (CTR) and respiratory quotient (RQ) can be calculated (Anderlei & Büchs, 2001; Anderlei, Zang, Papaspyrou, & Büchs, 2004). The BCpreFerm system from BlueSens (Herten, Germany) uses a comparable approach to determine OTR, CTR and RQ. Electrochemical sensors measure the oxygen and carbon dioxide concentration in the headspace of shake flasks. Besides the respiratory activity, non-invasive optical measurement techniques were developed for online biomass measurement. The cell growth quantifier (CGQ, aquila biolabs, Baesweiler, Germany) is composed of a thin sensor plate, which is installed below the shake flask (Bruder, Reifenrath, Thomik, Boles, & Herzog, 2016). Biomass is monitored through the transparent bottom by backscattered light detection. However, the spectrum of accessible process parameters was considerably extended with the development of fluorescent dyes being sensitve against oxygen and H^+ concentrations (Arain et al., 2006; John & Heinzle, 2001; John, Klimant, Wittmann, & Heinzle, 2003). By applying these sensor spots to shake flasks, parallel online monitoring of biomass, dissolved oxygen tension and pH is feasible (Sensor Flask + SFR vario, Presense, Regensburg, Germany).

Non-invasive optical measurement techniques are mainly used to monitor culture conditions in microtiter plates (Klöckner & Büchs, 2012). The BioLector device measures scattered light (biomass) and fluorescence (fluorescent proteins or metabolites) in each well of a continuously

shaken microtiter plate through the transparent bottom (Kensy, Zang, Faulhammer, Tan, & Büchs, 2009; Samorski, Müller-Newen, & Büchs, 2005). The small size of the above-mentioned sensor spots, also called optodes, makes them suited for application in microtiter plates. This enables additional online dissolved oxygen tension (DOT) and pH measurement with the BioLector (m2p-labs, Baesweiler, Germany). Applying sensor spots to measure DOT and pH in microtiter plates is also possible with the SensorDish® Reader (Presense, Regensburg, Germany). Recently, Flitsch et al. (2016) presented a device that enables online monitoring of the oxygen transfer rate (OTR) in each individual well of a 48-well microtiter plate. This technique was then combined with the BioLector measurement principle to further increase the information content (Ladner, Held, et al., 2016). However, in order to have access to information that cannot directly be measured by fluorescence or fluorescent dyes, a new device for multi-wavelength (2D) fluorescence spectroscopy in each well of a continuously shaken microtiter plate was introduced (Ladner, Beckers, Hitzmann, & Büchs, 2016). By applying chemometrics, concentrations of analytes, such as glycerol, glucose and acetate, as well as pH became accessible. Even though these systems are currently not commercially available, the introduced measurement techniques highlight future developments in the area of small-scale bioreactor online monitoring.

1.4 Combining fed-batch operation and online monitoring in small-scale shaken bioreactors

Efforts were made to combine the possibility of applying fed-batch mode with parallel online monitoring in small-scale shaken bioreactor systems (Neubauer et al., 2013, Chapter 1.2). One device enabling both feeding and online monitoring is the above mentioned BioLector Pro (m2p-labs, Baesweiler, Germany). Based on microchannels, which are introduced to the bottom plate of the microtiter plate, feeding is realized without disturbing the optical online measurement (Funke, Buchenauer, Mokwa, et al., 2010; Funke, Buchenauer, Schnakenberg, et al., 2010). In combination with the measured online parameters, simple process control is feasible. The micro-Matrix (Applikon Biotechnology, Delft, Netherlands) uses microinjection valves to realize a continuous feed stream from top of the microtiter plate. Additionally, online monitoring of for example DOT and pH is possible. However, high investment and operational costs have to be made for systems with sophisticated and continuous feeding technologies

combined with the possibility for online monitoring and process control. Furthermore, due to the peripheral equipment needed for feeding, the degree of parallelization is dependent on the amount of available devices.

1.5 Objectives and Overview

The aim of this thesis is to characterize and develop small-scale shaken bioreactors, such as shake flasks and microtiter plates, enabling continuous feeding without peripheral equipment. Special emphasis was placed on designing the small-scale fed-batch bioreactors to be compatible with online monitoring devices.

In shake flasks, continuos feeding was previously realized with the 250 mL membrane-based fed-batch shake flask (Bähr et al., 2012; Philip et al., 2017, 2018). Chapter 2 covers the further development of the 250 mL membrane-based fed-batch shake flask with regard to standardized dimensioning and optimization in design, handling and robustness. The 250 mL membrane-based fed-batch shake flask is then applied to investigate carbon- and nitrogen-limited fed-batch conditions in a protease producing *Bacillus licheniformis* culture. To demonstrate the advantage of parallel online measurement of the oxygen transfer rate (OTR) with the RAMOS device, a process performance indicator is deduced from the online OTR signal. Chapter 2 also includes the development and application of the 500 mL membrane-based fed-batch shake flask, representing a scaled-up version of the 250 mL membrane-based fed-batch shake flask system.

To enable higher throughput, a microtiter plate-based fed-batch system capabale of continuosly releasing glucose is presented in Chapter 3. The polymer-based controlled-release fed-batch microtiter plate is investigated under different initial culture conditions using the above mentioned protease producing *Bacillus licheniformis* culture. To prove that small-scale fed-batch cultivations are scalable, the shake flask-based glucose-limited fed-batch cultivation is transferred to polymer-based controlled-release fed-batch microtiter plates. In addition, the microtiter plate-based OTR online data, which are acquired with the µRAMOS device, are applied to establish a mechanistic fed-batch model.

In Chapter 4, the BioLector device is used to extend the range of accessible online process parameters of a microtiter plate operated in fed-batch mode. Therefore it is neccessary to design and develop a fed-batch microtiter plate that is compatible with the optical measurement system of the BioLector device, which allows online measurement of scattered light (biomass), fluorescence, dissolved oxygen tension and pH. For this purpose, the polymer-based glucose release system described in Chapter 3 is utilized.

Parts of the following chapter have been published previously as Habicher, T., John, A., Scholl, N., Daub, A., Klein, T., Philip, P., & Büchs, J. (2019). Introducing substrate limitations to overcome catabolite repression in a protease producing *Bacillus licheniformis* strain using membrane-based fed-batch shake flasks. *Biotechnology and Bioengineering*, *116*(6), 1326-1340. Arian John and Niklas Scholl assisted with the cultivation experiments with the 250 mL membrane-based fed-batch shake flasks (2.2.1-2.2.4, 2.2.7) (AVT-Biochemical Engineering, Prof. Dr.-Ing. Büchs, RWTH Aachen University). Dominik Engel performed the cultivation experiments with the 500 mL membrane-based fed-batch shake flasks (2.2.1-2.2.2, 2.2.5-2.2.7) (AVT-Biochemical Engineering, Prof. Dr.-Ing. Büchs, RWTH Aachen University).

Chapter 2

Membrane-based fed-batch shake flasks

2.1 Introduction

Shake flasks belong to the most frequently used reaction vessels in biotechnology (Büchs, 2001). However, they were originally designed to be operated in batch mode (Chapter 1.2). To realize continuous feeding in conventional 250 mL Erlenmeyer shake flasks, Bähr et al. (2012) introduced the membrane-based fed-batch shake flask. It consists of a centrally located feed reservoir that is connected to a diffusion tip via a flexible tube (Figure 2.1A). The diffusion tip has a cellulose membrane at its bottom. It represents an in-situ diffusion compartment (Figure 2.1B). The weight of the diffusion tip is adapted to let it rotate in-phase with the bulk liquid. Hence, the membrane constantly dips into the rotating liquid without changing the hydrodynamic conditions of the shake flask (Bähr et al., 2012). Due to the membrane, the fed-batch system is divided in two compartments, one containing the feed solution and the other one the culture broth (Figure 2.1C). Cells and high molecular weight products, such as proteases, are retained by the membrane and, therefore, are only present within the culture broth. Substrates, such as glucose and ammonium, are able to pass through the membrane in both directions. The direction and rate of diffusion depends on the concentration gradient between the feed reservoir and culture broth (Figure 2.1D). Characteristically, the reservoir contains a highly concentrated feed solution. This results in a continuous substrate release into the culture broth at a slightly declining rate. Due to the release, the substrate concentration within the feed reservoir decreases, which reduces the driving concentration gradient. Another

reason for the slightly declining rate is the effect of osmosis. Osmotic pressure differences lead to a flow of water into the reservoir, thereby diluting the feed solution (Figure 2.1D). However, since the membrane-based fed-batch shake flask is not restricted to a single type of membrane, membranes with various characteristics can be applied in order to meet individual needs (Philip et al., 2017).

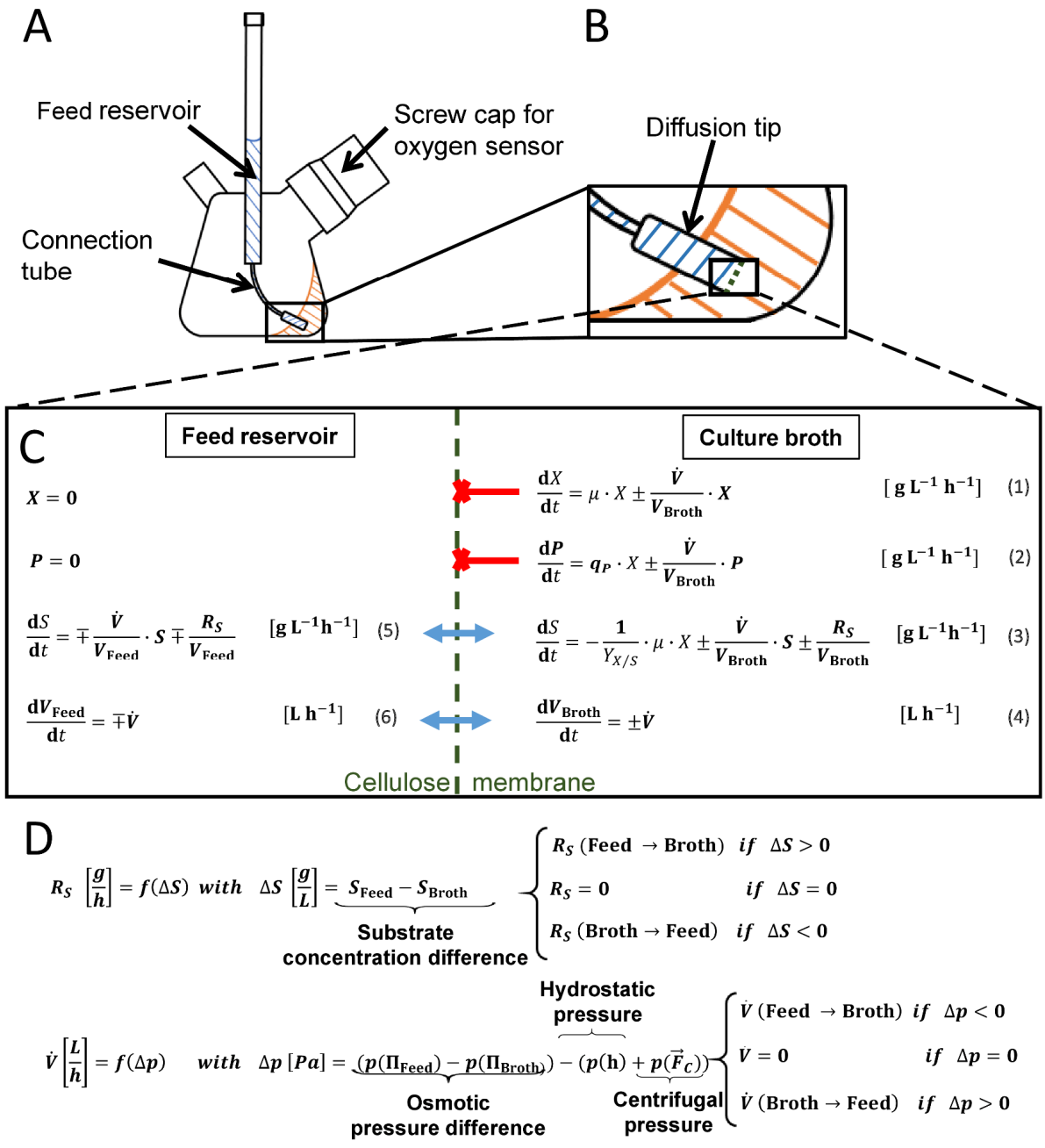

Figure 2.1: Principle of the membrane-based fed-batch shake flask with theoretical description of the fluxes. (A) Schematic representation of the membrane-based fed-batch shake flask. The screw cap for the oxygen sensor makes the membrane-based fed-batch shake flask compatible with the RAMOS device. (B) Close-up illustration of the diffusion tip with the cellulose membrane dipping into the culture broth. Since the weight of the diffusion

tip is adjusted to facilitate in-phase rotation with the bulk liquid, the hydrodynamic conditions within the shake flask remain unchanged and the membrane is in permanent contact with the culture broth. (C) Close-up view of the space around the membrane with the corresponding differential equations for biomass, product, substrate and liquid volume for the feed reservoir (Feed reservoir) and shake flask (Culture broth) compartment. Cells (e.g. *B. licheniformis*) and high molecular weight products (e.g. proteases) are not able to pass the membrane, whereas substrates (e.g. glucose) and water pass the membrane in both directions. (D) The feed flux (F_S) and water flux ($\dot{V}$) are assumed to be independent from each other. The concentration difference determines whether and to which extend a substrate is released from the feed reservoir (Feed reservoir) into the shake flask (Culture broth) and vice versa. The direction of the water flux is mainly determined by the osmotic pressure difference. The hydrostatic pressure and the pressure caused by the centrifugal acceleration of the feed solution (centrifugal pressure) have a negligible impact when working with ultrafiltration membranes, such as cellulose membranes. Abbreviations: μ, specific growth rate; R_S, substrate release rate; p, pressure; P, product concentration; q_P, specific production rate; S, substrate concentration; $\dot{V}$, water flux; V_{Broth}, volume of culture broth; V_{Feed}, volume of feed solution; X, biomass concentration; $Y_{X/S}$, biomass yield per consumed substrate.

In previous projects, the system was successfully used to adjust different feeding rates, feeding of various substrates, parallel feeding of substrates and pH stabilizing agents (Bähr et al., 2012; Philip et al., 2017, 2018). Since the scalability of small-scale fed-batch systems is an important aspect, a membrane-based fed-batch shake flask cultivation was also transferred to a lab-scale stirred tank reactor. With a constant volumetric feeding rate as scale-up criterion, comparable biomass and product concentrations were obtained (Philip et al., 2017).

The 250 mL membrane-based fed-batch shake flasks have been previously applied to *Escherichia coli* and *Hansenula polymorpha* cultures. However, the 250 mL membrane-based fed-batch shake flasks have not yet been applied to *Bacillus* species, which belong to the main producers of proteases. Proteases are highly relevant in the technical enzyme market, especially in detergents (Maurer, 2004). For the industrial production of detergent proteases, *Bacillus licheniformis* strains are extensively used (Maurer, 2004; Gupta et al., 2002; Rao et al., 1998). Despite the importance of *B. licheniformis* as an industrial workhorse, knowledge of the control mechanisms involved in the expression of proteases using endogenous promoters is limited (Voigt et al., 2006, 2015). Priest et al. (1977) pointed at the regulatory role of catabolite repression. Since then, different catabolites such as glucose (Frankena et al., 1986; Laishley & Bernlohr, 1968; Mao, Pan, & Freedman, 1992), ammonium (Giesecke et al., 1991; Hanlon, Hodges, & Russell, 1982) and oxygen (Çalık et al., 2000) were found to repress protease production in *B. licheniformis*. In more recent studies, transcriptome and proteome analysis were used to examine the response of *B. licheniformis* under different nutrient starvation conditions (Voigt et al., 2006, 2007; Wiegand et al., 2013). The obtained results once more

highlight the tight connection of protease expression and nutrient availability. Efforts were made to overcome carbon catabolite repression by using catabolite repression free expression systems and alternative carbon sources (Nathan & Nair, 2013; Singh, Schmalisch, Stülke, & Görke, 2008). Nevertheless, the most commonly applied strategy to avoid catabolite repression is the implementation of substrate-limited fed-batch processes (Maurer, 2004) (Chapter 1.1 and 1.2).

As described above, regulatory mechanisms of protease production with *Bacillus licheniformis* strains are complex. Different catabolites were found to influence protease production. Consequently, the investigation of the control mechanisms requires a large number of experiments, which becomes cost-, time- and labor intensive when working with stirred tank reactors. Membrane-based fed-batch shake flasks, however, are flexible regarding the spectrum of feedable compounds, are independent of peripheral equipment and highly parallelizable. Therefore, in this chapter, the 250 mL membrane-based fed-batch shake flask was standardized regarding its dimensions and optimized in design, handling and robustness. Subsequently, the system was used for the first time in combination with a protease producing *Bacillus licheniformis* strain. The in-house build RAMOS device enabled online monitoring of the oxygen transfer rate (OTR) (Anderlei & Büchs, 2001; Anderlei et al., 2004). By establishing a single component glucose release (Figure 2.2A) and a two component parallel glucose and NH_4^+ release (Figure 2.2B), defined glucose (C)-limited fed-batch conditions were introduced to the *Bacillus licheniformis* culture. NH_4^+-limited fed-batch conditions were achieved by establishing a single component NH_4^+ release (Figure 2.2C). The acquired online and offline data reveal the dynamics of the 250 mL membrane based fed-batch shake flasks. Furthermore, in-depth information on the behavior of the protease producing *Bacillus licheniformis* strain under glucose- and NH_4^+-limited fed-batch conditions were provided. The working principle of the 250 mL membrane-based fed-batch shake flask was then transferred to 500 mL shake flasks.

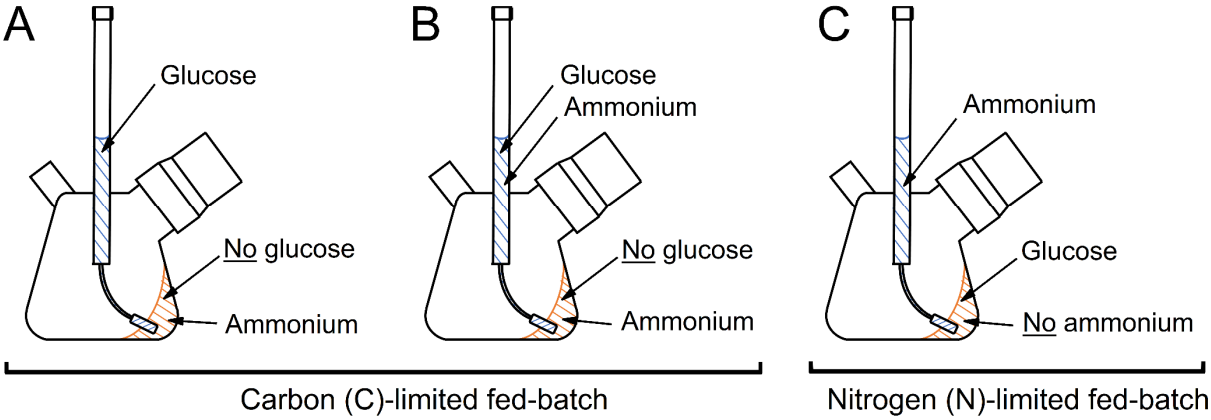

Figure 2.2: Schematic representation of different experimental set-ups using membrane-based fed-batch shake flasks. (A) Single component glucose feed resulting in carbon-limited fed-batch process. (C) Two component glucose and ammonium feed adjusted such that glucose is limited during fed-batch operation and ammonium is always available in excess. (D) Single component ammonium feed resulting in nitrogen-limited fed-batch process. For all different experimental set-ups, V3 mineral medium was used.

2.2 Material and Methods

2.2.1 Strain and media

The protease producing *Bacillus licheniformis* strain contains a plasmid for the expression of a subtilisin-like protease and a tetracycline resistance marker for selection and was kindly provided by BASF SE (Ludwigshafen am Rhein, Germany). Further information on the protease producing *Bacillus licheniformis* strain can be provided by BASF SE (Ludwigshafen am Rhein, Germany) upon request. The chemicals applied for the media preparation were of analytical grade and purchased from Carl Roth GmbH & Co. KG (Karlsruhe, Germany), Sigma-Aldrich Chemie GmbH (Steinheim, Germany), Merck (Darmstadt, Germany), VWR (Darmstadt, Germany) and from AppliChem (Darmstadt, Germany).

The complex Terrific Broth (TB) medium contained per liter: 10 g glycerol ($C_3H_8O_3$), 12 g tryptone, 24 g yeast extract, 12.54 g K_2HPO_4 and 2.31 g KH_2PO_4. After autoclaving (121 °C, 20 min), the medium was stored at 4 °C for not longer than 6 months. Prior to cultivation, a sterile filtered (0.2 µm filter) tetracycline stock solution was added to a final concentration of 20 mg L^{-1}.

The V3 mineral medium was prepared according to Meissner et al. (2015). The glucose concentration for the 2nd preculture and the batch main cultures was 25 g L^{-1} and 20 g L^{-1}, respectively. The $(NH_4)_2SO_4$ concentration was set to 10.6 g L^{-1} (2.9 g L^{-1} NH_4^+) for pre- and main cultures unless stated otherwise. Sterile tetracycline was added to obtain a final concentration of 20 mg L^{-1}. A general overview of the applied carbon and nitrogen sources in the culture media of fed-batch cultivations is given in Figure 2.2.

2.2.2 Cultivation conditions

Cultivations were performed in 250 or 500 mL shake flasks on an orbital climo-shaker ISFX-1 from Adolf Kühner AG (Biersfelden, Switzerland) with a filling volume V_{Broth} = 10 or 30 mL a shaking frequency n = 300 or 350 rpm and a shaking diameter d_0 = 50 mm at a temperature T = 30 °C. The applied cultivation conditions are specified in the following figures. An in-house build RAMOS device was used for online monitoring of shake flask cultivations. The RAMOS device enables online measurement of the oxygen transfer rate (OTR), the carbon dioxide transfer rate (CTR) and the respiratory quotient (RQ) in up to eight parallel shake flasks. Due to the low change of the absolute dissolved oxygen concentration, the measured oxygen transfer rate (OTR) can be assumed to be equal to the oxygen uptake rate (OUR) (Mühlmann, Forsten, Noack, & Büchs, 2018). A commercial version is available from Adolf Kühner AG (Biersfelden, Switzerland) or HiTec Zang GmbH (Herzogenrath, Germany).

Main cultures were carried out in batch or fed-batch mode. The pH was not actively controlled. Culture acidification was prevented by using MOPS buffer. With a MOPS buffer concentration of 0.2 M and 0.4 M, the initial pH value was 7.7 and 7.9, respectively. For batch experiments, the total amount of medium was inoculated (master mix). Subsequently, appropriate volumes were transferred to RAMOS flasks and conventional Erlenmeyer flasks with cotton plugs. Both flask types were treated identically and cultivated within the same temperature controlled shaker next to each other. Erlenmeyer flasks were used for sampling and once withdrawn from the shaker, were not put back (Wewetzer et al., 2015). The described procedure was similar for fed-batch experiments for which RAMOS-compatible membrane-based fed-batch shake flasks were used.

2.2.3 250 mL membrane-based fed-batch shake flask

The 250 mL membrane-based fed-batch shake flask is based on the prototype described by Bähr et al. (2012) and Philip et al. (2017). The tailor-made 250 mL Erlenmeyer shake flask has a centrally located GL 18 thread opening for the feed reservoir and a laterally placed GL 18 thread opening for inoculation and sampling (Figure 2.3A). The additional thread openings for air inlet (GL 18), air outlet (GL 18) and the oxygen sensor (GL 32) enable the application of the RAMOS device during fed-batch cultivation.

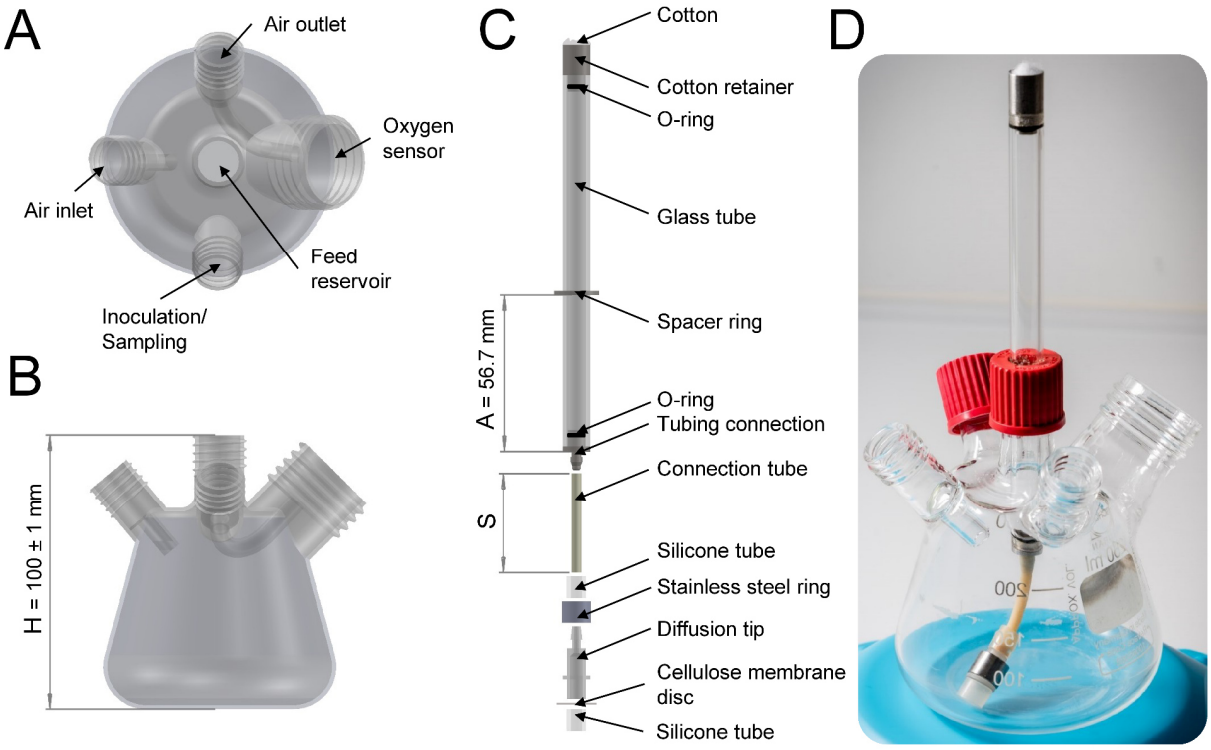

Figure 2.3: Features and components of the 250 mL membrane-based fed-batch shake flask. (A) Top view of the tailor-made 250 mL Erlenmeyer shake flask. (B) Side view of the tailor-made 250 mL Erlenmeyer shake flask. H = height of the shake flask. (C) Exploded view of the feed reservoir for the tailor-made 250 mL Erlenmeyer shake flask. A = distance between the lower edge of the spacer ring and tubing connection. S = length of the connection tube. (D) Assembled 250 mL membrane-based fed-batch shake flask.

The online 250 mL membrane-based fed-batch shake flask system was standardized regarding its dimensions. The height of the tailor-made 250 mL Erlenmeyer shake flask (H), which is the distance between the upper edge of the central opening and the bearing surface of the flask, was set to 100 mm (Figure 2.3B). Since tailor-made 250 mL Erlenmeyer shake flasks are manually manufactured, the height (H) of each shake flask ideally varies between ± 1 mm (Figure 2.3B). However, variations in height can disturb proper functioning of the membrane-based fed-batch

shake flask. With decreased height (H < 100 mm), the diffusion tip might bump into the shake flask wall while rotating. Continuous contact with the glass wall can directly cause damage to the membrane or can remove the silicone tube, which holds the membrane in place. With increased height (H > 100 mm), the diffusion tip might not dip into the culture broth. If the membrane is not in contact with the culture broth, substrate release is prevented. To guarantee continuous feeding, variations in flask height (H) were compensated by individually adjusting the length of the connection tube (S) on basis of

$$\mathbf{S = H_m \cdot C - A} \qquad [\mathbf{mm}] \qquad (2\text{-}1)$$

were H_m is the measured height of the shake flask. A is the standardized distance between the lower edge of the spacer ring and tubing connection, which was set to 56.7 mm (Figure 2.3C). C is an empirical constant with the value 0.9 that describes the relation between H_m and S + A. The constant C was determined by experimentally adjusting the connection tube length (S) within eight tailor-made 250 mL Erlenmeyer shake flasks. The adjustment of the connection tube length (S) was done by visual examination of the rotating diffusion tip on basis of slow motion videos taken with a smartphone camera (Galaxy S7 edge, Samsung, South Korea).

Besides the standardized dimensions, components of the feed reservoir were redesigned to reduce reservoir leaking and for improved handling and life span. The previously introduced stainless steel screw cap for the cotton retainer (Philip et al., 2017) was omitted (Figure 2.3C). This did not affect the stable positioning of the cotton during shaking, but allowed to reduce work steps and the top-heaviness of the system. The cotton retainer as well as the tubing connection are connected via UV bonding with the glass tube (UV curing at 366 nm, GB 368, Delo, Windach, Germany). With the previous design of these components, the UV adhesive had two functions: firstly, it bonded the stainless steel components to the glass tube and secondly, it served as sealing material. Due to frequent sterilization, however, the UV adhesive gets cracks before losing its adhesive properties. To prevent possible leakages caused by cracks in the UV adhesive, O-rings were introduced to the cotton retainer as well as tubing connection (Art. Nr.: 11488, Dichtelemente arcus GmbH, Seevetal, Germany) (Figure 2.3C). Thus, unexpected leakages were prevented and the life span of the membrane-based fed-batch shake flask increased. The assembled 250 mL membrane-based fed-batch shake flask is depicted in Figure 2.3D.

2.2.4 Preparation of the 250 mL membrane-based fed-batch shake flask

The assembly was based on the description by Philip et al. (2017). The commercially available membrane RCT-NatureFlex-NP from Reichelt Chemietechnik GmbH + Co. (Art. Nr.: 94587, Heidelberg, Germany) fabricated from regenerated cellulose was used for all fed-batch experiments with the 250 mL membrane-based fed-batch shake flask. Circular membrane disks with a diameter of 16 mm were punched out with a hollow puncher. The membrane disks were stretched on diffusion tips with an in-house build apparatus (Figure 2.4A). The in-house build apparatus enabled a crease-free and consistent spanning of the membranes. Membranes were held in place using a flexible and biocompatible silicone tube. To prevent the membrane from drying out, diffusion tips were filled with 0.2 mL of deionized water and placed into a cuvette filled with deionized water. Since in preliminary experiments leakage was never observed, the test for possible leakages as described by Philip et al. (2017) was omitted. Before each experiment, the reservoir was assembled, placed into the degassing unit and autoclaved at 121 °C for 20 min. The degassing unit is a tailor-made glass vessel with an outer diameter of 120 mm and a height of 170 mm (Figure 2.4B).

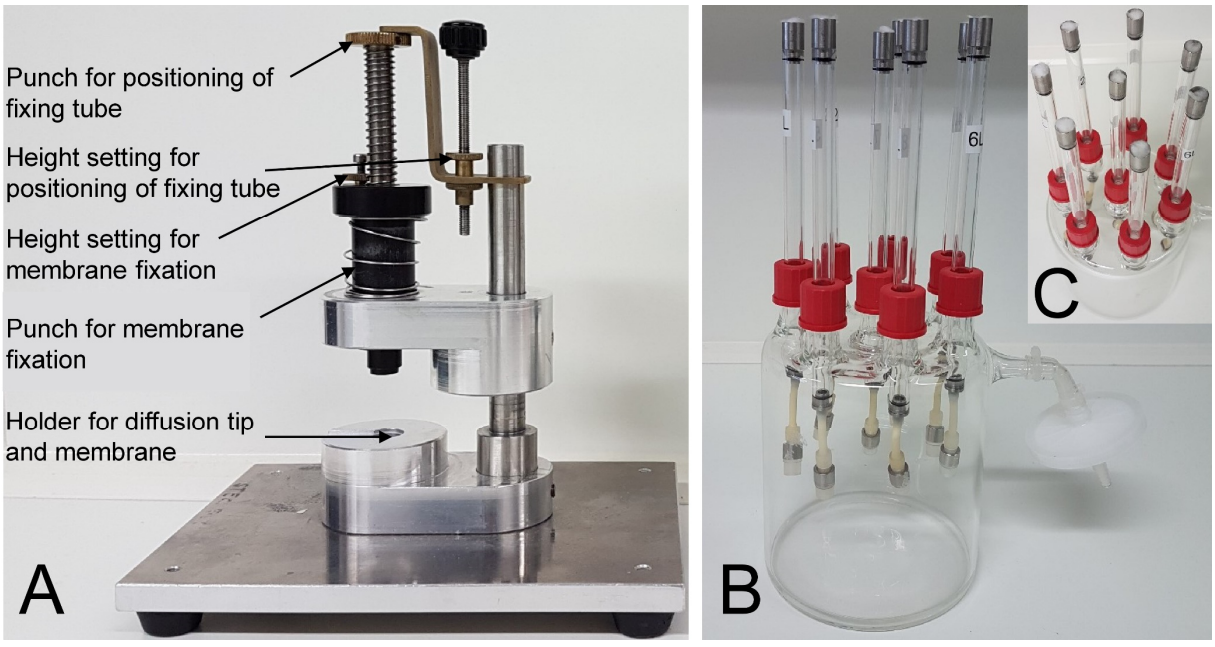

Figure 2.4: In-house build apparatus for membrane fixation and degassing unit for the 250 mL membrane-based fed-batch shake flask. (A) Set-up of the apparatus for membrane fixation. The procedure for membrane fixation was described by Bähr (2013). (B) Side view of the degassing unit containing fully assembled feed reservoirs. (C) Top view of the degassing unit showing the maximum capacity of eight feed reservoirs (8x GL 18 thread openings).

Different feeds were realized by changing the composition of the reservoir feed solution. Figure 2.2 gives an overview of the different experimental set-ups and the resulting substrate limitations. Applied concentrations of the feed solutions are specified in the following figures. Independent from concentrations, the feed reservoir was sterile filled with 2.8 mL of feed solution. Since the diffusion tip is pre-filled with 0.2 mL of deionized water, the feed solutions were prepared to reach the desired concentrations in the final volume of 3 mL. Gas bubbles in the feed reservoir were removed by placing the degassing unit into a desiccator. The desiccator was evacuated with a vacuum pump (LVS 301 p, Ilmvac GmbH, Ilmenau, Germany). An air filter enables sterile pressure compensation between the degassing unit and the desiccator (Figure 2.4B). The degassing unit was designed to degas eight feed reservoirs for 250 mL membrane-based fed-batch shake flasks in parallel (Figure 2.4C). Besides improving the handling during degassing, the compact design of the degassing unit also simplified autoclavation and filling of the feed reservoir. The membrane disks were discarded after each cultivation. Therefore, the described process was repeated for each experiment with newly punched membrane disks.

2.2.5 500 mL membrane-based fed-batch shake flask

The working principle of the 500 mL membrane-based fed-batch shake flask is based on the 250 mL membrane-based fed-batch shake flask described in Chapter 2.2.3. The tailor-made 500 mL Erlenmeyer shake flask is depicted in Figure 2.5 and contains thread openings for air inlet (GL 18), air outlet (GL 18), the oxygen sensor (GL 32) and an opening for inoculation and sampling (GL 25) (Laborbedarf Mohr, Aachen, Germany). The air inlet and outlet in combination with the thread opening for the oxygen sensor make the shake flask compatible with the RAMOS device (Figure 2.5A). The thread opening for the feed reservoir (GL 25) is located centrally to allow rotation of the diffusion tip in-phase with the liquid sickle. The height of the shake flask (H) is set to 135 mm (Figure 2.5B). The 500 mL Erlenmeyer shake flask is handmade and ideally contains variations in height (H) between ± 2 mm. Similar to the 250 mL membrane-based fed-batch shake flask, these variations are compensated by individually adjusting the length of the connection tube (S) on basis of Equation (2-1). The value of the empirical constant C was 0.9. It was determined with ten tailor-made 500 mL Erlenmeyer shake flasks according to the descibed procedure in Chapter 2.2.3.

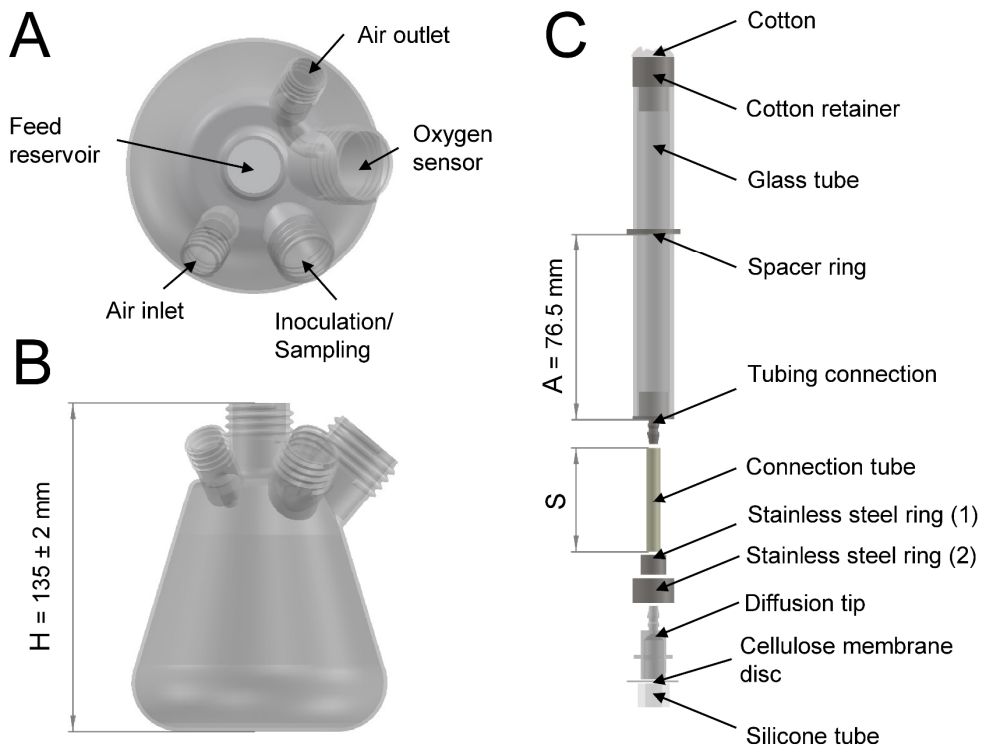

Figure 2.5: Features and components of the 500 mL membrane-based fed-batch shake flask. (A) Top view of the tailor-made 500 mL Erlenmeyer shake flask. (B) Side view of the tailor-made 500 mL Erlenmeyer shake flask. H = height of the shake flask. (C) Exploded view of the feed reservoir for the tailor-made 500 mL Erlenmeyer shake flask. A = distance between the lower edge of the spacer ring and tubing connection. S = length of the connection tube.

The individual components of the feed reservoir are depicted in Figure 2.5C. The feed reservoir consists of a DURAN® borosilicate glass tube with an inner diameter of 13.4 mm, an outer diameter of 17.0, a wall thickness of 1.8 mm and a length of 135.0 mm (DWK Life Sciences, Wertheim, Germany). The stainless steel (1.4301) cotton retainer, spacer ring and tubing connection were fabricated in-house and are connected with the glass tube via UV bonding (UV curing at 366 nm, GB 368, Delo, Windach, Germany) (Figure 2.5C). Since this was the first iteration of the 500 mL membrane-based fed-batch shake flask prototype development, the introduced O-rings for the cotton retainer and tubing connection were omitted (Chapter 2.2.3). Cotton was added as sterile barrier into the cotton retainer. As connection tube, a flexible PharMed® BPT tube with an inner diameter of 2.4 mm, an outer diameter of 5.6 mm and a wall thickness of 1.6 mm was chosen (Art. Nr.: R6503-26BPT, Saint Gobain, France). To allow in-phase rotation of the diffusion tip with the bulk liquid, the diffusion tip was loaded with two in-house fabricated rings of stainless steel (1.4301) (Figure 2.5C). The smaller stainless steel ring (1) has an inner diameter of 6.9 mm, an outer diameter of 10.5 mm, a wall thickness of

1.8 mm and a length of 8.0 mm. This ring fulfills two functions: firstly, it serves as weighting and secondly, it holds the larger stainless steel ring (2) in place while the shaker accelerates. The larger stainless steel ring (2) has an inner diameter of 10.4 mm, an outer diameter of 17.0 mm, a wall thickness of 3.3 mm and a length of 10.0 mm. The smaller (1) and larger (2) stainless steel ring have a mass of 3.1 and 11.2 g, respectively. With this total weight, the proper rotational movement of the diffusion tip is ensured for shaking frequencies between 300 and 350 rpm at a shaking diameter d_0 = 50 mm. If the shaking frequency or diameter are lowered, the weight of the stainless steel rings has to be increased accordingly.

The diffusion tip for the 500 mL membrane-based fed-batch shake flask system was designed to have a 3-fold enlarged active diffusion area compared to the diffusion tip of the 250 mL membrane-based fed-batch shake flask system. Thus, the inner diameter of the diffusion tip was increased from 4.8 to 8.3 mm resulting in an active diffusion area of 18.1 and 54.1 mm^2, respectively (Figure 2.6). On top of the diffusion tip, a cellulose membrane is fixed with a Versilic® silicone tube with an inner diameter of 7.0 mm, an outer diameter of 13.0 mm, a wall thickness of 3 mm and a length of 9.7 mm (Art. Nr.: 760590, Saint-Gobain, France).

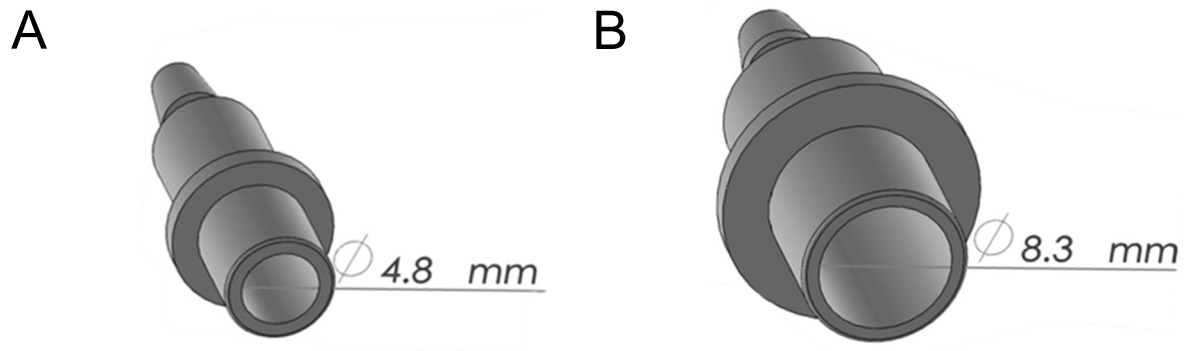

Figure 2.6: Diffusion tip for the 250 mL and 500 mL membrane-based fed-batch shake flask. (A) Diffusion tip for the 250 mL membrane-based fed-batch shake flask. The internal diameter is 4.8 mm resulting in an active diffusion area of 18.1 mm^2. (B) Diffusion tip for the 500 mL membrane-based fed-batch shake flask. The internal diameter is 8.3 mm resulting in an active diffusion area of 54.1 mm^2.

The assembled feed reservoir is fastened into the centrally placed GL 25 thread opening of the tailor-made 500 mL Erlenmeyer shake flask using a DURAN® PBT GL 25 screw cap with a hole (DWK Life Sciences, Wertheim, Germany). The hole diameter was enlarged to 17.5 mm according to the larger feed reservoir (outer diameter of 17.0 mm). To guarantee that the 500 mL membrane-based fed-batch system is airtight, a sealing ring (inner diameter of

16.0 mm, outer diameter of 22 mm, wall thickness of 3 mm and length of 2 mm) is placed between the spacer ring and the centrally placed GL 25 thread opening.

2.2.6 Preparation of the 500 mL membrane-based fed-batch shake flask

The assembly of the 500 mL membrane-based fed-batch shake flask is based on the description in Chapter 2.2.4. The commercially available membrane RCT-NatureFlex-NP from Reichelt Chemietechnik GmbH + Co. (Art. Nr.: 94587, Heidelberg, Germany) fabricated from regenerated cellulose was used for all fed-batch experiments with the 500 mL membrane-based fed-batch shake flask system. Circular membrane disks with a diameter of 24 mm were punched out with a hollow puncher. The membrane disks were stretched on the diffusion tip with an in-house build apparatus (Figure 2.7A). The working principle of the apparatus, described in Chapter 2.2.4, was adapted for the diffusion tips of the 500 mL membrane-based fed-batch shake flask system (Figure 2.6B). Membranes were held in place using a flexible and biocompatible silicone tube. To prevent the membrane from drying out, diffusion tips were filled with 0.9 mL of deionized water and stored in wells of a 24-well microtiter plate that was filled with deionized water. Since in preliminary experiments leakage was never observed, the test for possible leakages as described by Philip et al. (2017) was omitted. Before each experiment, the reservoir was assembled, placed into the degassing unit and autoclaved at 121 °C for 20 min. The degassing unit is a tailor-made glass vessel with an outer diameter of 160 mm and a height of 170 mm (Figure 2.7B).

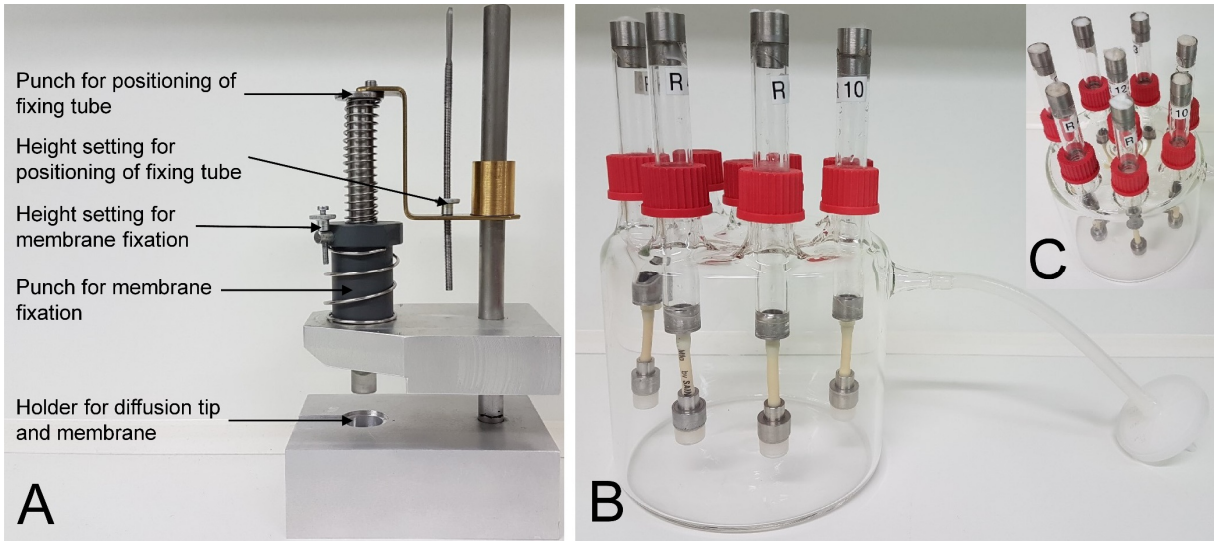

Figure 2.7: In-house build apparatus for membrane fixation and degassing unit for the 500 mL membrane-based fed-batch shake flask. (A) Set-up of the apparatus for membrane fixation. The procedure for membrane fixation was described by Bähr (2013). (B) Side view of the degassing unit containing fully assembled feed reservoirs. (C) Top view of the degassing unit showing the maximum capacity of eight feed reservoirs (8x GL 25 thread openings).

The feed reservoir was filled with 8.1 mL of a concentrated glucose solution. Since the diffusion tip is pre-filled with 0.9 mL of deionized water, the glucose solution was prepared to reach the desired concentration of 200 g L^{-1} in the final volume of 9 mL. Gas bubbles in the feed reservoir were removed by placing the degassing unit into a desiccator. The desiccator was evacuated with a vacuum pump (LVS 301 p, Ilmvac GmbH, Ilmenau, Germany). An air filter enables sterile pressure compensation between the degassing unit and the desiccator (Figure 2.7B). The degassing unit was designed to degas eight feed reservoirs for 500 mL membrane-based fed-batch shake flasks in parallel (Figure 2.7C). Besides improving the handling during degassing, the compact design of the degassing unit also simplified autoclavation and filling of the feed reservoir. The membrane disks were discarded after each cultivation. Therefore, the described process was repeated for each experiment with newly punched membrane disks.

2.2.7 Offline sample analysis

Optical density: The optical density was measured in disposable semi-micro cuvettes with a pathlength of 1 cm (Carl Roth GmbH & Co. KG, Karlsruhe, Germany) at a wavelength of 600 nm (OD_{600}) using the spectrophotometer Genesys 20 from Thermo Fisher Scientific (Waltham, USA). A 0.9 % NaCl-solution was used as blank and for sample dilution. The

samples were diluted to stay within the linear concentration range ($OD_{600} \leq 0.3$). On basis of an experimentally defined conversion factor, the resulting OD_{600} values can be transferred into biomass concentrations ($X\ [\mathrm{g\ L^{-1}}] = 0.74\ \cdot \mathrm{OD}_{600}$).

pH-value: Fresh and untreated samples were used to measure the pH at room temperature using the pH meter pH 510 from Eutech Instruments (Landsmeer, Netherlands). The pH meter was calibrated by means of a three-point calibration prior to each measurement (at least every 24 h). Due to the temperature dependency of the pK_a-value of the MOPS buffer, the measured pH value at room temperature (~ 25 °C) is roughly 0.06 higher than the actual pH value during the cultivation at 30 °C.

Ammonium: NH_4^+ concentrations were determined with the Ammonium Cell Test (Cat. No. 114559) in combination with the Spectroquant® NOVA 60 spectrophotometer, which both were from Merck (Darmstadt, Germany). The Ammonium Cell Test allowed the determination of the NH_4^+ concentration within a concentration range of 5.2 to 103.0 mg L^{-1}. Thus, samples were sterile filtered (0.2 µm filter) and diluted with deionized water to the given range. The measurement was carried out according to the manufacturer's procedure description.

Glucose and overflow metabolites: Glucose and overflow metabolite (acetate, 2,3-butanediol, succinate, lactate) concentrations were determined by high performance liquid chromatography (HPLC). The HPLC device (Ultimate 3000, Dionex, Sunnyvale, USA) was equipped with an organic acid-resin-precolumn (40 × 8 mm) and an organic acid-resin-column (250 × 8 mm), both from CS-Chromatographie Service GmbH (Langerwehe, Germany). Samples were sterile filtered (0.2 µm filter) and diluted with deionized water if the glucose concentration was > 50 g L^{-1}. Elution was carried out with 2.5 mM H_2SO_4 with a flow rate of 0.5 mL min^{-1} at a constant temperature of 70 °C. The compounds were detected by measuring the refractometric index with a Shodex RI-101 refractometer (Showa Denko Europe, Munich, Germany). Data analysis was done with the software Chromeleon 6.8 (Dionex, Sunnyvale, USA).

Protease assay: Protease activity measurement was based on the method developed by DelMar et al. (1979) and on the experimental procedure described by Meissner et al. (2015). The assay was carried out in a microplate reader (Synergy 4, BioTek, Winooski, USA) at a wavelength of 405 nm. The concentration of the substrate stock solution of N-succinyl-alanine-alanine-

proline-phenylalanine-p-nitroanilide (N-Suc-AAPF-pNA) was 60 mg mL^{-1} using water free dimethyl sulfoxide. Stocks were stored at -20 °C for not longer than 6 months. Prior to use, the substrate stock was diluted 1/50 with 0.1 M Tris HCl buffer, pH 8.6, 0.1 % (w/v) Brij 35 (reaction buffer). The reaction was started by adding 100 µL of diluted substrate stock to 50 µL of sample in a 96-well microtiter plate with clear and flat bottom (Rotilabo microtest plates, Art. Nr.; 9293.1, Carl Roth GmbH & Co. KG, Karlsruhe, Germany). The absorption measurement was conducted at 30 °C for 15 min. Samples were sterile filtered (0.2 µm filter) and diluted with reaction buffer to keep the absorption at 405 nm between 0.05 and 1. Protease activity was calculated based on the change of absorption at 405 nm, the extinction coefficient ε of 8,900 M^{-1} cm^{-1} and the pathlength of 0.43 cm. Within this chapter, all measured protease activity values were normalized to the activity measured at the point of glucose depletion within the batch experiment shown in Figure 2.9. For clarity, protease activities resulting from fed-batch experiments were also set in relation to the measured activity at the point of glucose depletion within the above mentioned batch experiment. Normalized protease activities are referred to as relative protease activities.

Consumed and released glucose and NH_4^+: Mass balances provided the basis for calculating the weight of the feed solution and of the culture broth before and after cultivation (Appendix 1). Samples of the feed solution and culture broth were analyzed for their glucose concentration. Based on the glucose concentration, the density of the solution at 30 °C was calculated according to Bettin et al. (1998). The density of the culture broth was assumed to be constant throughout cultivation (1.03 kg L^{-1}). On basis of the density and the previously determined weight of the solutions, the volume is calculated. Consequently, the measured glucose concentration within the solution is multiplied with the volume, which gives the available total mass of glucose. The difference of the total glucose mass in the membrane-based fed-batch system at the beginning and end of cultivation corresponds to the consumed glucose. The difference of the total glucose mass within the feed reservoir at the beginning and end of cultivation corresponds to the released glucose (Appendix 1).

For the two component feed, the procedure was kept identical and the density alteration caused by $(NH_4)_2SO_4$ was neglected. For the nitrogen-limited fed-batch with the $(NH_4)_2SO_4$-feed, the densities of aqueous $(NH_4)_2SO_4$-solutions as a function of temperature and concentration were

determined according to the empirical correlation by Novotny & Söhnel (1988). The determination of NH_4^+ consumption and release is identical to the described principle on basis of glucose (Appendix 1). It should be mentioned that the determination of the density based on single components concentrations (e.g. glucose and $(NH_4)_2SO_4$), is subject to potential errors as medium components diffuse into the feed reservoir during the cultivation.

Correction of offline samples: Due to osmotically induced water fluxes in the membrane-based fed-batch shake flasks, the culture broth was either concentrated or diluted (Figure 2.1D, Appendix 2). Since *B. licheniformis* cells and the produced proteases were retained by the membrane (molecular weight cut-off of 10-20 kDa) and thus were subjected to changing volumes, the optical densities (OD_{600}) and the protease activities were always corrected relative to the initial filling volume. This correction also included volume changes caused by evaporation. The volume correction based on mass balances of the empty and filled shake flask (without reservoir) at the beginning and end of cultivation. The density of the culture broth was assumed to be constant (1.03 kg L^{-1}). Thus, the ratio of the final and initial mass of the culture broth resulted in an individual correction factor for OD_{600} and protease activity for each data point.

2.3 Results and Discussion

2.3.1 Development of a preculture procedure

To ensure optimal and reproducible growth within the initial growth phase of the main culture, a two step preculture procedure was developed. A detailed flow chart of the preculture procedure is presented in Figure 2.8. The 1st (batch) preculture with the complex terrific broth medium (TB) was inoculated from a glycerol cryo stock, which was stored in complex TB medium (Figure 2.8A). The course of the OTR of the 1st preculture is shown in Figure 2.8B. The OTR shows no pronounced lag phase at the beginning of the cultivation. One reason for extended lag phases is the variation of the culture medium within the glycerol cryo stock and the 1st preculture. This is not only due to the change of available substrates from a complex to a mineral basis, but also due to physical changes within the culture environment as for example the osmolality (Paul et al., 2015; Schroeter et al., 2013). By using the same medium composition

for both the glycerol cryo stock and the 1st preculture, a lag phase could be avoided (Figure 2.8B).

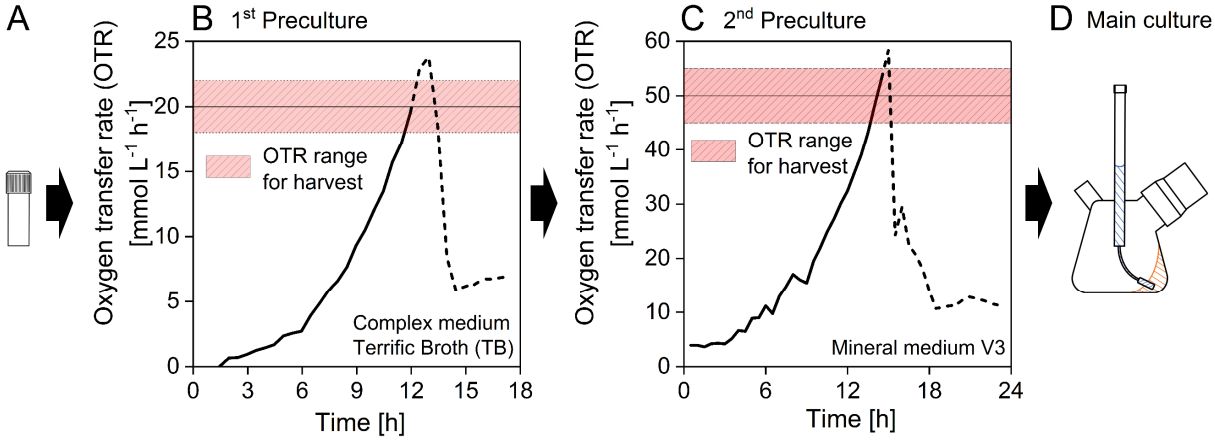

Figure 2.8: RAMOS-based two-step preculture procedure for inoculation of the main culture. (A) Complex TB medium based glycerol cryo stocks (10 % glycerol) were used to inoculate the 1st preculture. (B) For the 1st (batch) preculture, complex TB medium was used and cells were harvested in late exponential phase at an oxygen transfer rate (OTR) of 20 ± 2 mmol L^{-1} h^{-1}. The dashed line represents the further course of the 1st preculture. (C) The 2nd (batch) preculture was inoculated from the 1st with an optical density (OD_{600}) of 0.3. For the 2nd preculture V3 mineral medium was used and cells were harvested in late exponential phase at an OTR of 50 ± 5 mmol L^{-1} h^{-1}. The dashed line represents the further course of the 2nd preculture. (D) Main cultures were operated in batch and fed-batch mode as specified in the following figures. They were inoculated from the 2nd preculture with an OD_{600} of 2.5. For main cultures, exclusively V3 mineral medium was used. Cultivation conditions: T = 30 °C, 250 mL shake flasks, V_{Broth} = 10 mL, n = 350 rpm, d_0 = 50 mm.

Cells from the 1st preculture were harvested with an OTR of 20 ± 2 mmol L^{-1} h^{-1} in late exponential growth phase (Figure 2.8B, solid line) prior to glycerol depletion, which is characterized by a sharp drop of the OTR (Figure 2.8B, dashed line). Figure 2.8C shows the OTR of the 2nd preculture in mineral medium V3 inoculated with an OD_{600} of 0.3. In contrast to the 1st preculture, the initial growth phase of the 2nd preculture was characterized by a short lag phase of 3 h. As mentioned above, most probably the transfer from the complex to the mineral medium caused the lag phase. Consequently, performing a 2nd preculture using V3 mineral medium has two functions. First, the transfer of complex medium components into the main culture is avoided. Second, cells adapt to the medium applied in the main culture, thereby avoiding extended lag phases. Besides using the same culture medium for the last preculture and main culture, the time of harvest plays an important role in terms of inoculum quality and consistency. As soon as the preferred carbon source is depleted, *Bacillus* species undergo a variety of metabolic and morphologic changes (Fujita, 2009; Meissner et al., 2015; Voigt et al., 2006, 2007). Further, González-Pastor, Hobbs, & Losick (2003) described the

secretion of sporulation delaying protein (SDP) and sporulation killing factor (SKF), which prevent sporulation and cause cell lysis when *B. subtilis*, a close relative of *B. licheniformis*, faced nutrient starvation. Thus, cells from the 2nd preculture were always harvested with an OTR of 50 ± 5 mmol L^{-1} h^{-1} in the late exponential growth phase prior to glucose depletion. Main cultures were inoculated with an intial OD_{600} of 2.5 (Figure 2.8D). This high initial biomass concentration was necessary to avoid oxygen limitations within the 1st phase (batch phase) of the biphasic fed-batch cultivations (1st phase: batch phase, 2nd phase: substrate-limited fed-batch phase), as explained in Chapter 2.3.3. The developed preculture procedure was applied in each experiment of this chapter.

2.3.2 Batch cultivation

The results of *B. licheniformis* shake flask cultivations in batch mode are shown in Figure 2.9. The OTR increases exponentially to a maximum of 49 mmol L^{-1} h^{-1}, followed by a distinctive OTR drop at 11.5 h. The OTR drop correlates with the depletion of glucose, while NH_4^+ is always present in excess (always above 1.25 g L^{-1} NH_4^+, data not shown). The OD_{600} maximum of 14.5 correlates with the maximum OTR. After glucose depletion, OD_{600} decreases slightly, and then remains constant throughout the cultivation. Thus, the batch cultivation can be divided into a growth (0 – 11 h) and stationary phase (11- 27 h). In the growth phase, the pH drops to a value of 6.8 (Figure 2.9B). Once glucose is depleted, the pH increases again. The decreasing pH can be explained by NH_4^+ consumption and the secretion of overflow metabolites, such as acetate and succinate (Figure 2.9B) (Meissner et al., 2015). The increase of the pH after glucose depletion is due to the induction of genes that enable the consumption of the previously secreted organic acids (Voigt et al., 2007). It was further reported that under uncontrolled pH batch operation, the pH increases due to H^+ transport into the cells (Çalık et al., 2002). Since *B. licheniformis* maintains a constant intracellular (cytoplasmic) pH of about 7.5, cells react on variations of the extracellular pH by pumping H^+ ions in or out through the membrane (Çalık et al., 2002). The accumulated overflow metabolite concentrations are rather low, with the highest concentration of 0.6 g L^{-1} for acetate and 0.35 g L^{-1} for 2,3-butanediol (Figure 2.9B). The measured concentrations at the beginning of the cultivation originate from the inoculation with the preculture.

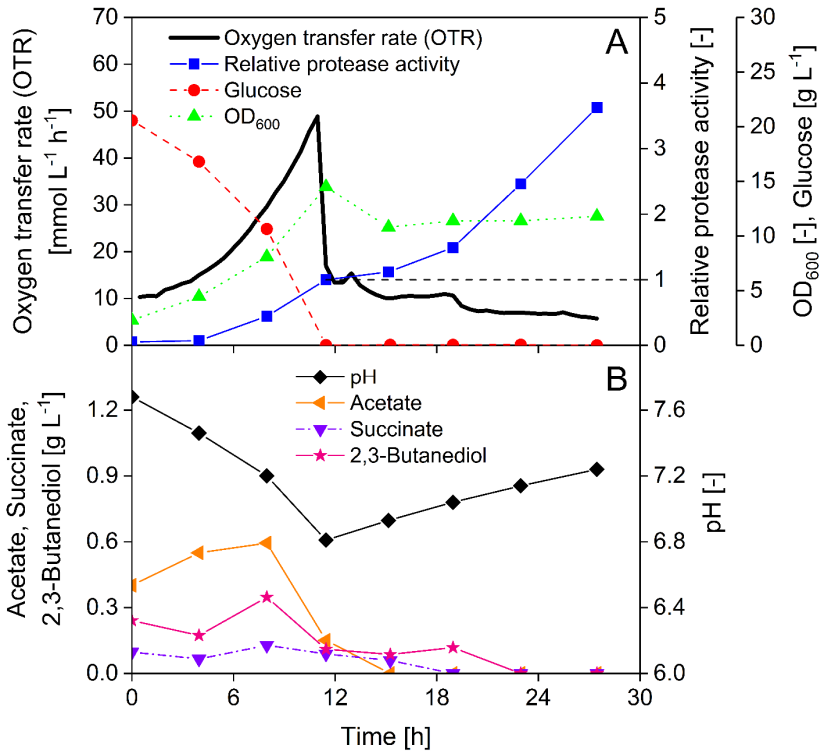

Figure 2.9: Performance of *Bacillus licheniformis* main culture in batch mode. (A) Oxygen transfer rate (OTR), relative protease activity, glucose concentration and optical density (OD_{600}). Protease activities are shown relative to the measured protease activity directly after glucose depletion at 11.5 h (dashed line). (B) pH value, acetate, succinate and 2,3-butanediol concentrations. Initial values: OD_{600} = 2.5, pH = 7.7, 20 g L^{-1} glucose, 2.9 g L^{-1} ammonium, 0.2 M MOPS buffer, V3 medium. Cultivation conditions: T = 30 °C, 250 mL shake flasks, V_{Broth} = 10 mL, n = 350 rpm, d_0 = 50 mm.

Protease activity is shown relative to the measured protease activity after glucose depletion and is referred to as relative protease activity (Figure 2.9A). The course of the relative protease activity is tightly coupled with the presence of glucose. Within the stationary phase (11- 27 h), where glucose is fully depleted and growth ceased, the relative protease activity is assumed to be linearly increasing with a rate of 0.17 h^{-1} reaching a final activity of 3.6 (Table 2-1). The preferred carbon source, such as glucose, has a major influence on the carbon catabolite control, by which *B. subtilis*, a close relative of *B. licheniformis*, coordinates the carbon and energy sources to maximize its efficiency (Fujita, 2009; Sonenshein, 2007). Thus, as long as glucose is present, genes encoding for enzymes that are responsible for carbon recruitment, e.g. proteases, are repressed (Voigt et al., 2007; Wiegand et al., 2013). Within the stationary phase, the only available carbon sources for protease synthesis should be the accumulated overflow metabolites. However, despite the depletion of the measured overflow metabolites at the end of cultivation, an OTR of 6 mmol L^{-1} h^{-1} is measurable (Figure 2.9A). The respiratory

activity indicates the consumption of undetected overflow metabolites, storage compounds or of nutrients deriving from lysed cells (Gebhard et al., 2016; Gonzalez-Pastor et al., 2003). In summary, glucose starvation causes completely undefined conditions in terms of nutrient availability. Therefore, a continuous and controlled release of glucose or other substrates is essential to avoid starvation and to study the behavior of *B. licheniformis* under defined substrate-limited conditions.

Table 2-1: Overview of investigated process conditions with corresponding release rates and slopes of relative protease activities

Process mode	Resulting process conditions	Substrate in feed reservoir	Substrate concentration [g L^{-1}]	Substrate release rate [a] [mg h^{-1}]	Slope of relative protease activity during starvation/limitation [b] [h^{-1}]	Reference
Batch	Glucose starvation	-	-	-	0.17	Figure 2.9
Fed-Batch	Glucose limitation	Glucose	200	5.9	0.19	Figure 2.2A, Figure 2.10A-C
Fed-Batch	Glucose limitation/ Ammonium limitation	Glucose	400	8.8	0.30	Figure 2.2A, Figure 2.10D-F
Fed-Batch	Glucose limitation	Glucose and Ammonium	400 21.8	8.3 0.6	0.24	Figure 2.2B, Figure 2.11
Fed-Batch	Ammonium limitation	Ammonium	16.4	0.2	0.24	Figure 2.2C, Figure 2.13

[a] Substrate release rate is given with the assumption of a constant substrate release rate over time.

[b] Slope of relative protease activity refers to a linearly assumed increase of the relative protease activity within starvation or limitation phases.

2.3.3 Carbon-limited fed-batch cultivation with single component feed

In the following experiment the process mode was switched from batch to fed-batch. Therefore, membrane-based fed-batch shake flasks were used to implement a single component glucose feed, resulting in a carbon-limited fed-batch process (Figure 2.2A). The result of a fed-batch experiment with 200 g L^{-1} of glucose in the feed reservoir and no additional glucose in the culture medium is shown in Figure 2.10A-C.

The initial growth phase is characterized by an increase of the OTR (Figure 2.10A). The steep increase right at the beginning of the cultivation can be attributed to warming up of the system when placed into the 30 °C incubation chamber. Glucose release is initiated once the culture broth gets in contact with the membrane, and thus glucose is released from the beginning of the cultivation. Initially, the glucose release rate is higher than the consumption rate. Consequently, glucose accumulates in the culture broth and all substrates are available in excess (Bähr et al., 2012; Jeude et al., 2006; Philip et al., 2017). Therefore, growth is unlimited and this cultivation phase represents a batch phase. When working with stirred tank reactors, the length of the initial batch phase is determined by the initially provided glucose concentration. As soon as glucose is depleted, fed-batch mode can be initiated by switching on the pumps for glucose feed. The membrane-based fed-batch shake flask releases glucose from the beginning. Therefore, the relation between the glucose release and glucose consumption rate determines the length of the initial batch phase. With the assumption of a constant glucose release rate, the length of the batch phase depends on the glucose consumption rate, which depends on the initial biomass concentration and the specific growth rate (Huber, Scheidle, Dittrich, Klee, & Büchs, 2009). In order to prevent extended batch phases with possible oxygen limitations (Philip et al., 2018), an appropriately high initial biomass concentration was chosen. Due to growth, the initial glucose consumption rate increases further and as soon as the consumption rate is higher than the release rate, the accumulated glucose decreases (Bähr et al., 2012; Huber, Scheidle, et al., 2009; Jeude et al., 2006; Philip et al., 2017). Prior to depletion, the OTR reaches its maximum of 23 mmol L^{-1} h^{-1} and drops to a level that is solely defined by the supply of glucose, and thus by the release rate. Glucose depletion was verified by measuring the glucose concentration in the culture broth (Figure 2.10A). Neither after the OTR drop nor over the remaining cultivation time glucose is measurable. In contrast to the batch phase, this cultivation phase is glucose-limited and thus termed fed-batch phase (Figure 2.10A). The fed-batch phase is characterized by a slightly decreasing OTR plateau of about 11 mmol L^{-1} h^{-1}. It is emphasized that this plateau should not be interpreted as an oxygen limitation (Bähr et al., 2012). The secondary OTR peaks are related to the additional consumption of overflow metabolites (Figure 2.10C). The small peak right after the OTR drop can be attributed to acetate consumption, whereas the OTR peak at 16.5 h is caused by 2,3-butanediol consumption. The pH decreases from 7.9 to 7.2 after 23.5 h and thereafter remains constant at approximately 7.2 (Figure 2.10C).Within the batch phase, growth is unlimited and the OD_{600} most probably follows the course of the OTR. At the same

time protease expression was low, reaching a relative protease activity of 1.0 after 11.5 h of cultivation. Under glucose-limited conditions, the OD_{600} increases, and flattens towards the end. The relative protease activity is assumed to be linearly increasing with a rate of 0.19 h^{-1} (Table 2-1), thereby reaching a final value of 11.8 (Figure 2.10A). Right after glucose depletion, the OTR of the batch process and the fed-batch process showed comparable values of approximately 13 mmol L^{-1} h^{-1} (Figure 2.9A, Figure 2.10A). However, under glucose starvation (batch process) growth ceased, whereas glucose-limited conditions enabled further growth. Furthermore, the slope of the relative protease activity slightly increased from 0.17 h^{-1} under glucose starvation in batch to 0.19 h^{-1} under glucose limitation in fed-batch (Table 2-1).

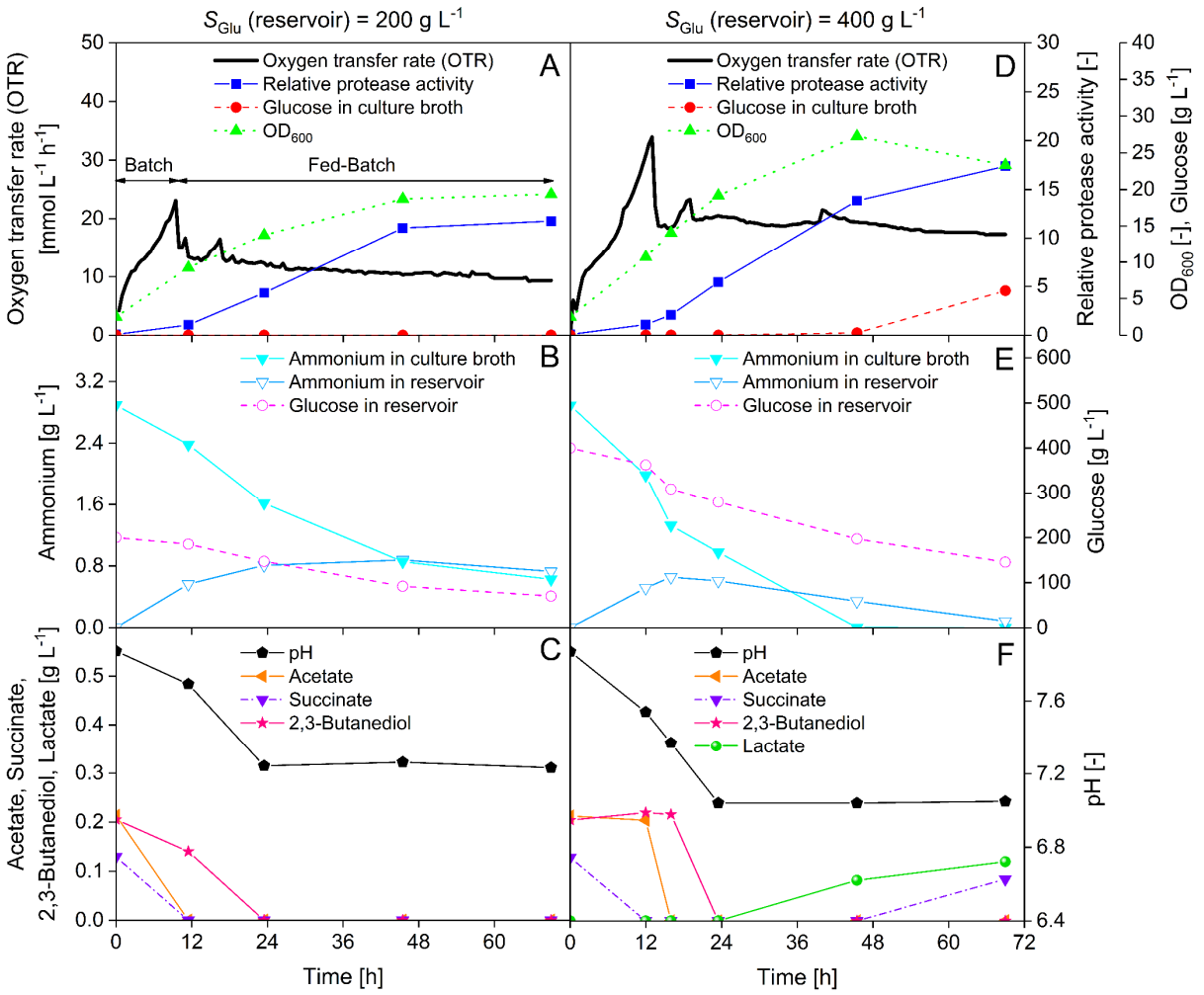

Figure 2.10: Carbon (C)-limited fed-batch cultivations of *Bacillus licheniformis* with varying glucose concentrations in the feed reservoir according to Figure 2.2A. (A-C) Glucose concentration of 200 g L^{-1} in the feed reservoir. (D-F) Glucose concentration of 400 g L^{-1} in the feed reservoir. (A, D) Oxygen transfer rate (OTR), relative protease activity, glucose concentration and optical density (OD_{600}). Protease activities were set in relation to the measured protease activity directly after glucose depletion at 11.5 h within the batch experiment shown in Figure 2.9. (B, E) Ammonium concentration in culture broth and ammonium and glucose concentration within feed reservoir. (C, F) pH value, acetate, succinate, 2,3-butanediol and lactate concentrations. Initial values

(culture broth): OD_{600} = 2.5, pH = 7.9, 0 g L^{-1} glucose, 2.9 g L^{-1} ammonium, 0.4 M MOPS buffer, V3 medium. Initial values (reservoir): V_{Feed} = 3 mL, active membrane diameter = 4.8 mm. Membrane: type = RCT-NatureFlex-NP, material = regenerated cellulose, thickness = 42 µm, cut-off = 10–20 kDa. Cultivation parameters: T = 30 °C, 250 mL membrane-based fed-batch shake flask, V_{Broth} = 10 mL, n = 350 rpm, d_0 = 50 mm.

Glucose release is based on the concentration gradient between the feed reservoir and the culture broth (Figure 2.1D). Due to the release, the glucose concentration in the feed reservoir decreased from 200 to 69.9 g L^{-1} over the full course of the cultivation (Figure 2.10B). However, glucose release is not the only explanation for decreasing concentrations in the feed reservoir. The osmolality of the 200 g L^{-1} glucose solution exceeds the osmolality of the culture broth and causes an osmotic flow of water across the cellulose membrane into the feed reservoir (Figure 2.1D, Appendix 2). Consequently, the volume of the reservoir increases, diluting its glucose concentration (Bähr et al., 2012; Philip et al., 2017). Since the glucose concentration declines, the driving concentration gradient diminishes, and thus, the release rate as well (Bähr et al., 2012). Since the remission of glucose release is rather small, the glucose release rate is specified as a constant (Table 2-1). The glucose concentration of 200 g L^{-1} within the feed reservoir resulted in a release of 5.9 mg h^{-1} (Table 2-1). The slightly declining release rate is reflected by the OTR within the fed-batch phase that declines as well (Figure 2.10A). Furthermore, the release rate also explains the course of the OD_{600}. Since biomass is increasing, more of the provided glucose is required for the maintenance metabolism and thus less is available for growth (Russell & Cook, 1995; Tännler, Decasper, & Sauer, 2008). This results in a constantly decreasing specific growth rate in cultures with constant feed rates (Öztürk et al., 2016).

Over the course of the cultivation the NH_4^+ concentration decreases, but never depletes (Figure 2.10B). Nonetheless, cell growth was not the only reason for decreasing NH_4^+ concentrations within the culture broth. At the beginning of the cultivation, the feed reservoir is filled solely with 200 g L^{-1} of glucose. Thus, the concentration gradient between the culture broth (2.9 g L^{-1}) and the feed reservoir (0 g L^{-1}) causes NH_4^+ to diffuse into the feed reservoir (Figure 2.1D). This phenomenon was also observed by Philip et al. (2017) for NH_4^+ and PO_4^{3-}. From 45.5 h onwards, the NH_4^+ concentration in the feed reservoir and the culture broth approximate (Figure 2.10B). Since within the culture broth NH_4^+ is further consumed, the

concentration deceeds the concentration in the feed reservoir. At that time, the NH_4^+ flow is reversed and NH_4^+ diffuses from the feed reservoir into the culture broth (Figure 2.1D).

The rate at which glucose is released into the culture broth can be varied in different ways (Bähr et al., 2012; Philip et al., 2017). The easiest is changing the initial glucose concentration in the feed reservoir. In the experiment shown in Figure 2.10D-F, the initial glucose concentration in the feed reservoir was increased to 400 g L^{-1}. The rest of the experimental set-up was kept identical to the experiment with 200 g L^{-1} (Figure 2.10A-C).

The higher initial glucose concentration in the feed reservoir results in an increased glucose release rate of 8.8 mg h^{-1} when compared to the 200 g L^{-1} experiment with 5.9 mg h^{-1} (Table 2-1, Figure 2.1D). As both experiments were inoculated with the same biomass concentration, the glucose consumption rate is similar at the beginning of the cultivation. In the experiment with 400 g L^{-1}, more glucose accumulates. Therefore, the batch phase is prolonged and the corresponding OTR peak enhanced (Figure 2.10A, D). The relative protease activity is again low after the batch phase (Figure 2.10D). The start of the fed-batch phase was confirmed by glucose measurement of samples taken at the time of the OTR maximum and shortly after the OTR drop (Figure 2.10D). Once glucose limitation is initiated, overflow metabolites are consumed parallel to the released glucose (Figure 2.10F). Succinate is already consumed at the OTR maximum, whereas acetate is metabolized directly after glucose limitation. Most probably, succinate is also consumed within the batch phase of the 200 g L^{-1} experiment (Figure 2.10C). The pronounced secondary OTR peak at 19 h is again attributed to 2,3-butanediol consumption.

The elevated glucose release rate in the experiment with 400 g L^{-1} initial glucose concentration is also reflected by the plateau of the fed-batch phase, resulting in a higher OTR level of about 20 mmol L^{-1} h^{-1} (Figure 2.10D). However, the OTR plateau shows one characteristic that is not observable within the 200 g L^{-1} experiment. In the middle of the fed-batch phase at 40 h another peak appears within the OTR plateau. Interestingly, a concentration of 0.3 g L^{-1} of glucose is measured in a sample taken shortly after the peak and the concentration even increases to 6.1 g L^{-1} at the end of cultivation (Figure 2.10D). Since overflow metabolites are already consumed at 23.5 h (Figure 2.10F), this is an indication for a metabolic switch. Indeed, NH_4^+ is not measurable in the culture broth from this point on (Figure 2.10E). Despite the enhanced

glucose release for the 400 g L^{-1} experiment, the initial NH_4^+ concentration was kept constant at 2.9 g L^{-1}. Thus, NH_4^+ depletes and becomes the growth limiting nutrient after 40 h, whereby glucose accumulates. Nevertheless, NH_4^+ is not fully depleted within the membrane-based fed-batch shake flask system. Based on the concentration gradient at the beginning of the cultivation, NH_4^+ diffused into the feed reservoir (Figure 2.10E). As soon as the concentration in the culture broth falls below the concentration in the feed reservoir, tiny quantities of NH_4^+ diffuse back into the culture broth (Figure 2.1D). At this point the process switched from carbon- to nitrogen-limitation. The sudden OTR increase at the beginning of the nitrogen limitation can be explained by a changing stoichiometry. Part of the provided glucose is metabolized for cell maintenance, which results in an increased oxygen demand per consumed glucose (Philip et al., 2018). Previously consumed succinate is produced again by *B. licheniformis* and even lactate is detected (Figure 2.10F). Growth also is affected by the nitrogen-limitation as the OD_{600} declines from 27.2 to 23.3 over the last period of cultivation (Figure 2.10D). Noticeable, the relative protease activity seemed not to be affected by the nitrogen limitation. It is assumed to increase linearly throughout the glucose and NH_4^+ limitation with 0.3 h^{-1} to a final relative value of 17.4 (Table 2-1, Figure 2.10D). During NH_4^+ limitation, the increase of the relative protease activity does not correlate with growth, which was already observed for glucose starvation conditions in batch (Figure 2.9A). Compared to the 200 g L^{-1} experiment, the final protease activity is increased by 47.5 %.

In a further experiment, the glucose concentration in the feed reservoir was raised to 600 g L^{-1}, thereby releasing 11.3 mg h^{-1} of glucose (Appendix 3). Due to the higher release and consumption rate of glucose, however, the OTR peak within the fed-batch plateau, and thus the NH_4^+ limitation, appeared earlier. This result affirmed that the OTR peak marks the time point of the initiation of the NH_4^+ limitation. The behavior of OD_{600}, glucose concentration in the culture broth, protease activity, NH_4^+ fluxes and overflow metabolites were highly comparable with the 400 g L^{-1} experiment (Figure 2.10D-F) in a qualitative- and more pronounced in a quantitative way. Hence, the slope of the relative protease activity was increased further to 0.36 h^{-1}.

2.3.4 Carbon-limited fed-batch cultivation with two component feed

The easiest solution to overcome a nitrogen limitation is to provide more NH_4^+ at the beginning of the cultivation. Nevertheless, preliminary batch experiments with elevated NH_4^+ concentrations showed an inhibiting effect on *B. licheniformis* growth (Appendix 4). Thus, the 250 mL membrane-based fed-batch shake flasks were used to feed glucose and NH_4^+ simultaneously. The feed reservoir was filled with a solution that additionally to 400 g L^{-1} glucose contained 21.8 g L^{-1} NH_4^+ (Figure 2.2B). At the same time, the initial NH_4^+ concentration in the culture broth was lowered to 1.6 g L^{-1} to reduce inhibition. Despite the fact that the glucose concentration was kept at 400 g L^{-1}, the glucose release rate of 8.3 mg h^{-1} slightly decreased when compared to the experiment with 400 g L^{-1} of glucose and no additional NH_4^+ within the reservoir (8.8 mg h^{-1}) (Table 2-1). The maximum OTR of 29.5 mmol L^{-1} h^{-1} is reached after 9.5 h, followed by a distinctive drop, which marks the initiation of the fed-batch phase (Figure 2.11A). The secondary OTR peak can again be attributed to parallel consumption of 2,3-butanediol (Figure 2.11C). In the previously described experiment with 400 g L^{-1} of glucose in the feed reservoir, an OTR peak within the fed-batch phase marks the NH_4^+ limitation (Figure 2.10D). In this experiment the OTR plateau shows no noticeable increase, and indeed NH_4^+ never reaches limiting concentrations. The NH_4^+ release of 0.6 mg h^{-1} rather increases the concentration over the course of the cultivation to a final value of 3.4 g L^{-1} (Table 2-1, Figure 2.11B). This means that the release of NH_4^+ compensates the NH_4^+ consumption throughout the cultivation. Due to the release, the concentration in the reservoir decreases constantly to a final concentration of 5.1 g L^{-1}. Similarly to glucose, the NH_4^+ release rate probably declines slightly due to the diminishing concentration gradient between feed reservoir and culture broth.

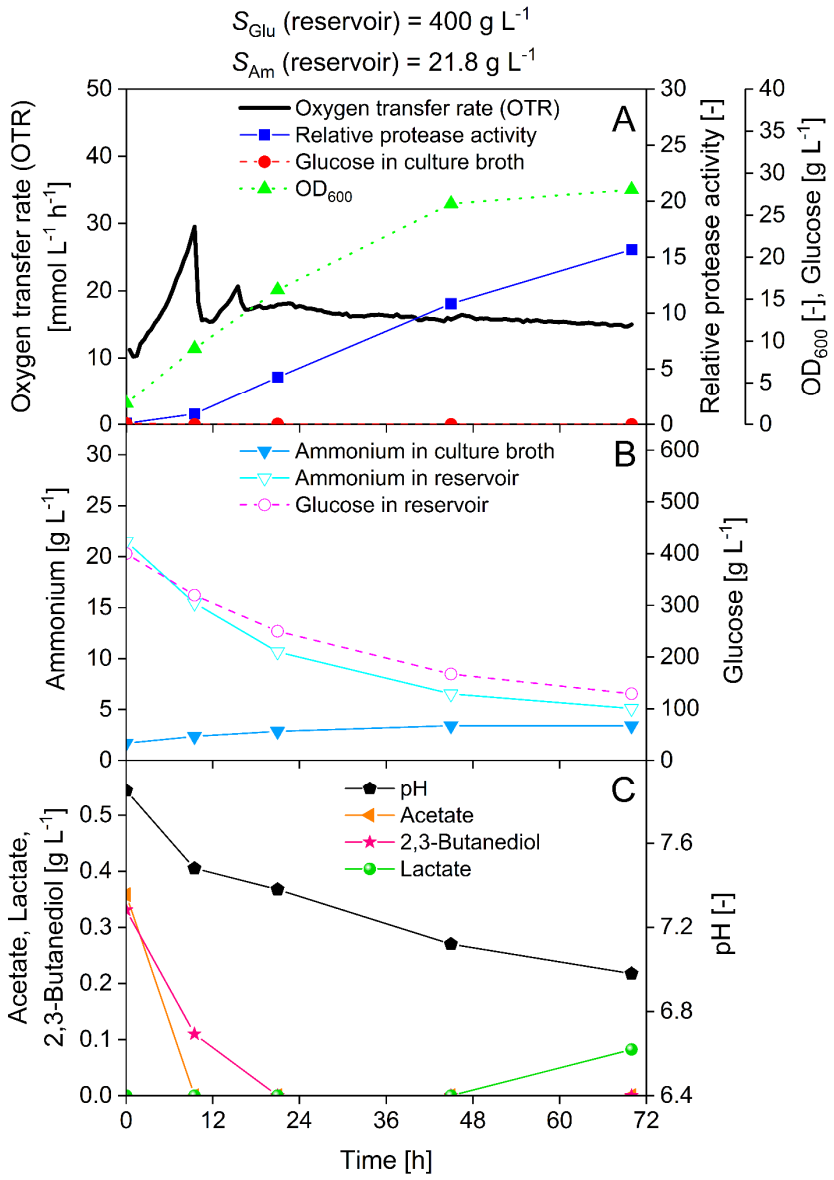

Figure 2.11: Carbon (C)-limited fed-batch cultivation of *Bacillus licheniformis* with glucose and ammonium within the feed reservoir according to Figure 2.2B. (A-C) Initial glucose concentration of 400 g L^{-1} and ammonium concentration of 21.8 g L^{-1} in the feed reservoir. (A) Oxygen transfer rate (OTR), relative protease activity, glucose concentration and optical density (OD$_{600}$). Protease activities were set in relation to the measured protease activity directly after glucose depletion at 11.5 h in the batch experiment shown in Figure 2.9. (B) Ammonium concentration in the culture broth and ammonium and glucose concentration in the feed reservoir. (C) pH value, acetate, 2,3-butanediol and lactate concentrations. Initial values (culture broth): OD$_{600}$ = 2.5, pH = 7.9, 0 g L^{-1} glucose, 1.6 g L^{-1} ammonium, 0.4 M MOPS buffer, V3 medium. Initial values (reservoir): V_{Feed} = 3 mL, active membrane diameter = 4.8 mm. Membrane: type = RCT-NatureFlex-NP, material = regenerated cellulose, thickness = 42 µm, cut-off = 10–20 kDa. Cultivation parameters: T = 30 °C, 250 mL membrane-based fed-batch shake flask, V_{Broth} = 10 mL, n = 350 rpm, d_0 = 50 mm.

As a consequence of the prevented switch from carbon to nitrogen limitation, glucose does not accumulate in the culture broth (Figure 2.11A). The OD$_{600}$ slightly increases also within the last period of cultivation and no succinate is produced (Figure 2.11C). This overall trend is

highly comparable to the 200 g L^{-1} fed-batch experiment (Figure 2.10A-C), where NH_4^+ limitation did not occur either. When comparing the carbon-limited fed-batch cultivations with the lower glucose release rate of 5.9 mg h^{-1} (200 g L^{-1} glucose, Figure 2.10A-C) to the cultivation with higher glucose release rate of 8.3 mg h^{-1} (400 g L^{-1} glucose and 21.8 g L^{-1} NH_4^+, Figure 2.11), the slope of the relative protease activity within the glucose-limited fed-batch phase increased from 0.19 to 0.24 h^{-1}, respectively (Table 2-1). Because of the increased glucose release rate, the final relative protease activity increased by 33 % and the final OD_{600} increased by 45 %.

To further decrease inhibition, the NH_4^+ concentration in the feed reservoir as well as in the culture broth was reduced (Figure 2.12). A NH_4^+ reduction in the feed reservoir with an initial concentration of 1.6 g L^{-1} in the culture broth had a minor effect on the batch growth phase (Figure 2.12A). However, when NH_4^+ was excluded from the culture broth, inhibition was clearly reduced resulting in a specific growth rate of 0.36 h^{-1} within the initial batch phase (27.3 g L^{-1} NH_4^+ in reservoir, Figure 2.12B). For comparison, the experiment depicted in Figure 2.10 has a specific growth rate of 0.24 h^{-1} within the initial batch phase. Since the specific growth rate determines the glucose consumption rate (Huber, Scheidle, et al., 2009), the experiment with 27.3 g L^{-1} in the feed reservoir and no initial NH_4^+ in the culture enters the glucose-limited fed-batch phase already after 4.5 h.

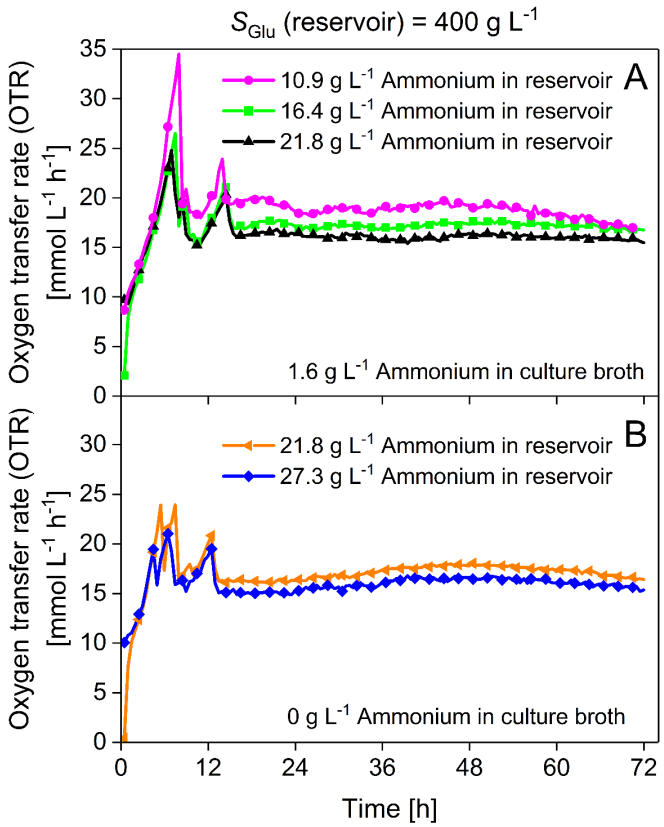

Figure 2.12: Carbon (C)-limited fed-batch cultivation of *Bacillus licheniformis* with 400 g L^{-1} glucose and varying initial ammonium concentrations within the feed reservoir and culture broth according to Figure 2.2B. (A,B) Oxygen transfer rates (OTRs) with varying ammonium concentrations within the feed reservoir and culture broth. The symbols represent every fourth measured oxygen transfer rate (OTR) data point. (A) Ammonium concentration was varied between 10.9, 16.4 and 21.8 g L^{-1} within the feed reservoir and kept constant at 1.6 g L^{-1} within the culture broth. (B) Ammonium concentration was varied between 21.8 and 27.3 g L^{-1} within the feed reservoir and kept constant at 0 g L^{-1} within the culture broth. Initial values (culture broth): OD_{600} = 2.5, pH = 7.9, 0 g L^{-1} glucose, 0.4 M MOPS buffer, V3 medium. Initial values (reservoir): V_{Feed} = 3 mL, active membrane diameter = 4.8 mm. Membrane: type = RCT-NatureFlex-NP, material = regenerated cellulose, thickness = 42 µm, cut-off = 10–20 kDa. Cultivation parameters: T = 30 °C, 250 mL membrane-based fed-batch shake flask, V_{Broth} = 10 mL, n = 350 rpm, d_0 = 50 mm.

Besides the increased specific growth rate, the batch phase is shortened due to the slightly decreased glucose release rate. It is mentioned in the section above that adding NH_4^+ to the feed reservoir diminishes the glucose release rate, although the glucose concentration was kept constant at 400 g L^{-1}. Within all experiments displayed in Figure 2.12, the OTR plateau in the fed-batch phase is higher for low NH_4^+ concentrations in the reservoir and vice versa. Due to the direct correlation between the OTR plateau and the glucose release rate, these experiments underline that addition of NH_4^+ to the feed reservoir reduces the glucose release rate. This observation is independent of the NH_4^+ concentration in the culture broth and occurred with 0, 0.8 and 1.6 g L^{-1} (Figure 2.12, Appendix 5A). Indeed, the fed-batch OTR plateau is highly

comparable when the feed solution is kept constant and the NH_4^+ concentration in the culture broth varies (Appendix 5B, C). Currently, there are no explanations for the underlying mechanisms.

2.3.5 Nitrogen-limited fed-batch with single component feed

The membrane-based fed-batch shake flask is also able to feed other components than glucose. Bähr et al. (2012) already presented data where NH_4^+ was fed to a *Hansenula polymorpha* culture. The experiment with switch from carbon to nitrogen limitation already suggested that protease expression is independent of the growth rate and also takes place under nitrogen-limited conditions (Figure 2.10D-F). To realize NH_4^+ feeding, the reservoir was filled with a 16.4 g L^{-1} NH_4^+ solution whereas the culture broth was supplemented with 60 g L^{-1} glucose, but no additional NH_4^+ (Figure 2.2C). The OTR in this experiment increased exponentially to a maximum of 46.7 mmol L^{-1} h^{-1} at 8.5 h (Figure 2.13A). In this phase NH_4^+ accumulated and, thus, all substrates are available in excess. Once the accumulated NH_4^+ is depleted, the nitrogen-limited fed-batch phase is initiated, indicated by the OTR drop to 22.5 mmol L^{-1} h^{-1} and the absence of NH_4^+ in the culture broth (Figure 2.13A). Since no NH_4^+ was added to the culture broth and depletion already occurs at 8.5 h, the overall NH_4^+ concentration is low during the batch phase. Therefore, growth inhibition is minimized and a specific growth rate of 0.35 h^{-1} is reached, which is comparable to the initial growth rates of glucose-limited experiments without initial NH_4^+ in the culture broth (Figure 2.12B). Within the fed-batch phase, the OTR declines rather than showing a constant plateau, which was visible in glucose-limited fed-batch cultivations (Figure 2.10A, D, Figure 2.11A and Figure 2.12). Furthermore, two secondary peaks occur at 10 and 18 h. Based on the samples, it is not possible to clearly assign those peaks to overflow metabolite consumption (Figure 2.13C). However, measurement of NH_4^+ in the culture broth clearly demonstrates that nitrogen limitation persists over the entire cultivation (Figure 2.13A).

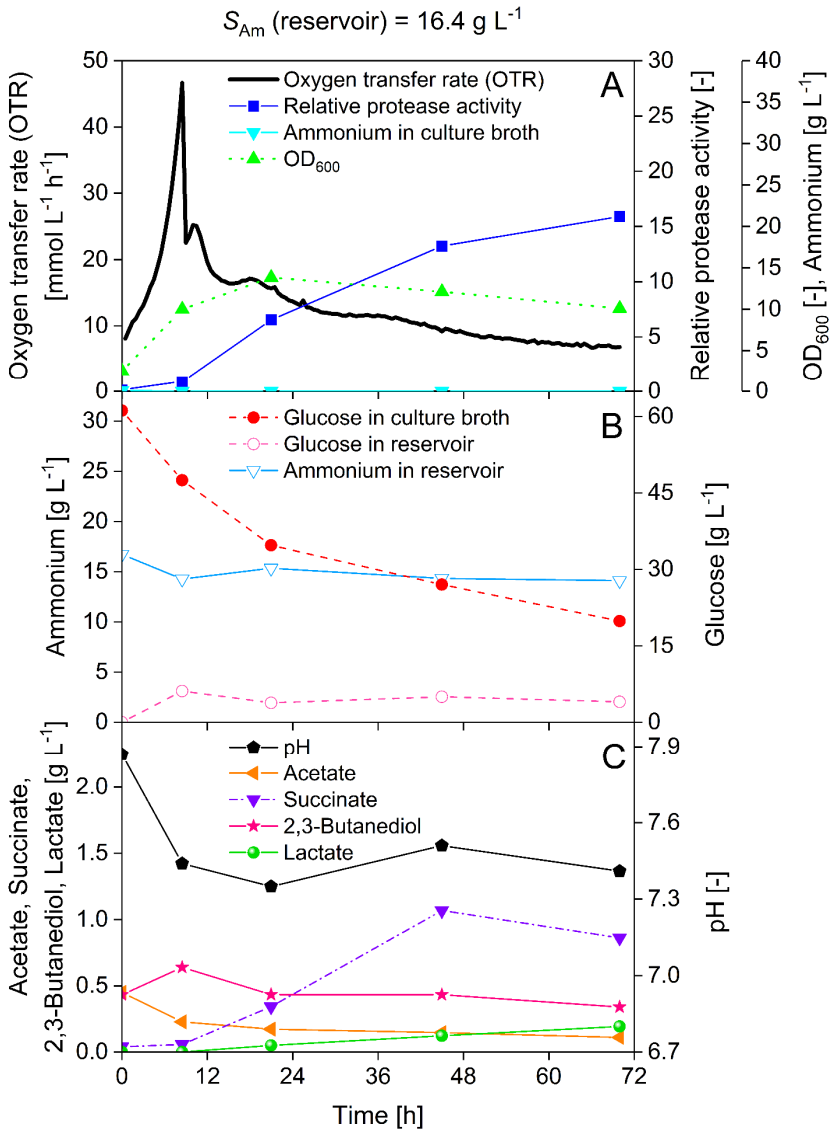

Figure 2.13: Nitrogen (N)-limited fed-batch cultivation of *Bacillus licheniformis* with ammonium within the feed reservoir according to Figure 2.2C. (A-C) Ammonium concentration of 16.4 g L^{-1} was supplied in the feed reservoir. (A) Oxygen transfer rate (OTR), relative protease activity, ammonium concentration and optical density (OD$_{600}$). Protease activities were set in relation to the measured protease activity directly after glucose depletion at 11.5 h in the batch experiment shown in Figure 2.9. (B) Glucose concentration in the feed reservoir and culture broth and ammonium concentration in the feed reservoir. (C) pH value, acetate, succinate, 2,3-butanediol and lactate concentrations. Initial values (culture broth): OD$_{600}$ = 2.5, pH = 7.9, 60 g L^{-1} glucose, 0 g L^{-1} ammonium, 0.4 M MOPS buffer, V3 medium. Initial value (reservoir): V_{Feed} = 3 mL, active membrane diameter = 4.8 mm. Membrane: type = RCT-NatureFlex-NP, material = regenerated cellulose, thickness = 42 µm, cut-off = 10–20 kDa. Cultivation parameters: T = 30 °C, 250 mL membrane-based fed-batch shake flask, V_{Broth} = 10 mL, n = 350 rpm, d_0 = 50 mm.

The OD$_{600}$ increases in the batch phase, though, under nitrogen limitation, *B. licheniformis* does not grow further and OD$_{600}$ even declines in the fed batch phase. In contrast to biomass, the relative protease activity is assumed to increase linearly with 0.24 h^{-1} within the NH_4^+-limited

fed-batch phase reaching a final value of 15.6 (Table 2-1, Figure 2.13A). Despite the cessation of growth, the slope of the relative protease activity is similar to the glucose-limited fed-batch experiment with parallel release of glucose and NH_4^+ (Table 2-1). Frankena et al. (1986) investigated different limitations in chemostat cultures at a variety of specific growth rates. Protease expression was shown to be inversely proportional to the specific growth rate under NH_4^+ limitation with glucose as carbon and energy source. These results correlate well with the here presented data. Interestingly, the NH_4^+ concentration in the feed reservoir remains rather constant (Figure 2.13B), even though it is constantly released at a rate of 0.2 mg h^{-1} (Table 2-1). Contrary to the other fed-batch experiments, the osmolality of the feed reservoir (1.0 osmol kg^{-1} at $t = 0$) within this experiment is below the osmolality of the culture broth (1.48 osmol kg^{-1} at $t = 0$) (Appendix 2). Due to the osmotic pressure, water diffuses from the feed reservoir into the culture broth (Figure 2.1D), and thus, the NH_4^+ solution within the feed reservoir is concentrated. Consequently, the concentration within the feed reservoir remains rather high. Nevertheless, the OTR within the fed-batch phase declines as previously described. However, the release kinetics of ions, such as NH_4^+, is also influenced by the charge of the membrane (Van der Bruggen et al., 1999). The producer did not provide detailed information on the membrane charge in dependence of the medium pH. Within this experiment, glucose is available in excess within the culture broth and drops from 60 to 19.9 g L^{-1} (Figure 2.13B). Due to the high concentration of glucose within the culture broth, back diffusion into the feed reservoir took place (Figure 2.13B, Figure 2.1D). The overflow metabolites succinate and lactate accumulate to 1.1 and 0.2 g L^{-1}, respectively (Figure 2.13C). Both metabolites have been associated with nitrogen limitation in the experiment with 400 g L^{-1} of glucose within the feed reservoir (Figure 2.10E, F). Overflow metabolites deriving from the preculture, such as acetate and 2,3-butanediol, remained rather constant with a slowly decreasing trend. The pH dropped during the initial batch phase and then fluctuated between 7.35 and 7.5 in the nitrogen-limited fed-batch phase. Similar to glucose, the NH_4^+ release rate is increased to 0.3 mg h^{-1} when the NH_4^+ concentration in the feed reservoir is raised to 21.8 g L^{-1} (Appendix 6). Hence, the slope of the relative protease activity was increased to 0.29 h^{-1}.

2.3.6 Comparison of batch, carbon-limited and nitrogen-limited fed-batch cultivations

Evaluation of the OTR courses of different fed-batch experiments resulted in a mean coefficient of variation of 5.5 % (Appendix 7). Furthermore, fed-batch cultivations that were conducted and analyzed in two different laboratories were compared on basis of the OTR course and the final relative protease activity (Appendix 8). The good reproducibility of membrane-based fed-batch shake flask cultivations allowed a detailed comparison of the applied substrate-limited conditions. The results summarized in Table 2-1 show that the substrate release rates positively correlate with the slopes of the relative protease activities. Further, glucose- (400 g L^{-1} glucose and 21.8 g L^{-1} NH_4^+ in reservoir) and nitrogen-limited conditions (16.4 g L^{-1} NH_4^+ in reservoir) result in similar slopes (Table 2-1). However, optimization of the productivity and the space-time yield was not the goal. Process optimization in terms of productivity and space-time yield requires the investigation of various fed-batch strategies with or without feedback control. Strategies with feedback control regulate the feed rate by monitoring the growth limiting substrate (direct feedback) or physical parameters (indirect feedback), such as pH or dissolved oxygen concentration (Öztürk et al., 2016). Strategies without feedback control comprise pulse, constant, linear or exponential feeding. The membrane-based fed-batch shake flask is currently limited to constant release rates. Therefore, the effect of glucose and NH_4^+-limited conditions was investigated based on the protease yield.

The total consumed glucose and the relative protease activity per consumed glucose ($Y_{P/S_{Glu}}$) were calculated (Appendix 9). To compare the batch and fed-batch cultivations, the $Y_{P/S_{Glu}}$ from the fed-batch experiments were set in proportion to the batch experiment. The results show that $Y_{P/S_{Glu}}$ is improved between 1.5 and 2.1-fold when *B. licheniformis* was cultivated in fed-batch mode. With a 2.1-fold increase, the highest $Y_{P/S_{Glu}}$ was obtained under nitrogen-limited conditions (16.4 g L^{-1} NH_4^+ in reservoir). Both carbon-limited cultivations with a glucose reservoir concentration of 200 g L^{-1} and a combined reservoir composition with 400 g L^{-1} of glucose and 21.8 g L^{-1} of NH_4^+ had a comparable increase of 1.6 and 1.5-fold, respectively. Interestingly, the elevated glucose release rate for the experiment with the doubled glucose concentration in the feed reservoir had no significant effect on $Y_{P/S_{Glu}}$. A similar observation was made for the increased NH_4^+ release rate with a reservoir concentration of 21.8 g L^{-1}. The fed-batch cultivation with the switch from carbon to nitrogen limitation showed a 1.8-fold increase,

and thus a slightly higher $Y_{P/S_{Glu}}$ when compared with fed-batch cultivations that were solely carbon-limited. Most likely, this is due to the partial nitrogen-limitation that occurred after 40 h of cultivation (Figure 2.10D-F).

Since in aerobic respiration glucose consumption can be assumed to be stoichiometrically coupled with oxygen uptake, the online OTR signal might represent an alternative to determine protease yields. Thus, the relative protease activities were related to the total amount of consumed oxygen (Y_{P/O_2}) and finally compared to the batch experiment (Appendix 9). The values highlight a 1.5 to 2.0-fold increase of Y_{P/O_2} for fed-batch operation. The results based on glucose consumption are highly comparable with the results obtained from the determination of the consumed oxygen. Only the experiment with the switch from carbon to nitrogen limitation showed a deviation of 0.3. Once nitrogen is depleted, growth stops and *B. licheniformis* uses the available glucose for cell maintenance. Hence, the stoichiometric relations change resulting in an increased demand of oxygen per consumed amount of glucose (Philip et al., 2018). This example shows that changing cultivation conditions have to be considered when using the oxygen-based yield coefficient. However, in the experimental set-ups with defined and persistent substrate limiting conditions, both glucose- and oxygen-based yields similarly revealed enhanced protease yields for glucose- and NH_4^+-limited conditions when compared to batch (Appendix 9). Thus, it was shown that under these conditions, the stoichiometric relations remain rather constant, and, therefore, the direct proportionality between glucose and oxygen consumption is given. A study of Stöckmann et al. (2003) indicates that stoichiometric relations can further be used to simulate substrate consumption, biomass formation and pH shift on basis of the consumed oxygen.

2.3.7 Comparison of 250 and 500 mL membrane-based fed-batch shake flask cultivations

The principle of the 250 mL membrane-based fed-batch shake flask was extended to 500 mL shake flasks. This enables to perform fed-batch cultivations with an increased filling volume while avoiding undesired oxygen limitations (Meier et al., 2016; Zimmermann, Anderlei, Büchs, & Binder, 2006). Due to the greater filling volume, larger quantities of the produced proteases can be harvested from fed-batch shake flask cultivations. Increased amounts of

proteases, for example, facilitate compatibility analysis with laundry detergents. Based on experiments with the 250 mL membrane-based fed-batch shake flask system, carbon-limited fed batch cultivations were conducted with the newly designed 500 mL membrane-based fed-batch shake flask system (Chapter 2.2.5). The comparability of both systems is investigated by means of online (Figure 2.14) and offline data (Figure 2.15).

In Figure 2.14, the OTR course of carbon-limited fed-batch processes using 250 and 500 mL membrane-based fed-batch shake flasks is depicted. The OTR course of both systems represents the initial unlimited batch phase, followed by a distinct OTR drop at around 8.5 h (Figure 2.14). This drop marks the initiation of the glucose-limited fed-batch phase. A detailed explanation of the OTR course resulting from membrane-based fed-batch cultivations can be found in Chapter 2.3.3. The initial batch phase as well as fed-batch phase are comparable between the fed-batch cultivations using the 250 and 500 mL membrane-based fed-batch shake flasks. This is caused by the similar volumetric glucose release rate in both systems. The diffusion tip of the 500 mL membrane-based fed-batch shake flask has an active diffusion area 3-fold greater than the diffusion tip of the 250 mL membrane-based fed-batch shake flask. Since the glucose concentration within the feed reservoir is kept constant in both systems (200 g L^{-1}), the enlarged active diffusion area led to an increased glucose release rate from 5.9 mg h^{-1} with the 250 mL membrane-based fed-batch shake flask to 18.6 mg h^{-1} with the 500 mL membrane-based fed-batch shake flask. Thus, the approximately 3-fold increase of the glucose release rate is proportional to the enlargement of the active diffusion area. To maintain the 3-fold higher glucose release rate (Philip et al., 2017), the total amount of glucose, and thus, the reservoir filling volume (V_{Feed}) was also increased 3-fold. As the filling volume of the 500 mL flask (V_{Broth}) is also increased 3-fold, both systems end up with comparable volumetric glucose release rates.

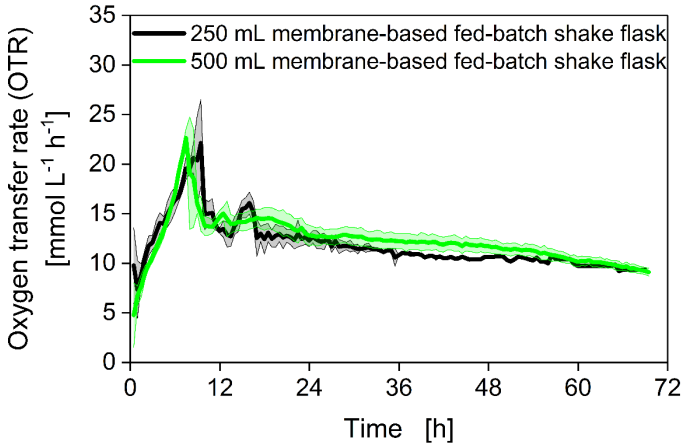

Figure 2.14: Comparison of carbon (C)-limited fed-batch cultivations of *Bacillus licheniformis* in the 250 and 500 mL membrane-based fed-batch shake flasks on basis of the OTR course according to Figure 2.2A. The course of the mean oxygen transfer rate (OTR) with standard deviation is shown over time. The OTR course of the 250 mL membrane-based fed-batch shake flask is already shown in Appendix 7A. In both systems, the initial glucose concentration in the feed reservoir was 200 g L^{-1}. Initial values for the 250 mL flask (culture broth): OD_{600} = 2.5, pH = 7.9, 0 g L^{-1} glucose, 2.9 g L^{-1} ammonium, 0.4 M MOPS buffer, V3 medium. Initial values (reservoir): V_{Feed} = 3 mL, active membrane diameter = 4.8 mm. Cultivation parameters: T = 30 °C, V_{Broth} = 10 mL, n = 350 rpm, d_0 = 50 mm. Initial values for the 500 mL flask (culture broth): OD_{600} = 2.5, pH = 7.7, 0 g L^{-1} glucose, 2.9 g L^{-1} ammonium, 0.2 M MOPS buffer, V3 medium. Initial values (reservoir): V_{Feed} = 9 mL, active membrane diameter = 8.3 mm. Cultivation parameters: T = 30 °C, V_{Broth} = 30 mL, n = 300 rpm, d_0 = 50 mm. Membrane: type = RCT-NatureFlex-NP, material = regenerated cellulose, thickness = 42 µm, cut-off = 10–20 kDa.

The volumetric glucose release rate is slightly enhanced for the 500 mL flask system (+ 5 %). Thus, the horizontal OTR plateau of the glucose-limited fed-batch phase is also slightly increased for the 500 mL flask system (Figure 2.14). The overall consumed oxygen, which is proportional to the amount of consumed glucose, is in accordance with an increase of 5 %. Since the reproducibility of fed-batch cultivations using 250 mL membrane-based fed-batch shake flasks is within this range (Appendix 7), this difference can be considered as average handling deviation.

Figure 2.15 shows fed-batch cultivations using 250 and 500 mL membrane-based fed-batch shake flasks under the same conditions as in Figure 2.14, however, with offline samples. The offline results of the 250 mL fed-batch shake flask were already presented and descibed in Chapter 2.3.3. The course of the relative protease activity, glucose concentration in culture broth and OD_{600} of the 500 mL membrane-based fed-batch shake flask cultivation are qualitatively as well as quantitatively comparable to the 250 mL membrane-based fed-batch shake flask cultivation (Figure 2.15A, C). Figure 2.15B and D hightlight that the glucose concentration in the feed reservoir is comparable as well. The same applies to the ammonium

concentration in the reservoir and culture broth (Figure 2.15B, D). As described above, the reservoir filling volume (V_{Feed}) as well as flask filling volume (V_{Broth}) were proportionally increased to the active diffusion area (summarized in Appendix 10). This results in similar concentration profiles with the 250 and 500 mL membrane-based fed-batch shake flasks.

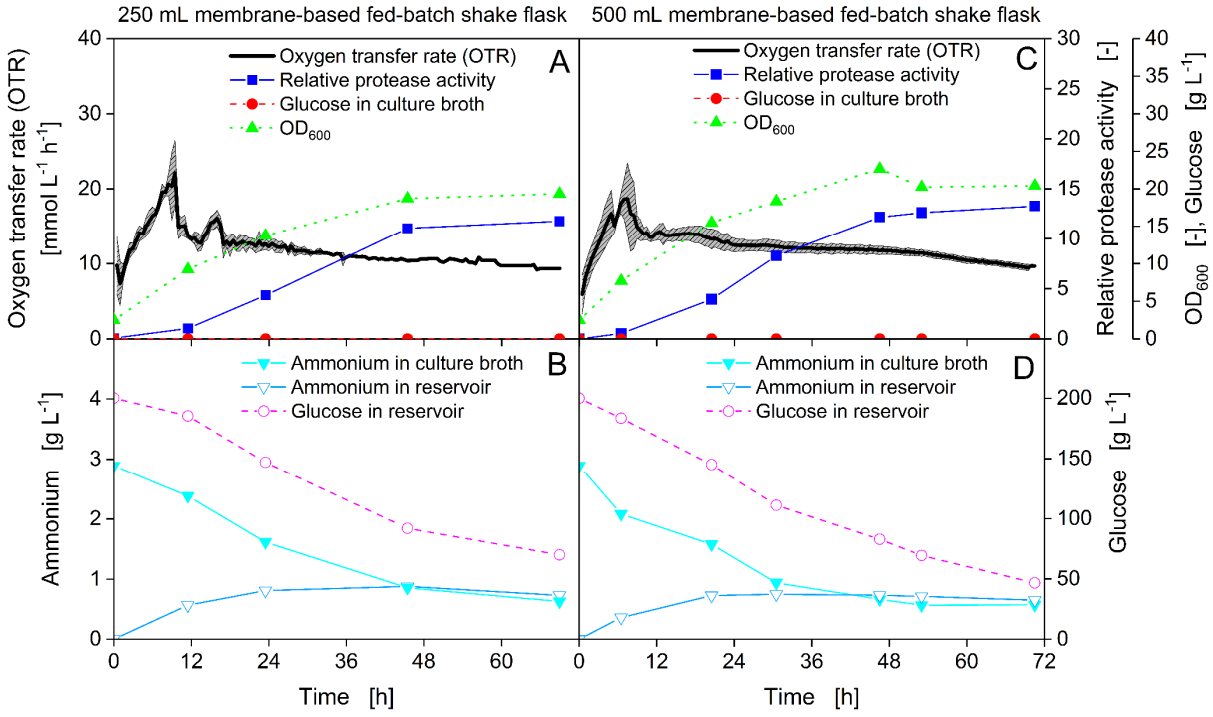

Figure 2.15: Comparison of carbon (C)-limited fed-batch cultivations of *Bacillus licheniformis* in 250 and 500 mL membrane-based fed-batch shake flasks on basis of online and offline data according to Figure 2.2A. (A, B) 250 mL membrane-based fed-batch shake flask cultivation already depicted in Figure 2.10A-C and Appendix 7A. (C, D) 500 mL membrane-based fed-batch shake flask cultivation. (A, C) Oxygen transfer rate (OTR), relative protease activity, glucose concentration and optical density (OD_{600}). Protease activities were set in relation to the measured protease activity directly after glucose depletion at 11.5 h within the batch experiment shown in Figure 2.9. (B, D) Ammonium concentration in culture broth and ammonium and glucose concentration within feed reservoir. Initial values for the 250 mL flask (culture broth): OD_{600} = 2.5, pH = 7.9, 0 g L^{-1} glucose, 2.9 g L^{-1} ammonium, 0.4 M MOPS buffer, V3 medium. Initial values (reservoir): V_{Feed} = 3 mL, active membrane diameter = 4.8 mm. Cultivation parameters: T = 30 °C, V_{Broth} = 10 mL, n = 350 rpm, d_0 = 50 mm. Initial values for the 500 mL flask (culture broth): $OD_{600} \approx 2.5$, pH = 7.7, 0 g L^{-1} glucose, 2.9 g L^{-1} ammonium, 0.2 M MOPS buffer, V3 medium. Initial values (reservoir): V_{Feed} = 9 mL, active membrane diameter = 8.3 mm. Cultivation parameters: T = 30 °C, V_{Broth} = 30 mL, n = 300 rpm, d_0 = 50 mm. Membrane used with 250 and 500 mL membrane-based fed-batch shake flask system: type = RCT-NatureFlex-NP, material = regenerated cellulose, thickness = 42 µm, cut-off = 10–20 kDa.

The results show that the principle of the 250 mL membrane-based fed-batch shake flask is scalable to 500 mL shake flasks. If the glucose concentration in the reservoir is kept constant and the flask and reservoir filling volumes are increased proportional to the active diffusion area, both systems have a similar volumetric glucose release rate. Thus, the online OTR signal

as well as offline data show highly comparable results. Consequently, established fed-batch cultivations in the 250 mL membrane-based fed-batch shake flasks can be easily scaled-up to the 500 mL system with increased culture volume. In the here presented case, the culture volume was increased 3-fold, resulting in a 3-fold higher amount of proteases.

2.4 Summary

In this chapter, the previously introduced 250 mL membrane-based fed-batch shake flask was standardized regarding its dimensions and optimized in design, handling and robustness. Consequently, *Bacillus licheniformis,* a well-known producer of proteases, was cultivated with carbon (glucose)- and nitrogen (ammonium)-limited fed-batch conditions. Catabolite repression of protease production by glucose and ammonium was succesfully avoided and yielded 1.5- and 2.1-fold increased protease activity relative to batch, respectively. An elevated feeding rate of glucose caused depletion of ammonium, which was detectable in the oxygen transfer rate (OTR) signal measured with the Respiration Activity MOnitoring System (RAMOS). Ammonium limitation was prevented and inhibition decreased by feeding ammonium simultaneously with glucose. The OTR signal clearly indicated the initiation of the fed-batch phase and gave direct feedback on the nutrient release kinetics. Increased feeding rates of glucose and ammonium led to an elevated protease activity without affecting the protease yield ($Y_{P/S_{Glu}}$). In addition to $Y_{P/S_{Glu}}$, protease yields were determined based on the metabolized amount of oxygen (Y_{P/O_2}). The results showed that the relative protease activity correlated with the amount of consumed glucose as well as with the amount of consumed oxygen.

The working principle of the 250 mL membrane-based fed-batch shake flasks was transferred to 500 mL Erlenmeyer shake flasks. By matching the volumetric glucose release rate, the 500 mL membrane-based fed-batch shake flask performed similar to the 250 mL membrane-based fed-batch shake flask. Having membrane-based fed-batch shake flask systems of a larger scale can be advantageous in applications where higher product amounts are needed, which otherwise would require time and cost intensive stirred tank reactor cultivations.

Parts of the following chapter have been submitted as Habicher, T., Rauls, E. K. A., Egidi, F., Keil, T., Klein, T., Daub, A., & Büchs, J. (2020). Establishing a fed-batch process for protease expression with *Bacillus licheniformis* in polymer-based controlled-release microtiter plates. *Biotechnology Journal*, *15*(2), 1900088. Edward K. A. Rauls and Franziska Egidi assisted with the cultivation experiments (3.2.1-3.2.4) (AVT-Biochemical Engineering, Prof. Dr.-Ing. Büchs, RWTH Aachen University).

Chapter 3

Polymer-based controlled-release fed-batch microtiter plate

3.1 Introduction

The high number of arising experiments during screening and early stages of development projects require microtiter plate-based cultivation systems to achieve the necessary throughput. Microtiter plates (MTPs) are increasingly used as cultivation systems (Klöckner & Büchs, 2012), however, development of simple and functional fed-batch microtiter plates with a continuous feed stream design remained challenging (Chapter 1.2). Enzyme-based glucose release systems are capable of continuously releasing glucose, are independent of peripheral equipment, are cost-efficient and can be integrated into existing laboratory equipment. However, in combination with *Bacillus licheniformis*, which is a well known producer of amylases and proteases (Gupta et al., 2002; Gupta, Gigras, Mohapatra, Goswami, & Chauhan, 2003), glucose release kinetics are hardly controllable. In polymer-based systems, amylases and proteases do not impair glucose release, thus representing an alternative to the enzyme-based system. For shake flask applications, polymer-based glucose release disks (FeedBeads) were already described by Jeude et al. (2006). On basis of this principle, a commercially available polymer-based controlled-release fed-batch microtiter plate was developed (Feed Plate®, Kuhner Shaker GmbH, Herzogenrath, Germany). The polymer-based glucose release system is not restricted to a single microtiter plate design. Different Feed Plate® formats, ranging from

24, 48 and 96 round- and square-wells, with different release characteristics are nowadays available.

In Figure 3.1A, a 48-well round- deep-well polymer-based controlled-release fed-batch microtiter plate is depicted. The silicone matrix with embedded glucose crystals is immobilized at the bottom of each well (Figure 3.1B). Once the well is filled with culture medium, glucose is released following a sequential process (Keil et al., 2019) (Figure 3.1C). First, water diffuses into the silicone matrix. The water dissolves the embedded glucose crystals, thereby creating cavities of highly concentrated glucose solution. Second, due to osmotic pressure, more water diffuses into the cavity. The water inflow causes swelling of the silicone matrix. Third, as soon as the swelling exceeds the elastic elongation of the silicone matrix, little cracks are established. Through these micro-channels, glucose is continuously released into the culture medium.

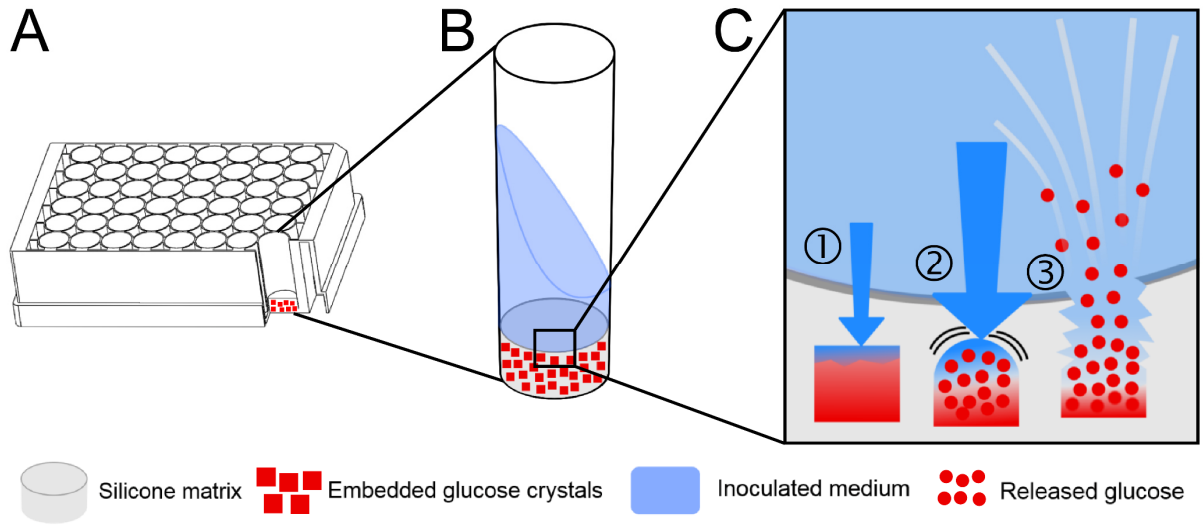

Figure 3.1: Principle of the polymer-based controlled-release fed-batch microtiter plate (Feed Plate®). (A) 48-well round- deep-well polymer-based controlled-release fed-batch microtiter plate with cross section view into a single well. (B) Close-up illustration of a single well showing the silicone matrix with embedded glucose crystals on its bottom. (C) Working principle of the polymer-based release system adapted from Keil et al. (2019). ① Water diffuses into the silicone matrix and starts dissolving glucose crystals, thereby creating a highly concentrated glucose solution. ② Due to the osmotic pressure, more water diffuses into the cavity. ③ At some point, little cracks and channels are established in the silicone matrix, which is followed by the release of the glucose solution into the culture medium.

Recently, Keil et al. (2019) provided a detailed characterization of glucose release kinetics with varying media conditions and temperatures. When compared to the enzymatic release system, the polymer-based release system showed to be less sensitive against moderate changes of pH and temperature (Keil et al., 2019; Toeroek et al., 2015). Besides its stable glucose release

characteristics, the polymer-based controlled-release fed-batch microtiter plate is ready-to-use, disposable and integrable into existing laboratory infrastructure, like microtiter plate- and liquid handling systems (Keil et al., 2019). Glucose release is diffusion driven, and thus, independent from peripheral equipment, such as micro pumps or microinjection valves. This enables saving expenses for additional laboratory equipment while maintaining a high degree of parallelization.

On basis of the descibed characteristics, the polymer-based controlled-release fed-batch microtiter plate represents a promising tool for high-throughput applications, such as optimal strain screening, for medium screening and for applications in early stages of development projects. Its use with *Bacillus* strains has not been reported yet. Consequently, the applicability of the polymer-based controlled-release microtiter plate to establish a fed-batch process with the above applied protease producing *Bacillus licheniformis* strain (Chapter 2) was investigated and is described in this chapter. Online monitoring of the oxygen transfer rate (OTR) within each individual well was realized with a µRAMOS device (Flitsch et al., 2016). The reproducibility of fed-batch cultivations was examined using five individual polymer-based controlled-release fed-batch microtiter plates from two different production lots. To investigate the effect of different initial cultivation conditions, the biomass concentration, the filling volume and the osmotic pressure were varied. Cultivations within the polymer-based controlled-release fed-batch microtiter plate were then transferred to the 250 mL membrane-based fed-batch shake flask with the volumetric release rate as scale-up criterion. Finally, the acquired fed-batch online data were used to establish and validate a mechanistic model.

3.2 Material and Methods

3.2.1 Strain and media

The protease producing *Bacillus licheniformis* strain contains a plasmid for the expression of a subtilisin-like protease and a tetracycline resistance marker for selection and was kindly provided by BASF SE (Ludwigshafen am Rhein, Germany). Further information on the protease producing *Bacillus licheniformis* strain can be provided by BASF SE (Ludwigshafen

am Rhein, Germany) upon request. The chemicals applied for media preparation were of analytical grade and purchased from Carl Roth GmbH & Co. KG (Karlsruhe, Germany), Sigma-Aldrich Chemie GmbH (Steinheim, Germany), Merck (Darmstadt, Germany), VWR (Darmstadt, Germany) and from AppliChem (Darmstadt, Germany). The composition of the complex Terrific Broth (TB) medium and the V3 mineral medium can be taken from Chapter 2.2.1. The V3 mineral medium was previously described in publications from Meissner et al. (2015) and Wilming et al. (2013).

3.2.2 Cultivation conditions

Precultures were performed in 250 mL shake flasks and carried out on an orbital climo-shaker ISFX-1 from Adolf Kühner AG (Biersfelden, Switzerland) with a filling volume V_{Broth} = 10 mL, a shaking frequency n = 350 rpm, a shaking diameter d_0 = 50 mm and a temperature T = 30 °C. For online monitoring, the in-house build RAMOS device was used. A commercial version is available from Adolf Kühner AG (Biersfelden, Switzerland) or HiTec Zang GmbH (Herzogenrath, Germany). Precultures were divided in two steps, whereby the 1st preculture was carried out in complex TB medium and the 2nd in V3 mineral medium. A detailed description of the RAMOS-based two-step preculture procedure can be found in Chapter 2.3.1.

Membrane-based fed-batch main cultures were performed in 250 mL shake flasks with a filling volume V_{Broth} = 16 mL. Shaking conditions and online monitoring was similar to the above described preculture procedure. For fed-batch main cultivations, no initial glucose was supplemented to the V3 mineral medium. A detailed description of the preparation of the membrane-based fed-batch shake flasks can be found in Chapter 2.2.4.

Microtiter plate-based fed-batch main cultivations were conducted using 48-well round-deep-well microtiter plates with a glucose-containing polymer on the bottom of each well (Art. Nr.: SMFP08004, Kuhner Shaker GmbH, Herzogenrath, Germany) (Figure 3.1), a filling volume V_{Broth} = 0.5, 0.8 or 1.0 mL, a shaking frequency n = 1000 rpm, a shaking diameter d_0 = 3 mm and a temperature T = 30 °C. For online monitoring of each individual well,

a µRAMOS device was used (Flitsch et al., 2016). The microtiter plate was covered with a sterile barrier (900371-T, HJ-Bioanalytik GmbH, Erkelenz, Germany) to avoid contamination.

3.2.3 Determination of glucose release

Glucose release of polymer-based controlled-release fed-batch microtiter plates was measured with a filling volume of 1.0 mL, a shaking frequency n = 1000 rpm, a shaking diameter d_0 = 3 mm and a temperature T = 30 °C. The plate was covered with a Rotilabo® sealing foil (Art. Nr.: X172.1, Carl Roth GmbH & Co. KG, Karlsruhe, Germany) to eliminate evaporation. It was assumed that glucose distributes equally within the culture volume. Therefore, concentrating effects caused by swelling of the polymer matrix were not taken into consideration. For each data point, three individual wells (n = 3) were harvested and sterile filtered (0.2 µm filter). The glucose concentration was analyzed by high performance liquid chromatography (HPLC). The HPLC device (Ultimate 3000, Dionex, Sunnyvale, USA) was equipped with a protection cartridge (4 × 3 mm) (Art. Nr.: AJ0-4490, Securityguard™ Standard) and an ion-exclusion column (300 × 7.8 mm) (Art. Nr.: 00H-0138-K0, Rezex™), both from Phenomenex® (Aschaffenburg, Germany). Elution was carried out with 50 mM H_2SO_4 with a flow rate of 0.8 mL min^{-1} at a constant temperature of 70 °C. Glucose was detected by measuring the refractometric index with a Shodex RI-101 refractometer (Showa Denko Europe, Munich, Germany). Data analysis was done with the software Chromeleon 6.8 (Dionex, Sunnyvale, USA).

3.2.4 Offline sample analysis

Offline samples were analyzed regarding the optical density at 600 nm (OD_{600}), the pH-value and the protease activity. A detailed description of the applied procedures can be found in Chapter 2.2.7. The protease activity measurement is based on the method developed by DelMar et al. (1979) and on the experimental procedure described by Meissner et al. (2015). The protease activity was measured from samples taken at the end of the cultivation and was normalized to the measured protease activity directly after glucose depletion at 11.5 h of the reference batch experiment (Figure 2.9). The normalized protease activity is referred to as relative protease activity.

It is assumed that cells and proteases are not able to penetrate into the polymer matrix. Hence, in addition to evaporation, swelling has a concentrating effect on cells and proteases. In Figure 3.2, the experimental procedure to determine swelling and evaporation is presented. Two individual polymer-based fed-batch microtiter plates were used to determine evaporation (0.038 g per well) and swelling (0.089 g per well) under cultivation conditions after 70 h. The mass balancing procedure was performed with a precision balance (EWJ 3000-2, Kern und Sohn GmbH, Balingen, Germany). The measured mass difference was converted to volume with an assumed density of 1 g cm^{-3}. Evaporation was assumed to be constant for experiments with different filling volumes in microtiter plates. On basis of the determined values for evaporation and swelling, the measured protease activity and OD_{600} were corrected to the initial filling volume (Figure 3.2).

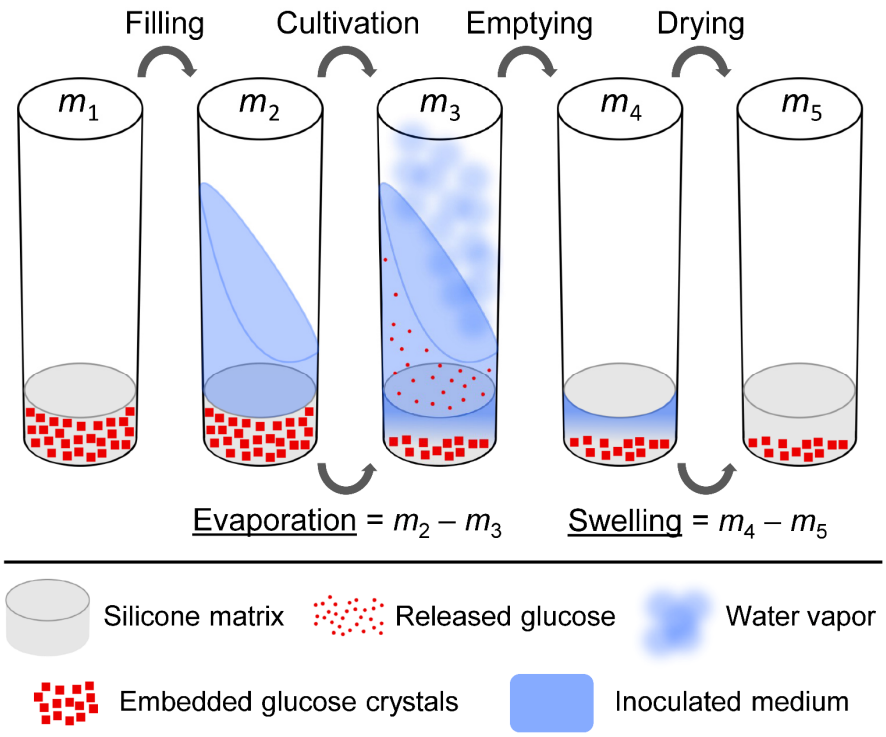

Figure 3.2: Procedure for the determination of evaporation and swelling of the polymer matrix at the bottom of each well in the polymer-based controlled-release fed-batch microtiter plate. The single wells represent the whole polymer-based controlled-release fed-batch microtiter plate (48-well round- deep-well). Weight measurements were carried out before (m_1), and after filling of the plate with inoculated medium (m_2), after the cultivation (m_3), after emptying the wells with the help of cotton buds (m_4) and after drying at 80 °C for 24 h (m_5). The mass difference between m_2 and m_3 corresponds to evaporation. The amount of water penetrating into the silicone matrix is named swelling and was quantified by the difference between m_4 and m_5.

In membrane-based fed-batch shake flasks, the volume loss was caused by evaporation and back diffusion of water into the reservoir. As with polymer-based controlled-release fed-batch microtiter plates, protease activity and OD_{600} were corrected to the initial filling volume. The applied procedure can be taken from Chapter 2.2.7.

Sterile filtered samples (0.2 µm filter) were used to measure the osmolality with the Osmomat 030 (Gonotec GmbH, Berlin, Germany). The device was calibrated with calibration standards of 0.85 or 2.00 osmol kg^{-1} (Gonotec GmbH, Berlin, Germany).

3.2.5 Fed-batch model

For the fed-batch model in microtiter plates Monod kinetics were used. The equation for biomass concentration X is

$$\frac{\mathbf{d}\boldsymbol{X}}{\mathbf{d}\boldsymbol{t}} = \boldsymbol{\mu} \cdot \boldsymbol{X} \qquad [\mathbf{g} \cdot \mathbf{L^{-1}} \cdot \mathbf{h^{-1}}] \qquad (3\text{-}1)$$

were μ is the specific growth rate. μ is calculated on basis of the Monod equation

$$\boldsymbol{\mu} = \boldsymbol{\mu_{max}} \cdot \frac{\boldsymbol{S_{Glu}}}{\boldsymbol{S_{Glu}} + \boldsymbol{K_{S_{Glu}}}} \qquad [\mathbf{h^{-1}}] \qquad (3\text{-}2)$$

were $K_{S_{Glu}}$ is the Monod constant, μ_{max} the maximum specific growth rate and S_{Glu} the glucose concentration. In case of possible oxygen limited conditions, the Monod equation can be extended with an additional Monod term $O_2/(O_2 + K_{O2})$ to introduce the oxygen concentration O_2 as additional growth limiting substrate. The accumulated volumetric glucose release $F_{S_{Glu}}$ is described with the empirical equation

$$\boldsymbol{F_{S_{Glu}}} = \frac{(\boldsymbol{A} \cdot \mathbf{e}^{\boldsymbol{B \cdot t}} + \boldsymbol{C} \cdot \mathbf{e}^{\boldsymbol{D \cdot t}})}{\boldsymbol{V_{Broth}}} \qquad [\mathbf{g} \cdot \mathbf{L^{-1}}] \qquad (3\text{-}3)$$

were A, B, C and D are fitting parameters and V_{Broth} the volume of the culture broth. Glucose concentration is described with

$$\frac{\mathbf{d}S_{\mathbf{Glu}}}{\mathbf{d}t} = -\frac{1}{Y_{X/S\mathbf{Glu}}} \cdot \mu \cdot X - m_{S\mathbf{Glu}} \cdot X + F'_{S\mathbf{Glu}} \qquad [\mathbf{g \cdot L^{-1} \cdot h^{-1}}] \qquad (3\text{-}4)$$

were $Y_{X/S\mathrm{Glu}}$ is the biomass yield per consumed glucose and $m_{S\mathrm{Glu}}$ the maintenance coefficient related to glucose. $F'_{S\mathrm{Glu}}$ is the volumetric glucose release rate that is obtained by differentiating $F_{S\mathrm{Glu}}$ with respect to time t. The oxygen concentration within the liquid is calculated with

$$\frac{\mathbf{d}O_2}{\mathbf{d}t} = -\frac{1}{Y_{X/O2}} \cdot \mu \cdot X - m_{O2} \cdot X + OTR \qquad [\mathbf{mol \cdot L^{-1} \cdot h^{-1}}] \qquad (3\text{-}5)$$

were Y_{X/O_2} is the biomass yield per consumed oxygen, m_{O_2} the maintenance coefficient related to oxygen and OTR the oxygen transfer rate that is calculated with

$$OTR = k_L a \cdot (O_{2,\max} - O_2) \qquad [\mathbf{mol \cdot L^{-1} \cdot h^{-1}}] \qquad (3\text{-}6)$$

were $k_L a$ is the volumetric mass-transfer coefficient and $O_{2,\max}$ the maximum dissolved oxygen concentration defined as

$$O_{2,\max} = L_{O2} \cdot p_{amb} \cdot y_{O2} \qquad [\mathbf{mol \cdot L^{-1}}] \qquad (3\text{-}7)$$

with L_{O_2} as the oxygen solubility within the culture broth, p_{amb} the ambient pressure and y_{O_2} the mole fraction of oxygen within air. $O_{2,\max}$ was assumed to be a constant parameter.

3.2.6 Model simulation and fitting

The system of ordinary differential equations (ODE's) for biomass X, glucose S_{Glu} and oxygen O_2 was solved in MATLAB R2018a using the *ODE23tb* solver. The initial conditions for biomass concentration X_0 were deduced from the OD_{600} values on basis of an experimentally determined conversion factor with $X\ [\mathrm{g\ L^{-1}}] = 0.74 \cdot \mathrm{OD}_{600}$. The initial glucose concentration $S_{\mathrm{Glu},0}$ of 0.33 mg corresponded to the fitted volumetric glucose release $F_{S\mathrm{Glu}}$ at time $t = 0$. The start value for the oxygen concentration $O_{2,0}$ was the maximum dissolved oxygen concentration $O_{2,\max}$ (0.0002095 mol $\mathrm{L^{-1}}$). Values and units of the constant parameters are listed in

Appendix 11. The unknown parameters $m_{S_{Glu}}$ and m_{O_2} were fitted on basis of experiments with different initial biomass concentrations. The sum of least squares between the experimental and simulated data was globally minimized with the MATLAB minimization solver *fmincon* in combination with the global search function *gs*. Lower and upper bounds for $m_{S_{Glu}}$ and m_{O_2} were defined on basis of values from literature (Frankena et al., 1986; Sauer et al., 1996; Tännler et al., 2008). Model validation was done with experiments with different initial biomass concentrations and filling volumes.

3.3 Results and Discussion

3.3.1 Reproducibility of microtiter plate-based fed-batch cultivations

Screening processes in microtiter plates are usually performed without online monitoring. Therefore, clone rankings most often are based on final product concentrations or enzyme activities instead of yields, as for example $Y_{P/S_{Glu}}$. A solution for this problem is to define a constant volumetric glucose release rate and, if identical conditions are applied, to assume that the amount of released glucose after a certain time point remains constant in all wells. In doing so, it is of importance to investigate the plate-to-plate reproducibility of cultivations using the polymer-based release system.

Figure 3.3 shows the OTR curve of fed-batch cultivations with an initial OD_{600} of 0.5 and a filling volume of 0.5 mL. The OTR course is characterized by an initial batch phase, followed by an OTR drop, which marks the initiation of the glucose-limited fed-batch phase. In Figure 3.3A, the mean OTR of 32 parallel cultivations [n =32] in a single polymer-based controlled-release fed-batch microtiter plate is depicted. The OTR-based well-to well mean coefficient of variation (mean CV) is 8.8 %. In order to investigate the plate-to-plate reproducibility, five different MTP's from two production lots (Lot 1 and Lot 2) were used (Figure 3.3B). Due to the amount of investigated plates, the number of parallel cultivations on each plate was reduced. On basis of the mean OTR of all MTP's (Figure 3.3B, solid black line), the mean CV resulted in a value of 9.2 %. Toeroek et al. (2015) also achieved a mean plate-to-plate CV of less than 10 % using an enzymatic glucose release system with online

biomass concentration monitoring. However, different production lots were not considered in that study.

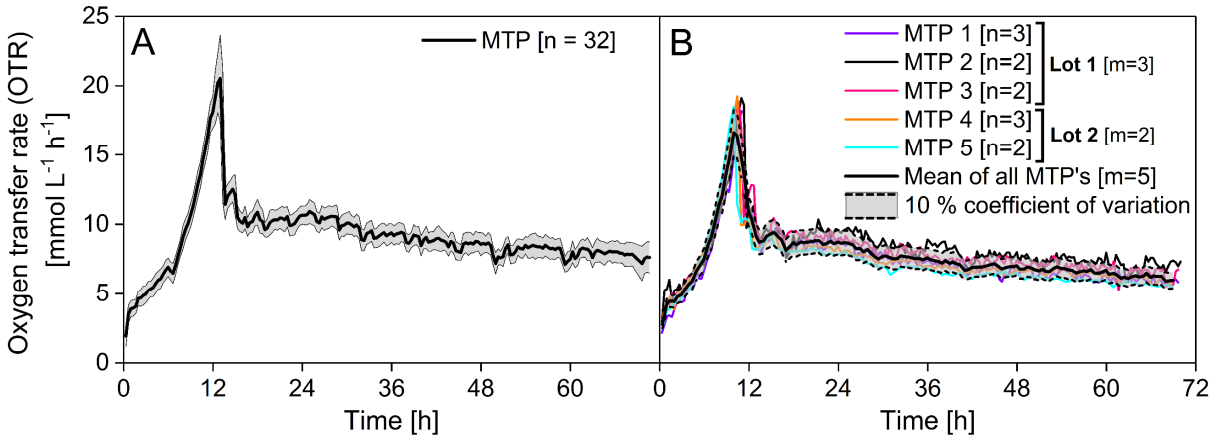

Figure 3.3: Reproducibility of individual fed-batch cultivations using polymer-based controlled-release fed-batch microtiter plates. (A) Reproducibility of fed-batch cultivations using a single polymer-based controlled-release fed-batch microtiter plate (MTP). The mean oxygen transfer rate (OTR) of 32 parallel cultivations is depicted as black line (n = number of included wells). The shadow symbolizes the standard deviation. (B) Reproducibility of fed-batch cultivations using polymer-based controlled-release fed-batch microtiter plates from two different production lots (Lot numbers). The mean oxygen transfer rates (OTR) of three plates from Lot 1 (MTP 1, MTP 2 and MTP 3; m = 3) and two plates from Lot 2 (MTP 4 and MTP 5; m = 2) are shown (m = number of included plates). Experiments on each plate were conducted in triplicates and inoculated starting with an individual glycerol stock followed by a two-step preculture procedure. Wells that could not be sealed tightly by the measurement device or had a noisy p_{O2} signal were excluded. The black line represents the mean oxygen transfer rate (OTR) of all five MTP's from the two production lots. The shadow symbolizes a defined coefficient of variation (CV) of 10 %. Cultivation conditions: polymer-based controlled-release fed-batch microtiter plate (48-well round- and deep-well), OD_{600} = 0.5, V_L = 0.5 mL, n = 1000 rpm, d_0 = 3 mm, T = 30 °C.

When determining the reproducibility on basis of cultivation experiments, it should be considered that the biological system and the online monitoring system add separate individual error. This error should not be attributed to the release system. Thus, glucose release experiments without cells resulted in a mean CV of only 4.5 % using the polymer-based controlled-release system (Keil et al., 2019).

3.3.2 Influence of the initial biomass concentration on microtiter plate-based fed-batch cultivations

The effect of the initial biomass concentrations on the final protease activities in *B. licheniformis* fed-batch cultivations was investigated. In Figure 3.4, the OTR course of cultivations with an initial OD_{600} of 0.1, 0.5, 1.0, 1.5 and 2.5 is depicted. Independent of the

initial biomass concentration, the OTR increases exponentially at the beginning of the cultivation (Figure 3.4A). In this phase, glucose accumulates and is available in excess (batch phase). This is due to the generally low initial biomass concentration, which causes a low glucose consumption rate. By increasing the initial biomass concentration, the consumption rate increases as well, and thus, less glucose accumulates within the batch phase. Consequently, the length of the batch phase is shortened and the maximum OTR value is decreased (Figure 3.4A). Additional factors that influence glucose accumulation, which however were not relevant within this experiment, are the specific growth rate and potential lag phases (Huber, Scheidle, et al., 2009). Once the accumulated glucose is reduced to limiting levels, the OTR drops sharply, which marks the initiation of the glucose-limited fed-batch phase. Since the filling volume was kept constant within each well, the volumetric release rate was equal for all cultivations, which was reflected by a highly comparable OTR plateau of about 7.5 mmol L^{-1} h^{-1} within the fed-batch phase (Figure 3.4A). The slightly declining trend of the OTR plateau can be attributed to the glucose release that diminishes over time (Figure 3.8A). The secondary OTR peaks within the fed-batch plateau, for example visible at 4 and 9 h within the experiment with an OD_{600} of 2.5, indicate the parallel consumption of the overflow metabolites acetate and 2,3-butanediol (Chapter 2.3.3). As overflow metabolites mainly derive from the preculture, the peaks become less pronounced with decreasing inoculation volume. Despite a low inoculation volume for the experiment with an initial OD_{600} of 0.1, a pronounced shoulder within the fed-batch OTR plateau is visible. Because of the low initial biomass, glucose accumulation was intensified and most probably caused additional formation of overflow metabolites that are consumed once entering glucose-limited conditions.

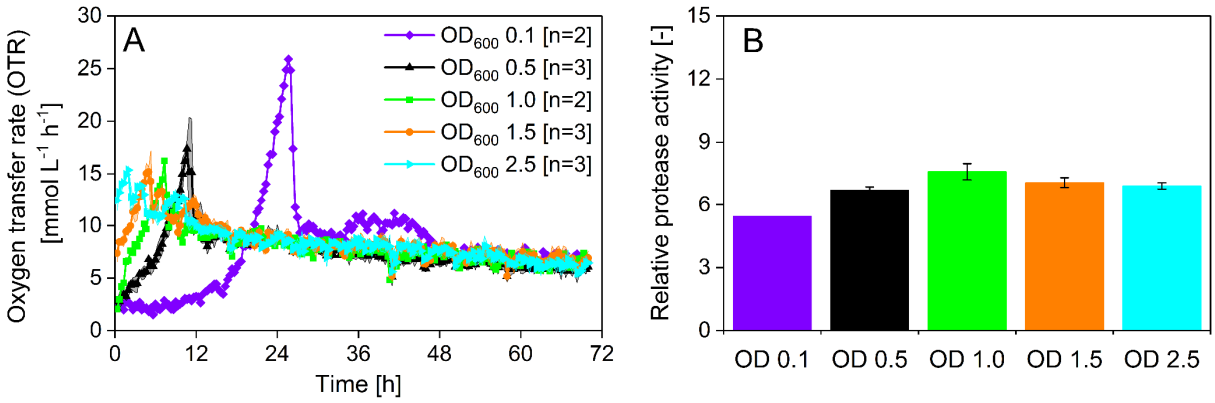

Figure 3.4: Influence of the initial biomass concentration (OD_{600}) on fed-batch cultivations of *Bacillus licheniformis* using the polymer-based controlled-release fed-batch microtiter plate. (A) Mean oxygen transfer rate (OTR) over time. Each experiment was conducted in triplicates (despite OD_{600} 0.1, n = 2), however

wells that could not be sealed tightly by the measurement device or had a noisy p_{O_2} signal were excluded. Shadows symbolize the standard deviation (for n > 2). (B) Mean relative protease activity at the end of the cultivation. Error bars symbolize the standard deviation [n = 3]. Protease activities were set in relation to the measured protease activity directly after glucose depletion at 11.5 h within the batch experiment, shown in Figure 2.9. Cultivation conditions: polymer-based controlled-release fed-batch microtiter plate (48-well round- deep-well), V_{Broth} = 0.5 mL, n = 1000 rpm, d_0 = 3 mm, T = 30 °C.

The experiments with an initial OD_{600} of 0.5, 1.0, 1.5, and 2.5 show no major difference of the final relative protease activity (Figure 3.4B). However, the experiment with the lowest initial biomass (OD_{600} of 0.1) has a slightly decreased relative protease activity. One possible reason for this is the enhanced glucose accumulation within the batch phase, which possibly enhances overflow metabolite formation and culture acidification. Additionally, the prolongation of the batch phase cuts the time in which *B. licheniformis* is exposed to glucose-limited fed-batch conditions. It was found that under batch conditions protease biosynthesis is repressed, whereas under glucose-limited fed-batch conditions protease activities increase (Chapter 2.3.6). Thus, it is hypothesized that too low initial biomass concentration have a negative effect on the final relative protease activities.

3.3.3 Influence of the initial filling volume on microtiter plate-based fed-batch cultivations

The total glucose release rate within the polymer-based controlled-release fed-batch microtiter plate is defined by the composition of the silicone matrix and the amount of the embedded glucose crystals. The user cannot change these characteristics, although the filling volume can be varied in order to change the volumetric release rate. The experiment in Figure 3.5 shows the results of different filling volumes when using the polymer-based controlled-release fed-batch microtiter plate.

The initial increase of the OTR within the batch phase is highly comparable for the experiment with 0.5, 0.8 and 1.0 mL filling volume (Figure 3.5A). This is due to identical cultivation conditions with equal initial biomass concentrations. However, the maximum OTR, the length of the batch phase and the level of the OTR plateau within the fed-batch phase directly correlate with the filling volume. While the batch phase is shortened with increasing filling volume, the maximum OTR as well as the level of the OTR plateau within the fed-batch phase are reduced.

The filling volume that influences the volumetric glucose release rate (Equation (3-3)) solely causes these differences.

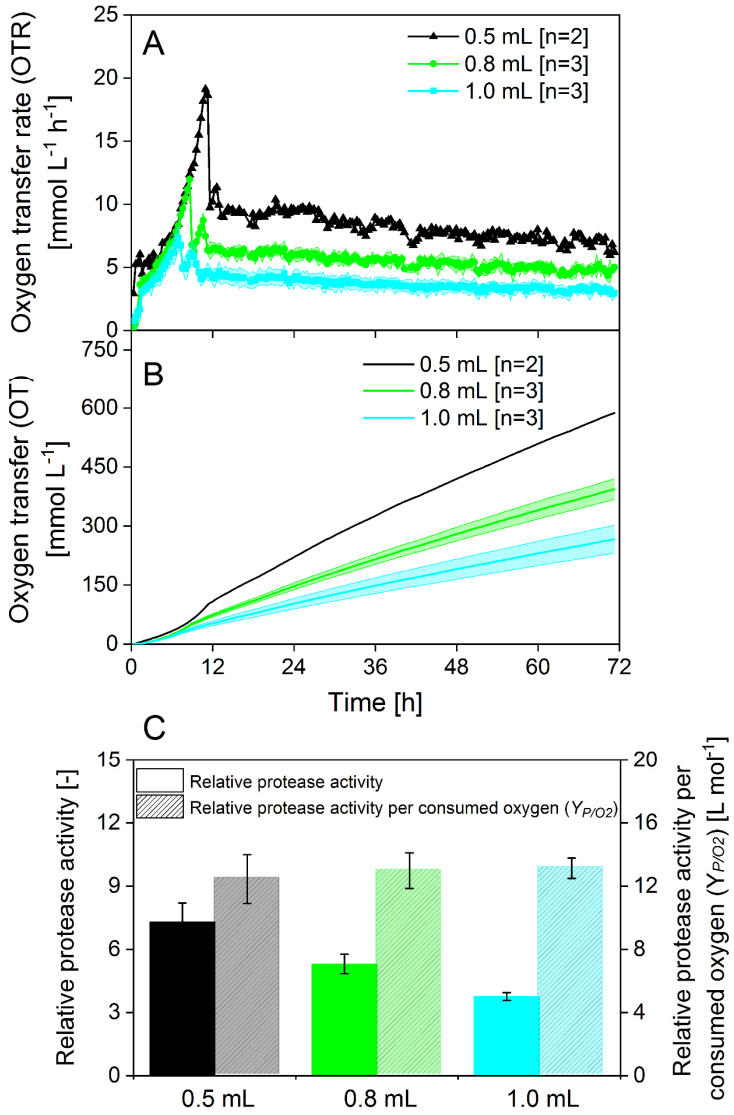

Figure 3.5: Influence of the initial filling volume (V_{Broth}) on fed-batch cultivations of *Bacillus licheniformis* using the polymer-based controlled-release fed-batch microtiter plate. (A) Mean oxygen transfer rate (OTR) over time. Each experiment was conducted in triplicates, however wells that could not be sealed tightly by the measurement device or had a noisy p_{O_2} signal were excluded. Shadows symbolize the standard deviation (for n > 2). (B) Mean accumulated oxygen tranfer (OT) over time. The OT is equivalent to the consumed oxygen. Shadows symbolize the standard deviation (for n > 2). (C) Mean relative protease activity (filled bars) and relative protease activity per consumed oxygen (Y_{P/O_2}) (dashed bars) at the end of the cultivation. Error bars symbolize the standard deviation [n = 3]. Protease activities were set in relation to the measured protease activity directly after glucose depletion at 11.5 h within the batch experiment, shown in Figure 2.9. Cultivation conditions: polymer-based controlled-release fed-batch microtiter plate (48-well round- deep-well), OD_{600} = 0.5, V_{Broth} = 0.5 mL, n = 1000 rpm, d_0 = 3 mm, T = 30 °C.

Final relative protease activities with different volumetric release rates are shown in Figure 3.5C (filled bars). The relative protease activities are inversely proportional to the filling volume. However, to investigate the physiological and regulatory effect of different volumetric release rates on protease biosynthesis with *B. licheniformis*, instead of the relative protease activity, protease yields have to be compared. It was demonstrated that protease yields related to consumed oxygen (Y_{P/O_2}) are a suitable alternative to the glucose-based yields ($Y_{P/S_{Glu}}$) (Chapter 2.3.6). Consequently, the accumulated oxygen transfer (OT), which is equivalent to the total consumed oxygen (Figure 3.5B), was used to calculate Y_{P/O_2}. The results highlight that the different volumetric release rates have no effect on Y_{P/O_2} and $Y_{P/S_{Glu}}$ (Figure 3.5C, dashed bars, Appendix 12). This observation is in good agreement with the results described in Chapter 2.3.6 and underlines that the investigated volumetric release rates do not influence protease yield for this *B. licheniformis* strain. In addition, the comparability between Y_{P/O_2} and $Y_{P/S_{Glu}}$ was confirmed. In contrast to the yields, however, increasing volumetric glucose release rates enhance the relative protease productivity (Appendix 13).

In additional experiments with an initial OD_{600} of 1.5, the batch phase was artificially prolonged by supplementing 2.5 and 5 g L^{-1} glucose to the culture medium, while the filling volume of 0.5 mL and consequently the volumetric release rate was kept constant (Appendix 14A). The relative protease activity is slightly enhanced with glucose supplementation when compared to the experiment without initial glucose (0 g L^{-1}) (Appendix 14B). Since the supplemented glucose is mainly used for growth, the fed-batch phase is initiated with different biomass concentrations, which could explain the higher final protease activity. Nevertheless, the protease activity per consumed oxygen (Y_{P/O_2}) and per consumed glucose ($Y_{P/S_{Glu}}$) remains rather constant (Appendix 12).

3.3.4 Influence of the medium osmolality on microtiter plate-based fed-batch cultivations

To highlight the effect of increased osmolality, the V3 mineral medium was supplemented with a concentrated sodium chloride solution. In Figure 3.6, the influence of media formulations with osmolalities of 0.63 (no sodium chloride added), 1.09 and 1.72 osmol kg^{-1} are shown. Within the batch phase, the increase of the OTR is reduced for experiments with increased

osmolality (Figure 3.6A). However, the initial biomass concentration was kept constant, and thus, the osmotic pressure attenuates growth. Under osmotic stress, *B. licheniformis* activates mechanisms to accumulate compatible intracellular osmolytes (Paul et al., 2015; Schroeter et al., 2013). Although this mechanism enables *B. licheniformis* strains to withstand high salt concentrations, growth yields diminish (Schroeter et al., 2013). It was further found that the osmoadaptation goes along with an increased cellular demand for energy (Paul et al., 2015). Thus, it is most likely that the higher energy demand slows down growth.

Within the fed-batch phase, the OTR level is inversely proportional to the medium osmolality (Figure 3.6A). As the filling volume was kept constant, the decreased OTR level within the fed-batch phase indicates that the osmotic pressure causes a reduction of glucose release (Keil et al., 2019). In order to confirm this, final glucose concentrations were measured in wells with identical medium formulation but without biomass. The glucose concentration was 26, 17 and 8 g L^{-1} within wells with 0.63, 1.09 and 1.72 osmol kg^{-1}, respectively (Appendix 12). The proportion between the final glucose concentrations correlated with the proportion between the final OT's (Figure 3.6B, Appendix 12). Consequently, glucose release was affected by physically altered release characteristics within the polymer matrix. These results are confirmed by experiments with altered MOPS buffer concentrations (Appendix 15A). When comparing cultivations with similar osmolality using MOPS buffer and sodium chloride (1.08 ± 0.01 osmol kg^{-1}), the level of the OTR plateau within the fed-batch phase is highly comparable (Appendix 15B). Thus, the osmotic pressure affects glucose release (Keil et al., 2019).

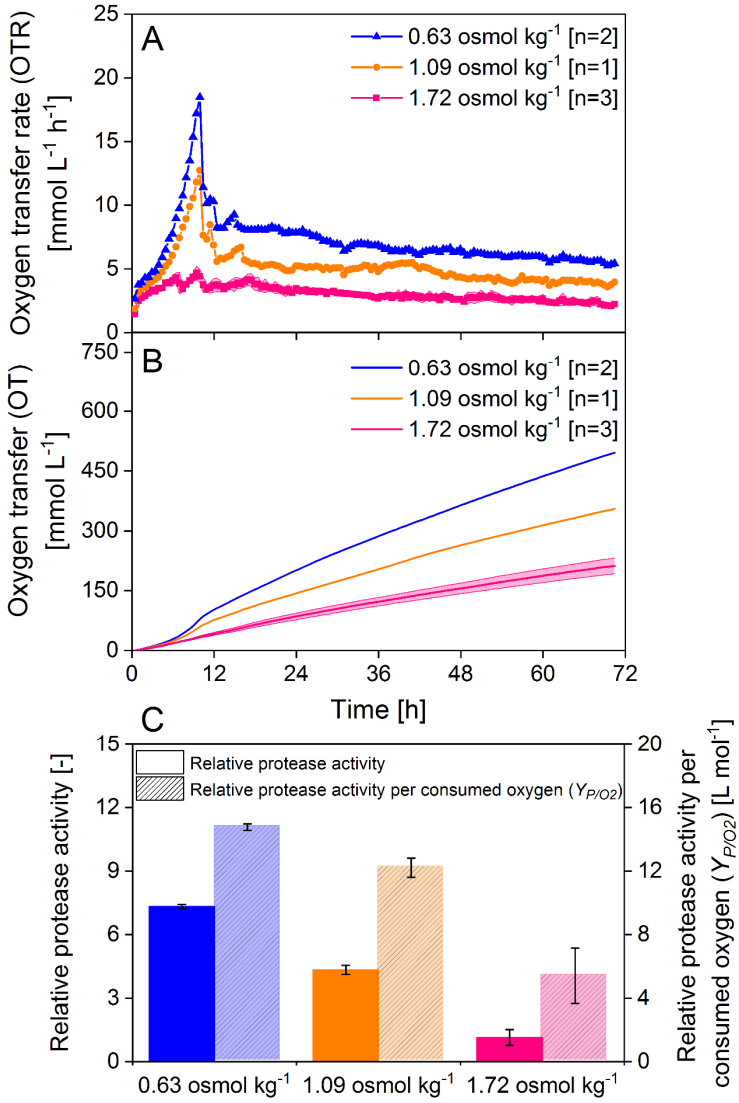

Figure 3.6: Influence of the medium osmolality on fed-batch cultivations of *Bacillus licheniformis* using the polymer-based controlled-release fed-batch microtiter plate. A concentrated sodium chloride (NaCl) solution was utilized to increase the osmolality of the culture medium. The osmolality of the standard medium formulation (without the addition of sodium chloride) is 0.63 osmol kg^{-1}. (A) Mean oxygen transfer rate (OTR) over time. Each experiment was conducted in triplicates, however wells that could not be sealed tightly by the measurement device or had a noisy p_{O2} signal were excluded. Shadows symbolize the standard deviation (for n > 2). (B) Mean accumulated oxygen transfer (OT) over time. The OT is equivalent to the consumed oxygen. Shadows symbolize the standard deviation (for n > 2). (C) Mean relative protease activity (filled bars) and relative protease activity per consumed oxygen ($Y_{P/O2}$) (dashed bars) at the end of the cultivation. Error bars symbolize the standard deviation [n = 3]. Protease activities were set in relation to the measured protease activity directly after glucose depletion at 11.5 h within the batch experiment, shown in Figure 2.9. Cultivation conditions: polymer-based controlled-release fed-batch microtiter plate (48-well round- deep-well), OD_{600} = 0.5, V_{Broth} = 0.5 mL, n = 1000 rpm, d_0 = 3 mm, T = 30 °C.

The volumetric release rate, which is highest for the lowest osmolality and vice versa, correlates with the final relative protease activity (Figure 3.6C, filled bars). The protease yield per

consumed oxygen (Y_{P/O_2}) and per consumed glucose ($Y_{P/S_{Glu}}$) does not give comparable results between the different volumetric release rates (Figure 3.6C, dashed bars, Appendix 12). Independent of the release characteristics of the polymer-based controlled-release fed-batch microtiter plate, the increased osmolality again has a physiological influence on *B. licheniformis*. Most probably, the osmotic pressure not only slows down growth, but also has a negative effect on protease biosynthesis.

3.3.5 Scale-up of microtiter plate-based fed-batch cultivations to shake flasks

To show scalability of microtiter plates to shake flasks, the polymer-based controlled-release fed-batch microtiter plate process was transferred to 250 mL membrane-based fed-batch shake flasks. Consequently, the volumetric release rate within the 250 mL membrane-based fed-batch shake flask was adjusted to meet the volumetric glucose release rate within the polymer-based controlled-release fed-batch microtiter plate. The results of both small-scale fed-batch cultivation systems are shown in Figure 3.7.

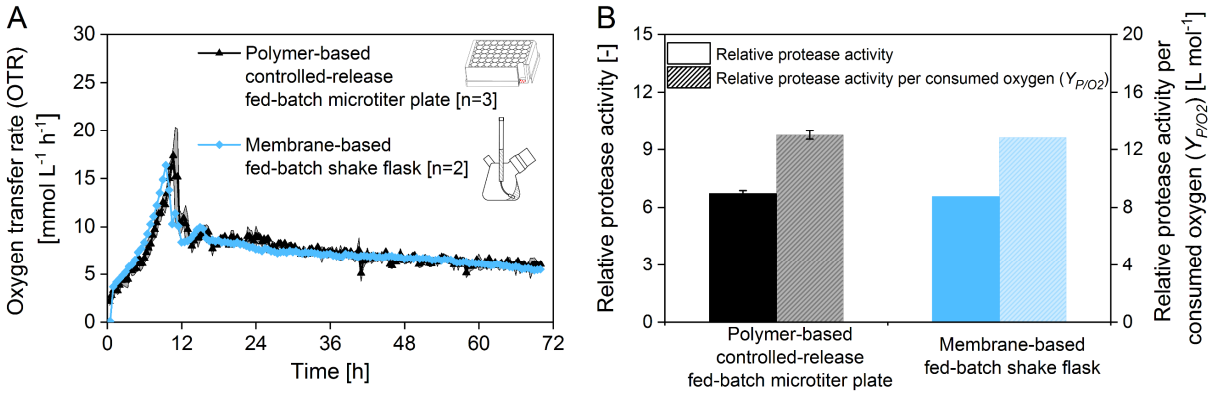

Figure 3.7: Scale-up of microtiter plate-based fed-batch cultivations to shake flasks with the volumetric glucose release rate as scale-up criterion. (A) Mean oxygen transfer rate (OTR) of the polymer-based controlled-release fed-batch microtiter plate and of the membrane-based fed-batch shake flask over time. Shadows symbolize the standard deviation of parallel cultivations (n > 2). (B) Mean relative protease activity (filled bars) and relative protease activity per consumed oxygen (Y_{P/O_2}) (dashed bars) at the end of the cultivation. Error bars symbolize the standard deviation (for n > 2). Protease activities were set in relation to the measured protease activity directly after glucose depletion at 11.5 h within the batch experiment, shown in Figure 2.9. µRAMOS cultivation conditions (microtiter plate): polymer-based controlled-release fed-batch microtiter plate (48-well round- deep-well), OD_{600} = 0.5, V_{Broth} = 0.5 mL, n = 1000 rpm, d_0 = 3 mm, T = 30 °C. RAMOS cultivation conditions (shake flask): membrane-based fed-batch shake flask (250 mL Erlenmeyer flask), OD_{600} = 1.0, V_{Broth} = 16 mL, n = 350 rpm, d_0 = 50 mm, T = 30 °C. Set-up membrane based fed-batch shake flask: V_{Feed} = 3 mL, S_{Glu} (reservoir) = 200 g L^{-1}, active diffusion diameter = 4.8 mm. Membrane: type = RCT-NatureFlex-NP, material = regenerated cellulose, thickness = 42 µm, molecular weight cut-off = 10–20 kDa.

The OTR course of the membrane-based fed-batch shake flask and the polymer-based controlled-release fed-batch microtiter plate cultivation is highly comparable (Figure 3.7A). Especially the OTR level within the fed-batch phase of both cultivation systems underlines the fact that very similar volumetric glucose release rates are met. This is also reflected by the similar amount of consumed glucose (Appendix 12). The final relative protease activity, Y_{P/O_2}, $Y_{P/S_{Glu}}$ and the protease productivity compare well in both systems (Figure 3.7B, Appendix 12, Appendix 13). Additionally, mean pH and OD_{600} were related between the two systems at the end of cultivation. The pH was 7.07 and 7.02 whereas the OD_{600} 9.8 and 10.9 for the polymer-based controlled-release fed-batch microtiter plate and the membrane-based fed-batch shake flask, respectively.

In a recent publication, the transferability of membrane-based fed-batch shake flask cultivations to stirred-tank reactors was validated (Müller, Hütterott, Habicher, Mußmann, & Büchs, 2019). Despite inevitable differences between the scales, such as pH control and initiation of the feed, comparable results were achieved when equal volumetric glucose release rates were applied. This demonstrates that glucose-limited fed-batch cultivations can be consistently scaled-up from microtiter plates to lab-scale stirred tank reactors. The microtiter plate-based fed-batch process, however, normally differs from a fed-batch process in lab-scale stirred tank reactors in terms of the feeding strategy and the total amount of fed glucose. Despite this fact, similar basic physiological conditions concerning catabolite repression, pH-range and oxygen availability are met between the scales. In contrast to batch mode, this basic comparability between the scales allows to investigate process parameters, such as osmolality, in early developmental stages using microtiter plates. Finally, if fed-batch cultivations with sophisticated feeding strategies conducted in lab-scale stirred tank reactors are transferred to production-scale stirred tank reactors, additional factors, such as mixing effects, have to be considered. These factors related to production-scale, however, are a subject of its own, and are not treated in this work.

3.3.6 Modelling fed-batch cultivations in microtiter plates

Simulation of fed-batch cultivations with the polymer-based controlled-release fed-batch microtiter plates requires knowledge of the glucose release rate. Since the polymer-based release mechanisms are complex, glucose release was determined experimentally with V3

mineral medium without cells (Figure 3.8A). Glucose release slightly flattens over time, and thus, the release rate decreases from 0.27 to 0.1 mg h^{-1}.

The unknown maintenance coefficients $m_{S_{Glu}}$ and m_{O_2} were fitted to the described model (Equation (3-1) - (3-7)) on basis of the experiments with an initial OD_{600} of 0.1, 1.0 and 2.5 (Figure 3.8B). The global minimum of the sum of least squares was found for $m_{S_{Glu}} = 0.0638\ g_{S_{Glu}}\ g_X^{-1}\ h^{-1}$ and for $m_{O_2} = 0.0018\ mol_{O_2}\ g_X^{-1}\ h^{-1}$. When comparing the fitted values to another protease producing *B. licheniformis* strain from literature ($m_{S_{Glu}} = 0.0414\ g_{S_{Glu}}\ g_X^{-1}\ h^{-1}$ and $m_{O_2} = 0.0011\ mol_{O_2}\ g_X^{-1}\ h^{-1}$) (Frankena, van Verseveld, & Stouthamer, 1985), the maintenance requirements are slightly increased. The higher maintenance requirements also explain the lower values for $Y_{X/S_{Glu}}$ and Y_{X/O_2} when compared to the same strain from literature. However, the fitted maintenance coefficients were within the physiological range of various *Bacillus* species (Sauer et al., 1996; Tännler et al., 2008). Since the model equations did neither contain terms describing overflow metabolite production nor overflow metabolite consumption, secondary OTR peaks are observable for the measured but not for the simulated OTR course (Figure 3.8B).

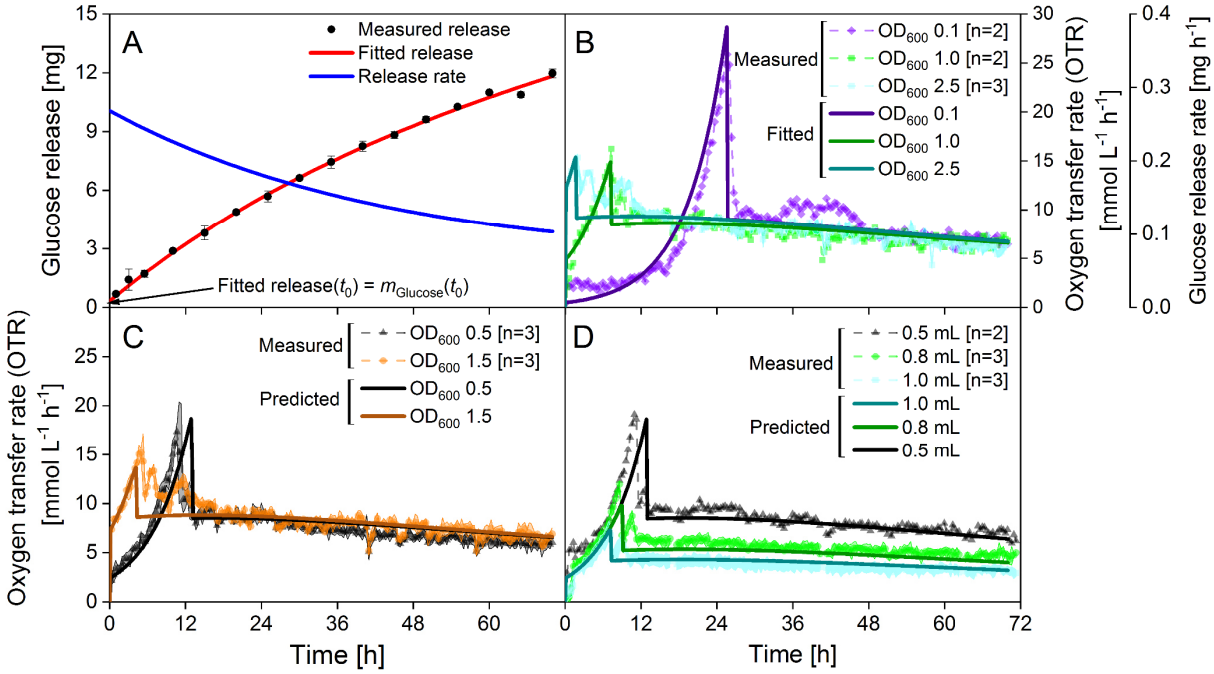

Figure 3.8: Glucose release of the polymer-based controlled-release fed-batch microtiter plate and model-based simulation of the OTR course of *Bacillus licheniformis* fed-batch cultivations with varied initial biomass concentration and filling volume. (A) Glucose release was determined experimentally by measuring the glucose concentration in V3 mineral medium without cells over time. Each data point represents the mean of three individual wells [n = 3]. The measured release was fitted and differentiated resulting in the glucose release

rate. The intersection of the fitted glucose release with the y-axis (t = 0) corresponds to the amount of initially provided glucose. The volumetric release (F_{SGlu}) and release rate (F'_{SGlu}) are obtained by dividing the filling volume V_{Broth}. (B) Maintenance coefficients m_S and m_{O2} were fitted to the experiments with an initial OD_{600} of 0.1, 1.0 and 2.5 by performing a global minimization (global search (*gs*) and *fmincon* MATLAB functions) of the sum of least-squares based on the described fed-batch model (Equation (3-1) - (3-7)). (C,D) The model with the fitted parameters m_S and m_{O2} was validated on basis of experiments with varying initial biomass concentrations (C) and filling volumes (D).

To validate the established fed-batch model, additional conditions, such as different initial biomass concentrations and filling volumes, were simulated using the fitted maintenance coefficients. The model-output of experiments with varied initial biomass concentrations and filling volumes is shown in Figure 3.8C and D, respectively. In both cases, the simulated OTR course correctly reflects the initial batch phase, the initiation of the fed-batch phase and the level of the fed-batch OTR plateau. It can be concluded that the determined maintenance coefficients in combination with the other model parameters are suitable to describe the OTR course of cultivations in polymer-based controlled-release fed-batch microtiter plates.

3.4 Summary

In this chapter, the polymer-based controlled-release fed-batch microtiter plate was used to investigate fed-batch cultivations of a protease producing *Bacillus licheniformis* culture. Therefore, the oxygen transfer rate (OTR) was online-monitored within each well of the polymer-based controlled-release fed-batch microtiter plate using a µRAMOS device. Cultivations in five individual polymer-based controlled-release fed-batch microtiter plates of two production lots showed good reproducibility with a mean coefficient of variation of 9.2 %. Decreasing initial biomass concentrations prolonged batch phase while simultaneously postponing the fed-batch phase. The initial liquid filling volume affects the volumetric release rate, which is directly translated in different OTR levels of the fed-batch phase. An increasing initial osmotic pressure within the mineral medium decreases both glucose release and protease yield ($Y_{P/O2}$). With the volumetric glucose release rate as scale-up criterion, microtiter plate- and shake flask-based fed-batch cultivations were highly comparable. On basis of the small-scale fed-batch cultivations, a mechanistic model was established and validated. Model-based simulations coincided well with the experimentally acquired data.

Parts of the following chapter have been submitted as Habicher, T., Czotscher, V., Klein, T., Daub, A., Keil, T. & Büchs, J. (2019). Glucose-containing polymer rings enable fed-batch operation in microtiter plates with parallel online measurement of scattered light, fluorescence, dissolved oxygen tension and pH. *Biotechnology and Bioengineering*, *116*(9), 2250-2262. Alexander Lobanov contributed in developing the manufacturing process of microtiter plates containing polymer rings (4.2.3) (AVT-Biochemical Engineering, Prof. Dr.-Ing. Büchs, RWTH Aachen University). Vroni Czotscher assisted with manufacturing of fed-batch microtiter plates and performed cultivation experiments (4.2.1-4.2.5) (AVT-Biochemical Engineering, Prof. Dr.-Ing. Büchs, RWTH Aachen University).

Chapter 4

BioLector measurements in fed-batch microtiter plates

4.1 Introduction

Online monitoring of microtiter plate-based cultivations is mainly realized via non-invasive optical measurement systems (Klöckner & Büchs, 2012). A well-known optical online monitoring system for microtiter plates, which is used in the academic as well as industrial sector, is the BioLector device. The underlying measurement principle is based on an optical fiber bundle that is connected to an x-y-positioning device (Figure 4.1A). This design enables scattered light (biomass) and fluorescence (fluorescent proteins and metabolites) measurement in each well of a microtiter plate (Kensy et al., 2009; Samorski et al., 2005). In order to monitor similar process parameters as in standard stirred tank reactors, efforts have been made to facilitate online measurement of the dissolved oxygen tension and pH by immobilized fluorescent dyes (optodes) (Arain et al., 2006; John & Heinzle, 2001; John et al., 2003). In combination with these optodes, the BioLector device allows for parallel online measurement of scattered light, fluorescence, dissolved oxygen tension and pH. This makes the BioLector an efficient device for strain and medium screening, growth characterization, cultivation parameter optimization etc. (www.m2p-labs.com/references/publications/).

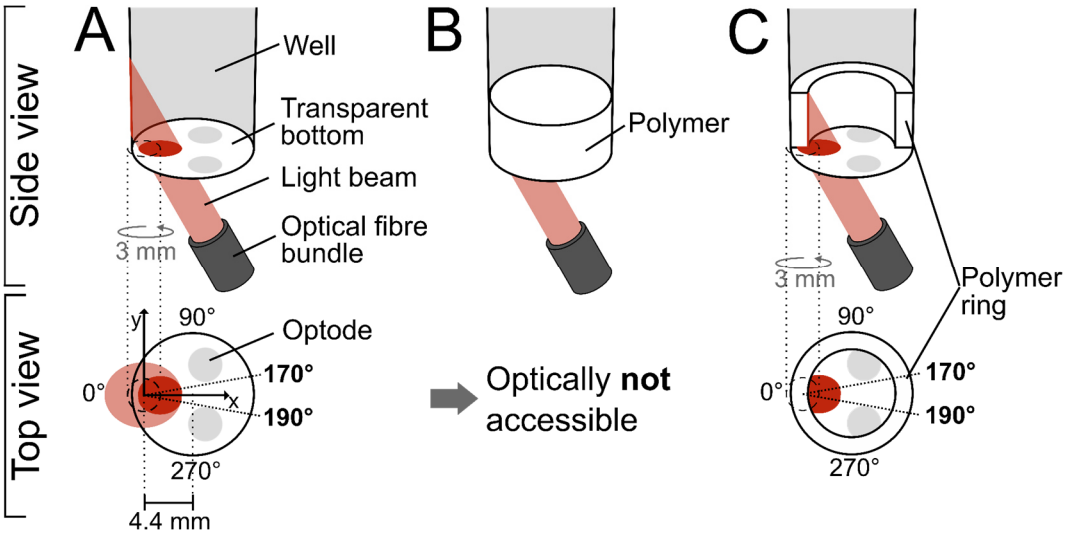

Figure 4.1: Schematic representation of online biomass monitoring with the BioLector in a standard well and in wells containing polymer-based glucose release systems. (A) Default scattered light (biomass) measurement position in a standard well of a 48-well round- deep-well microtiter plate with transparent bottom. For online biomass monitoring, the default measurement position of the x-y-positioning device is shifted 4.4 mm to the left from the center of the well. Due to the orbital shaking of the microtiter plate (shaking diameter d_0 = 3 mm; dashed circle), the light beam illuminates a ellipsoidal area (top view, light red ellipsoidal area). The default measurement position represents the origin of the coordinate system of the x-y-positioning device (x = 0, y = 0) and is the center of the illuminated ellipsoidal area. From a complete shaking revolution (0° - 360°), online biomass measurements are only recorded at an angle of 170° to 190° (dark red area). (B) Default biomass (scattered light) measurement position in a well of a commercially available polymer-based controlled-release fed-batch microtiter plate (Feed Plate®). The glucose-containing polymer matrix covers the bottom of the well of the 48-well round- deep-well microtiter plate. (C) Default biomass measurement in a well with a polymer ring. The polymer ring is placed at the bottom of the well of a 48-well round- deep-well microtiter plate. The default biomass measurement position is illustrated.

Independent of the online monitoring possibilities, applying fed-batch mode is still crucial for many fermentation processes (Chapter 1.1). Systems that combine both online monitoring and feeding are compared in Chapter 1.4. The applicability of such systems, however, also depends on low investment- and operating costs, compatibility with existing laboratory equipment, versatility and reproducibility (Neubauer et al., 2013). Enzyme-controlled glucose auto-delivery systems fulfill most of these requirements while being compatible with online monitoring devices using optical measurement techniques, such as plate readers or the BioLector device. Nevertheless, glucose release is sensitive against amylases, proteases and changing cultivation conditions, such as pH and temperature, resulting in hardly controllable release characteristics (Toeroek et al., 2015).

The polymer-based controlled-release fed-batch microtiter plate (Feed Plate®), which was described in Chapter 3, has similar characteristics as the enzyme-controlled glucose release system. It is independent of peripheral equipment, ready-to-use, disposable, highly parallelizable, cost efficient and compatible with existing laboratory equipment. Amylases and proteases do not impair the glucose release characteristics. Furthermore, glucose release was shown to be highly reproducible and less sensitive against changing cultivation conditions compared to the enzymatic release system (Keil et al., 2019). Nevertheless, to date the enzymatic glucose release system is advantageous to the current polymer-based release system in terms of online monitoring. Since the glucose-containing polymer matrix covers the bottom of each well, the polymer-based controlled-release fed-batch microtiter plate is not compatible with commercially available optical online monitoring devices (Figure 4.1B).

In this chapter, a polymer-based glucose release microtiter plate enabling online monitoring with the BioLector device is presented. Hence, the stable and reproducible glucose release characteristics of the existing polymer-based controlled-release fed-batch microtiter plate system have been extended to allow online monitoring through the transparent bottom of the microtiter plate (Figure 4.1C). The optical accessibility of the culture broth was realized by manufacturing polymer rings. These rings were placed at the bottom of each well so that the light beam is able to penetrate inside the culture broth (Figure 4.1C). To avoid measurement interferences caused by the polymer ring, the scattered light measurement position and the polymer ring geometry were adjusted accordingly. The applicability of the polymer ring, introducing fed-batch conditions in a microtiter plate, with parallel BioLector online monitoring is demonstrated with *Escherichia coli* cultures.

4.2 Material and Methods

4.2.1 Strain and media

Escherichia coli BL21 (DE3) pRhotHi-2-EcFbFP was used as a model organism and was kindly provided by T. Drepper from the Institute of Molecular Enzyme Technology (Heinrich-Heine-University, Düsseldorf, Germany). The expression of flavin mononucleotide-based fluorescent protein (EcFbFP) is under the control of a lactose operator (Huber, Ritter, et al., 2009).

However, the fluorescent protein was shown to be synthesized in a catabolite controlled manner without the addition of an inducer (Bähr et al., 2012; Philip et al., 2018). Maturation of EcFbFP is independent of oxygen; thus, fluorescence intensities are detectable under oxygen limited conditions (Drepper et al., 2007, 2010).

The chemicals applied for media preparation were of analytical grade and purchased from Carl Roth GmbH & Co. KG (Karlsruhe, Germany), Sigma-Aldrich Chemie GmbH (Steinheim, Germany), Merck (Darmstadt, Germany) and Fluka Chemie AG (Buchs, Switzerland).

The complex medium Terrific Broth (TB) was used for the first preculture and contained 10 g L^{-1} glycerol ($C_3H_8O_3$), 12 g L^{-1} tryptone (Carl Roth GmbH & Co. KG, Karlsruhe, Germany), 24 g L^{-1} yeast extract (Carl Roth GmbH & Co. KG, Karlsruhe, Germany), 12.54 g L^{-1} K_2HPO_4 and 2.31 g L^{-1} KH_2PO_4. After autoclaving (121 °C, 20 min), the medium was stored at 4 °C for no longer than 6 months. Prior to cultivation, 50 mg L^{-1} of kanamycin were added.

The modified mineral medium Wilms-MOPS was prepared according to Philip et al. (2017) and was used for the second preculture and all main cultures (Wilms et al., 2001). For batch cultivations, the medium was supplemented with 20 g L^{-1} of glucose, whereas no glucose was added to the medium for fed-batch experiments (0 g L^{-1}). Prior to cultivation, 50 mg L^{-1} of kanamycin were added. Despite the glucose concentration, the Wilms-MOPS medium formulation was identical for batch and fed-batch cultivations.

4.2.2 Cultivation conditions

The first and second preculture was performed in 250 mL shake flasks and carried out on an orbital climo-shaker ISFX-1 from Adolf Kühner AG (Biersfelden, Switzerland) with a filling volume V_{Broth} = 10 mL, a shaking frequency n = 350 rpm, a shaking diameter d_0 = 50 mm and at T = 30 °C. For online monitoring of the oxygen transfer rate (OTR), the in-house build RAMOS device was used. A commercial version is available from Adolf Kühner AG (Biersfelden, Switzerland) or HiTec Zang GmbH (Herzogenrath, Germany). The preculture procedure was divided in two steps, whereby the first preculture was carried out in complex TB medium and the second in Wilms-MOPS medium. Glycerol cryo stocks were used to inoculate

the first preculture. Cells from the first preculture were harvested in late exponential growth phase on glycerol and used to inoculate the second preculture with an initial optical density at 600 nm (OD_{600}) of 0.1. Cells from the second preculture were harvested in late exponential growth phase on glucose and used to inoculate the main culture. The initial OD_{600} of the main culture ranges between 0.1 and 1 and is specified in the figure legend or caption.

Batch and fed-batch main cultures were conducted in 48-well round- deep-well microtiter plates (MTP-R48-B, m2p labs GmbH, Baesweiler, Germany) with a filling volume V_{Broth} = 0.8 or 1.2 mL, a shaking frequency n = 1000 rpm, a shaking diameter d_0 = 3 mm, at 30 °C and a relative humidity φ = 80 – 85 %. A commercially available BioLector (m2p labs GmbH, Baesweiler, Germany) was used for online monitoring. For DOT and pH measurement, 48-well round- deep-well microtiter plates with optodes were utilized (MTP-R48-BOH, m2p labs GmbH, Baesweiler, Germany). To reduce evaporation and prevent cross contamination, the microtiter plates were covered with a gas permeable sealing foil with evaporation reduction layer (F-GPR48-10, m2p labs GmbH, Baesweiler, Germany). Parallel cultivations with the µRAMOS device enabled online monitoring of the OTR within each individual well of the 48-well round- deep-well microtiter plate (Flitsch et al., 2016). When the µRAMOS device was used, microtiter plates were covered with a pierced polyolefin sealing foil (900371-T, HJ-Bioanalytik GmbH, Erkelenz, Germany).

4.2.3 Manufacturing of microtiter plates with polymer rings

The polymer matrix with embedded glucose crystals was ordered on request in form of flat sheets with a thickness of 5 mm from Kuhner Shaker GmbH (Herzogenrath, Germany). The use of a combined hollow punch with an outer diameter of 12 mm and variable inner diameter enabled the manufacturing of polymer rings of constant height and outer diameter and varying inner diameters of 6, 7, 8 and 9 mm (Figure 4.2A). In order to obtain polymer rings of comparable shape, a controlled movement during stamping is necessary. Therefore, the hollow punch was pressed manually against a steel tube that was fixed into a bench drill stand (Figure 4.2B).

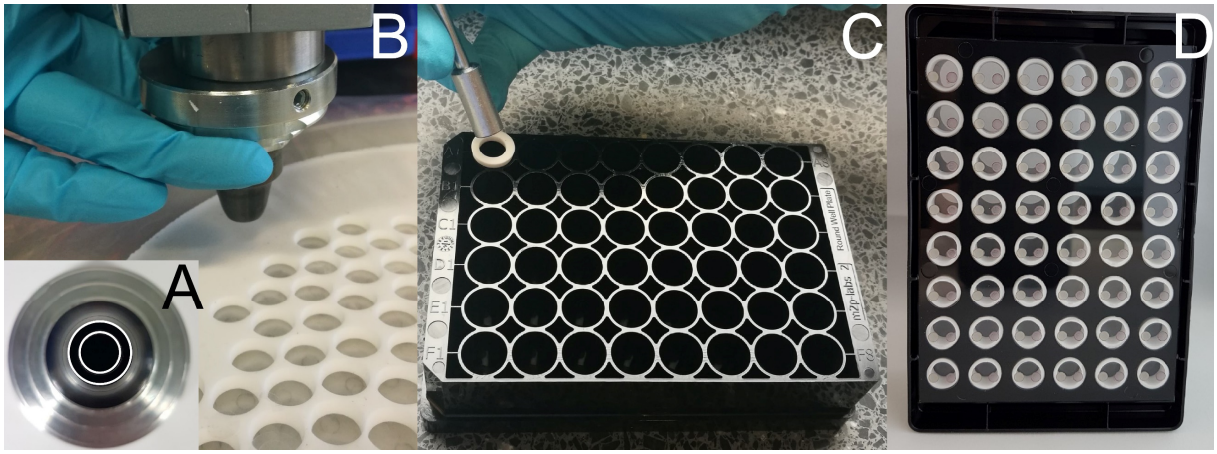

Figure 4.2: Overview of the manufacturing process of microtiter plates with polymer rings. (A) Assembled hollow punch with an outer diameter of 12 mm and inner diameter of 8 mm. The outer diameter as well as inner diameter can be varied by applying the appropriate hollow punch. (B) The assembled hollow punch is pressed manually against a steel tube that is then clamped into a bench drill stand. The bench drill stand has a handle (not visible on the photograph) that allows for a repeatable downward movement and, thus, a standardized and reproducible stamping of polymer rings. (C) Polymer rings were inserted into the well of a 48-well round- deep-well microtiter plate and gently pushed to the bottom using a socket wrench. (D) Completed microtiter plate with polymer rings in each well.

Finally, the handle of the bench drill stand facilitated a defined downward movement and thus a standardized and reproducible production of polymer rings. Each polymer ring was then inserted into the well and gently pushed to the bottom using an eight socket wrench (Figure 4.2C). Optimal placing on the bottom was checked through the transparent bottom of the microtiter plate (Figure 4.2D). Due to the ease of handling, the manufacturing procedure was carried out under non-sterile conditions with a non-sterile polymer matrix. To avoid contaminations during cultivation, kanamycin was added to the culture broth.

4.2.4 Determination of glucose and overflow metabolites

Glucose and overflow metabolite concentrations (acetate and lactate) were determined by high-performance liquid chromatography (HPLC). The HPLC device (Ultimate 3000; Dionex, Sunnyvale, CA) was equipped with an organic acid-resin- precolumn (40 × 8 mm) and an organic acid-resin-column (250 × 8 mm), both from CS-Chromatographie Service GmbH (Langerwehe, Germany). Samples were sterile filtered (0.2-µm filter) and stored at -20 °C until measurement. Elution was carried out with 2.5 mM H_2SO_4 with a flow rate of 0.5 mL min^{-1} at a constant temperature of 70 ° C. The compounds were detected by measuring the

refractometric index with a Shodex RI-101 refractometer (Showa Denko Europe, Munich, Germany). Data analysis was done with the software Chromeleon 6.8 (Dionex).

4.2.5 BioLector settings

Biomass was online monitored via scattered light intensity at a wavelength λ = 620 nm with a gain of 25. EcFbFP fluorescence intensity was online monitored at an excitation wavelength $\lambda_{Excitation}$ = 450 nm and an emission wavelength $\lambda_{Emission}$ = 492 nm with a gain of 100. DOT and pH were measured via optodes at $\lambda_{Excitation}$ = 520 nm/$\lambda_{Emission}$ = 600 nm with a gain of 70 and $\lambda_{Excitation}$ = 470 nm/$\lambda_{Emission}$ = 525 nm with a gain of 30, respectively. The angle section in which the measurement is conducted is from 170 ° - 190 ° for scattered light (Figure 4.1A), pH and DOT and from 150 ° - 210 ° for EcFbFP fluorescence.

Adjustment of the measurement position of the optical fiber bundle was done via the user interface of the BioLector. Within the set-up menu, new microtiter plate layouts can be created or existing ones modified (.mtp – file). The software uses the 48-well microtiter plate as basis for the internal coordinate system for the x-y-positioning device (x_1 = 14 and y_1 = 75, Appendix 16A). For clarity, within this chapter the default measurement position of the x-y-positioning device is given as x = 0 and y = 0. Fluorescence is always measured at the same position as biomass. The measurement positions of DOT and pH are given as relative coordinates to biomass within the software. Therefore, changing biomass measurement positions requires an adjustment of DOT and pH measurement positions. To keep the same measurement position from well to well, the optical fiber bundle is moved 13 mm in x and y direction (Appendix 16B).

4.3 Results and Discussion

4.3.1 Adjustment of the online biomass monitoring position

The principle of online biomass monitoring with the BioLector device is graphically illustrated in Figure 4.1A. In a 48-well microtiter plate, the light beam penetrates into the wells through the transparent bottom. In contrast, the wells of a commercially available 48-well polymer-

based fed-batch microtiter plate (Feed Plate®) are optically not accessible due to the polymer matrix that covers the bottom (Figure 4.1B). Thus, polymer rings were introduced to enable fed-batch operation mode with simultaneous online monitoring (Figure 4.1C).

Since the white surface of the polymer ring might cause optical effects, such as light reflection, the scattered light intensity was measured in wells with a polymer ring. Figure 4.3A shows the influence of the measurement position (x-axis offset of the x-y-positioning device) on light reflection, quantified via scattered light measurements at 620 nm, for ring geometries with an inner diameter of 6, 7, 8 and 9 mm. Measurements were done without adding liquid to the well. Graphical visualizations of the measurement position display the path of the light beam (Figure 4.3B). At the default measurement position with an x-axis offset of 0 mm, the well without polymer ring shows a negligible scattered light intensity, while for wells with polymer ring, scattered light intensities are substantially increased (Figure 4.3A, x = 0 mm). The low scattered light intensity in the well without polymer ring is due to the black wall of the microtiter plate, which absorbs light instead of reflecting it. The increased scattered light intensities in wells with a polymer ring are caused by light reflections on the white surface of the polymer ring. Furthermore, measured intensities correlate with the inner diameter of the polymer ring. Graphical visualizations depicted in Figure 4.3B (x = 0 mm) highlight that with decreasing inner diameter of the polymer ring the surface at the bottom of the polymer ring being illuminated by the light beam increases. It can be concluded that from the horizontal white surface a bigger proportion of the light is backscattered to the optical fiber bundle when compared to the vertical white surface. This explains the higher scattered light intensities for wells containing a polymer ring with smaller inner diameter.

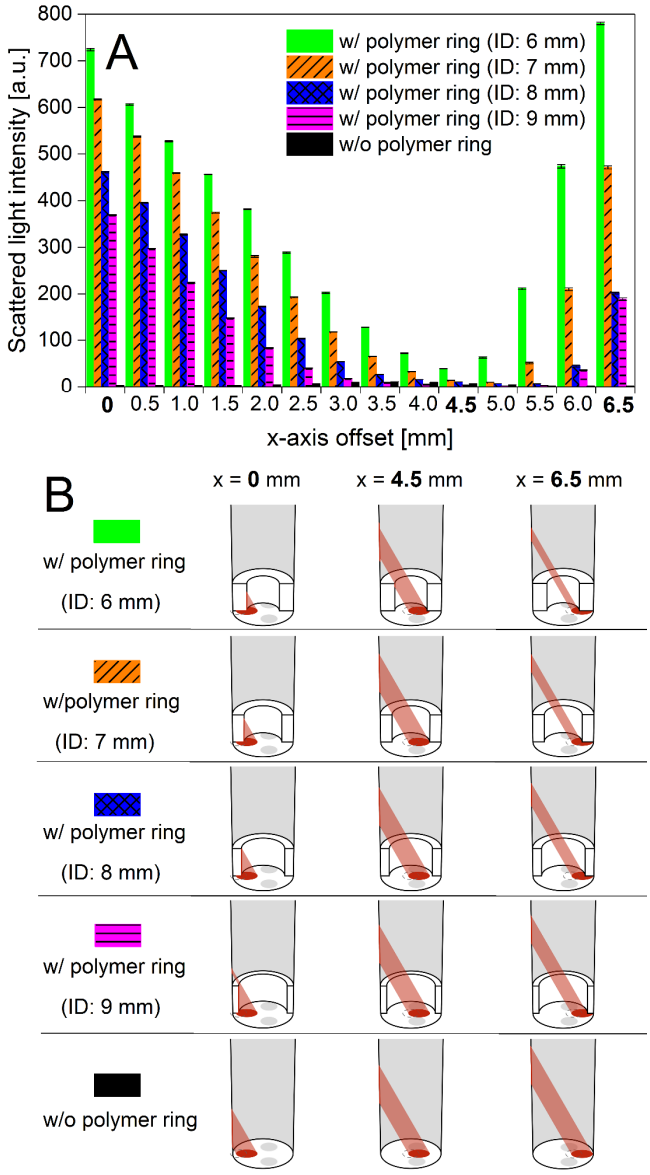

Figure 4.3: Determination of the light reflection on polymer rings with varying inner diameters in dependency of the x-axis offset of the x-y-positioning device. (A) The reflection (scattered light intensity; λ = 620 nm) was measured in wells of a 48-well round- deep-well microtiter plate with polymer rings of a constant outer diameter of 12 mm and varying inner diameters (ID of 6, 7, 8 and 9 mm) as well as in wells without polymer ring. The x-y-positioning device was moved stepwise 6.5 mm in x-direction with constant y-position. Measurements were done within five individual wells [n = 5] at a shaking frequency n = 1000 rpm with a shaking diameter d_0 = 3 mm. No liquid was added to the wells. (B) Graphical illustration of the light beam within wells with and without polymer ring at an x-axis offset of 0, 4.5 and 6.5 mm. The light beam is exemplarily illustrated only at 180°. To visualize the light beam inside the wells, the front part of the polymer ring is not depicted.

In order to reduce the reflection of the polymer rings, the measurement position was adjusted by moving the x-y-positioning device in 0.5 mm steps in x-direction. Consequently, scattered light intensities constantly decreased in wells with a polymer ring (Figure 4.3A). When considering all ring geometries, the lowest scattered light intensities are reached at an x-axis

offset of 4.5 mm. At this position, the light beam marginally illuminates parts of the white surface of the polymer ring (Figure 4.3B; x = 4.5 mm). By moving the x-y positioning device further, scattered light intensities increase again. Increasing intensities are due to the light beam illuminating the other side of the horizontal surface of the polymer rings, which is graphically visualized in Figure 4.3B for the position x = 6.5 mm.

4.3.2 Glucose release characteristics of the polymer ring

Glucose release characteristics of the standard- and slow release polymer matrix were investigated. The results of glucose release experiments are depicted in Figure 4.4. A polymer ring with an inner diameter of 8 mm, manufactured with the standard release polymer matrix, is characterized by a constant glucose release rate of 0.37 mg h^{-1} after 12 h (under cultivation conditions) (Figure 4.4). Within the first 12 h, 15.6 mg of glucose was released. This strong, abrupt initial glucose release is attributed to the inner part of the polymer ring surface that has been cut during the manufacturing process. In contrast to a smooth polymerized surface, cutting changes the surface properties and makes the embedded glucose crystals more easily accessible.

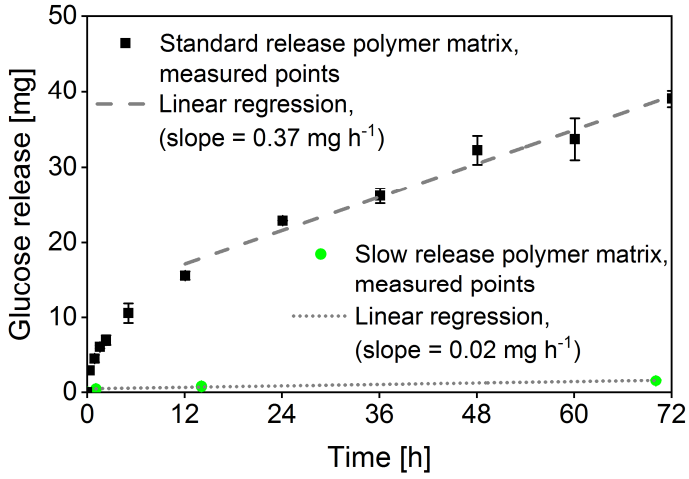

Figure 4.4: Glucose release of the polymer ring with an inner diameter of 8 mm using the standard- and slow release polymer matrix. The amount of released glucose is shown over time. For each data point, three individual wells were analyzed regarding their glucose concentration [n = 3]. For the standard release polymer matrix, linear regression was done starting with the measurement point at 12 h. For the slow release polymer matrix, linear regression was done starting with the measurement point at 1 h. Culture medium: Wilms-MOPS medium, 0 g L^{-1} glucose, 0.2 M MOPS, no biomass. Cultivation conditions: 48-well round- deep-well microtiter plate, n = 1000 rpm, d_0 = 3 mm, V_{Broth} = 1 mL, T = 30 °C.

A polymer ring with an inner diameter of 8 mm, manufactured with the slow release polymer matrix, releases negligible amounts of glucose (under cultivation conditions) (Figure 4.4). In contrast to the standard release polymer matrix, a strong and abrupt initial glucose release is not observed with the slow release polymer matrix. Since glucose release from this polymer matrix is negligible, it is used for batch-like cultivations. Thus, online monitoring in wells without polymer ring (reference) can be compared to wells with polymer ring. The use of a glucose-containing polymer matrix for batch cultivations was necessary in order to have a similar white color to the standard release polymer matrix, which is used for fed-batch cultivations.

4.3.3 Online monitoring of DOT and pH in wells with polymer ring

In order to investigate possible negative impacts of the polymer ring on online DOT and pH measurements, parallel batch cultivations of *E. coli* BL21 (DE3) were conducted in wells with polymer ring of varied inner diameter (6, 7, 8 and 9 mm) and wells without polymer ring. Polymer rings were made from the slow release polymer matrix; thus, glucose release is negligibly small (Figure 4.4). Figure 4.5 shows the course of DOT and pH in wells with and without polymer ring of batch cultivations including photographs of the wells prior to inoculation.

In Figure 4.5A, the DOT measurement of the cultivation without polymer ring serves as reference. The course of the DOT represents typical batch growth of an *E. coli* BL21 (DE3) culture using Wilms-MOPS mineral medium (Wewetzer et al., 2015) (Appendix 17B). The cultivations with a polymer ring with an inner diameter of 8 or 9 mm behave similar to the reference (w/o polymer ring, black line). In contrast, cultivations with a polymer ring with an inner diameter of 6 or 7 mm exhibit an altered course. For these two cultivations, the DOT decreases more rapidly within the first hours (0 - 6 h) and increases rather slowly after the oxygen-limited phase (DOT = 0 %) at 10 h. The course of the DOT of the cultivation with the polymer ring with 6 mm differs more from the reference when compared to the cultivation with the polymer ring with 7 mm.

The pH of the reference cultivation (w/o polymer ring, black line), depicted in Figure 4.5B, represents the typical pH course of an *E. coli* BL21 (DE3) batch cultivation

(Wewetzer et al., 2015) (Appendix 17C). The pH course of cultivations with a polymer ring with an inner diameter of 7, 8 or 9 mm are similar to the reference, whereby the cultivation with a polymer ring with an inner diameter of 6 mm shows major deviation. Thereby, the pH increases only slowly after 10 h and remains below the reference until the end of the cultivation.

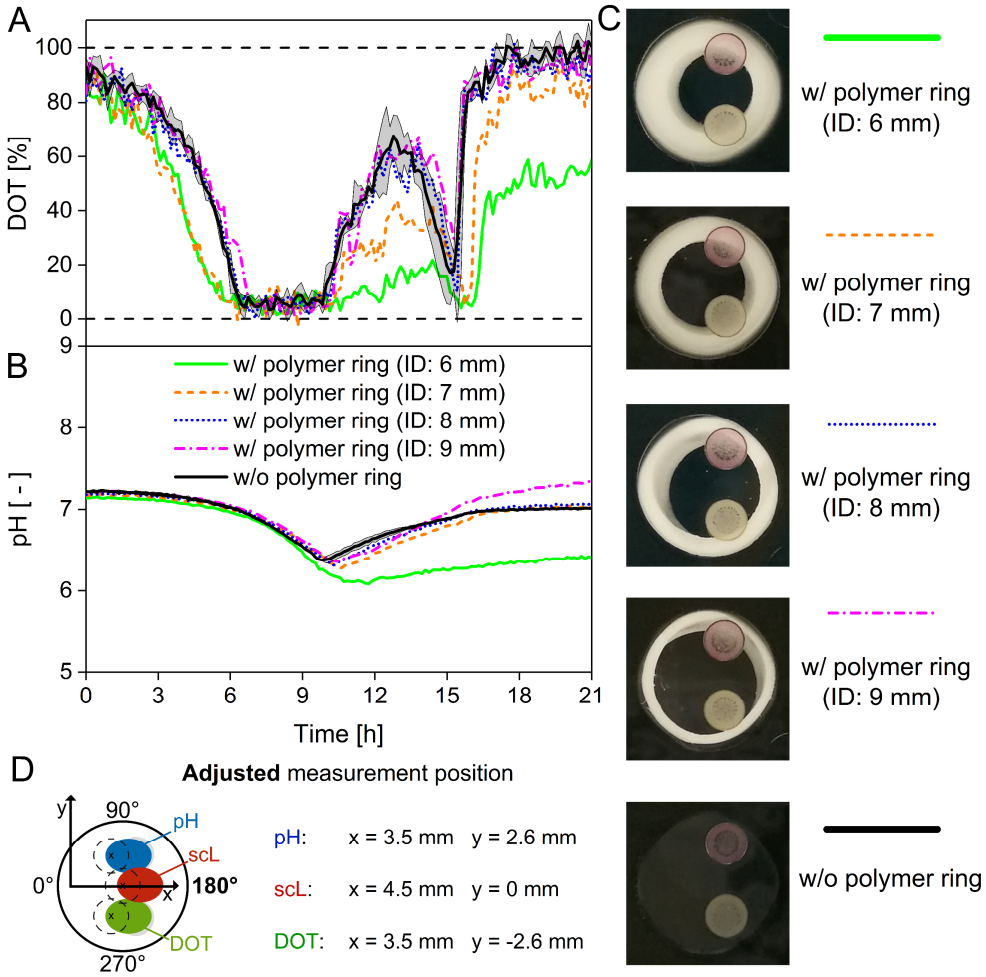

Figure 4.5: Online monitoring of DOT and pH with the adjusted measurement position (x = 4.5 mm) during a batch cultivation in wells with polymer ring of varying inner diameter and wells without polymer ring. (A) DOT and (B) pH of a batch cultivation with *E. coli* BL21 (DE3). Polymer rings had an outer diameter of 12 mm, a variable inner diameter of 6, 7, 8 and 9 mm and were made from the slow release polymer matrix. Glucose release from this applied polymer matrix is negligible. Measurements with polymer ring were done in single wells [n = 1]. Measurements in wells without polymer ring were done in four individual wells [n = 4]. Culture medium: Wilms-MOPS medium, 20 g L^{-1} glucose, 0.2 M MOPS, OD_{600} = 0.5. Cultivation conditions: 48-well round- deep-well microtiter plate with optodes, n = 1000 rpm, d_0 = 3 mm, V_{Broth} = 0.8 mL, T = 30 °C. (C) Bottom view photographs of wells with optodes and with and without inserted polymer ring. (D) Visualization (top view) of the adjusted measurement position for scattered light (scL) with the corresponding measurement positions for DOT and pH. Intensities are recorded at an angle section of 170° - 190° (exemplarily illustrated only at 180°).

The photographs in Figure 4.5C display wells with polymer ring and without polymer ring. It is clearly visible that with decreasing inner diameters a bigger proportion of the optodes is covered by the polymer ring. Since the covered part of the optodes is not in direct contact with the culture broth, it can be hypothesized that the conditions below the polymer ring (covered part) do not represent the actual DOT and pH within the culture broth. The acquired fluorescence signal, however, represents a mix between the covered and uncovered part of the optode. This explains the deviating course of the pH and DOT for the cultivation with the polymer ring with an inner diameter of 6 mm. In the case of the polymer ring with an inner diameter of 7 mm, pH was comparable to the reference, although DOT was not. The corresponding photograph in Figure 4.5C (ID: 7 mm) indicates that the optodes are not always positioned symmetrically to the corresponding well. It is visible that the reddish DOT spot is closer to the well wall than the yellowish pH spot. As a result, a larger area of the DOT spot is covered by the polymer ring compared to the pH spot. Polymer rings with an inner diameter of 8 and 9 mm cover only a minor part of the optodes (Figure 4.5C). Thus, with these polymer ring geometries online monitoring of pH and DOT is similar to wells without polymer ring. Nevertheless, due to the wall thickness of only 1.5 mm, polymer rings with an inner diameter of 9 mm regularly broke during the manual manufacturing process. For this reason, polymer rings with an inner diameter of 8 mm were used for subsequent cultivations with parallel DOT and pH monitoring. Due to the adjustment of the ring geometry, the DOT and pH measurement position remained unchanged, while scattered light and fluorescence measurements were always conducted at the adjusted position (x = 4.5 mm, y = 0 mm, Figure 4.5D).

4.3.4 Online monitoring of batch cultivations in wells with polymer ring

E. coli BL21 (DE3) batch cultivations were performed in wells with and without polymer ring to directly compare scattered light, DOT, pH, and fluorescence measurement on basis of the previously described adjustments of the measurement position and ring geometry (Figure 4.3 and Figure 4.5). Figure 4.6 shows the results of batch cultivations with varying initial biomass concentrations in wells with and without polymer ring (inner diameter 8 mm).

Independent of the initial OD_{600} of 0.2, 0.5 and 1, the scattered light intensity increases exponentially within the initial oxygen unlimited growth phase (DOT > 0 %), whereas the DOT

decreases (Figure 4.6A, B). The oxygen-unlimited growth phase is shortened with an increasing initial OD_{600} of 0.2, 0.5 and 1, entering the oxygen-limited phase after about 8, 6 and 4 h, respectively. Once the cultures are oxygen-limited (DOT = 0 %), the scattered light intensity exhibits a linear increase. The oxygen limitation persists as long as the primary carbon source, glucose, is available. The time point when the DOT increases, marks the depletion of glucose (Wewetzer et al., 2015) (Appendix 17B). At this point, the curve of the scattered light intensity flattens and pH shifts from a downward to an upward trend (Figure 4.6C, Appendix 17A, B). This pH shift is caused by the consumption of previously accumulated overflow metabolites, such as lactate and acetate (Wewetzer et al., 2015) (Appendix 17C). The oxygen-limited conditions enhance the accumulation of acetate (Losen, Frölich, Pohl, & Büchs, 2004). Overflow metabolite consumption is visible by a distinct spike of the DOT at 17, 14 and 11 h for cultures with an initial OD_{600} of 0.2, 0.5 and 1, respectively (Figure 4.6B, Appendix 17B, C). The EcFbFP fluorescence intensity does not increase within the initial unlimited growth phase, but ascends under oxygen-limited conditions and during overflow metabolite consumption (Figure 4.6C). EcFbFP is known for a strong interference with the pH signal from the fluorescent optode (Kunze, Roth, Gartz, & Büchs, 2014). The comparison of online and offline measured pH values in batch reveals the distorting impact of EcFbFP fluorescence on pH measurement (Appendix 18). For example, with an EcFbFP fluorescence intensity of 100 a.u. the online pH results in a 0.35 higher value than the offline pH (Appendix 18). The falsified online pH measurement is solely caused by the fluorescent reporter protein EcFbFP (Kunze et al., 2014). The polymer ring itself does not affect pH measurement (Figure 4.5B).

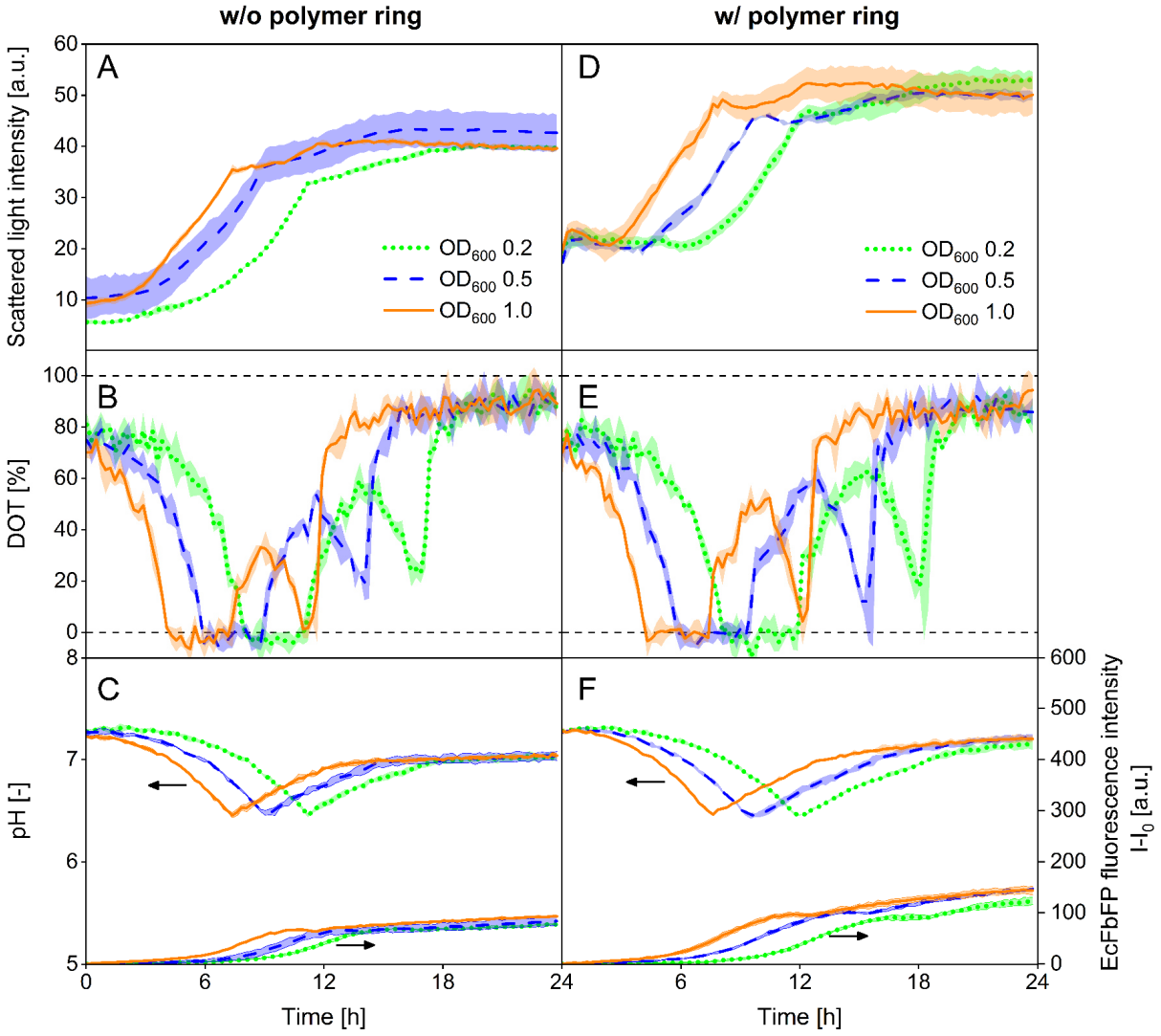

Figure 4.6: Batch cultivations of *E. coli* BL21 (DE3) with varying initial biomass concentrations in wells without and with polymer ring. (A-C) Batch cultivations of *E. coli* BL21 (DE3) in wells without polymer ring. (D-F) Batch cultivations of *E. coli* BL21 (DE3) in wells with polymer ring (outer diameter of 12 mm and inner diameter of 8 mm). The slow release polymer matrix was used. Glucose release from this polymer matrix is negligible. (A,D) Scattered light intensity, (B,E) DOT, (C,F) pH and EcFbFP fluorescence intensity over time. Each experiment was done in triplicates [n = 3], shadows symbolize the standard deviation. Adjusted measurement position for biomass and fluorescence (x = 4.5 mm, y = 0 mm). Culture medium: Wilms-MOPS medium, 20 g L^{-1} glucose, 0.2 M MOPS. Cultivation conditions: 48-well round- deep-well microtiter plate with optodes, n = 1000 rpm, d_0 = 3 mm, V_{Broth} = 0.8 mL, T = 30 °C.

Parallel batch cultivations in wells with and without polymer ring are highly comparable concerning online measurement of DOT, pH and EcFbFP fluorescence intensity (Figure 4.6E, F). However, the initially constant scattered light intensity points at light reflections that prevent the detection of low biomass concentrations (Figure 4.6D). With increasing biomass concentration, the course of the scattered light intensity matches with the

cultivations without polymer ring. Higher final scattered light values might be due to secondary light reflection of the white ring surface.

4.3.5 Online monitoring of fed-batch cultivations in wells with polymer ring

The adjustment of the measurement position and ring geometry enabled comparable online monitoring in wells with polymer ring and wells without polymer ring (Figure 4.6). In the following experiment, a polymer ring with similar geometry (inner diameter of 8 mm), and capable of continuously releasing glucose, was inserted into the wells. For online monitoring with the BioLector, the adjusted measurement position was applied (Figure 4.5D). The results of the *E. coli* BL21 (DE3) fed-batch cultivation with parallel online monitoring using the BioLector and µRAMOS device is shown in Figure 4.7.

The fed-batch cultivation is divided in four distinct phases. Within phase *I,* the scattered light intensity and the oxygen transfer rate (OTR) increase exponentially (Figure 4.7A, B). The DOT behaves reversely, thereby decreasing exponentially (Figure 4.7B). This exponential behavior is due to accumulation of glucose and the resulting unlimited growth conditions (batch phase). Glucose accumulation occurs due to the (1) low initial biomass concentration that results in low initial glucose consumption, (2) the start of the glucose release already with the start of the cultivation and (3) the high abrupt initial glucose release (Figure 4.4). However, an initial unlimited batch phase with an excess of glucose is characteristic for fed-batch processes (Korz, Rinas, Hellmuth, Sanders, & Deckwer, 1995; Riesenberg et al., 1991; Xu, Jahic, Blomsten, & Enfors, 1999). In contrast to the batch cultivations with polymer ring (Figure 4.6D), the initial scattered light intensity of the fed-batch cultivation is not indicative for light reflections (Figure 4.7A). With the exception of the increased filling volume of 1.2 mL, the measurement position, ring geometry and cultivation conditions remained identical. This observation indicates that the filling volume has an influence on light reflections, and thereby on the detection of low initial biomass concentrations. Nevertheless, the fluid dynamics within the ring compartment are still unknown and therefore explanations concerning the underlying optical effects would remain speculative.

In phase *II*, the culture runs into an oxygen limitation, which is visible in the DOT of 0 % as well as in the observed horizontal OTR plateau (Figure 4.7A, B). As described in literature, the horizontal OTR plateau is characteristic for oxygen limited conditions, thereby indicating the maximum oxygen transfer capacity (OTR_{max}) at the applied operating conditions of the microtiter plate (Anderlei & Büchs, 2001). Oxygen-limited conditions, however, are avoided in fed-batch cultivations with controlled stirred tank reactors. The reason for the oxygen limitation in the microtiter plate-based cultivation is the strong and abrupt initial glucose release of the polymer rings (Figure 4.4, Standard release matrix). The strong and abrupt initial glucose release results in an enhanced accumulation of glucose within the batch phase, which causes oxygen-limited conditions. The initiation of the oxygen limitation is also reflected in the course of the scattered light intensity that switches from exponential to linear growth (Figure 4.7A). Similar to the batch experiments in Figure 4.6C and F, under oxygen-limited conditions the pH continues to fall, whereby the EcFbFP fluorescence intensity slightly increases (Figure 4.7C). The persisting downward trend of the pH points at overflow metabolism caused by an excess of glucose.

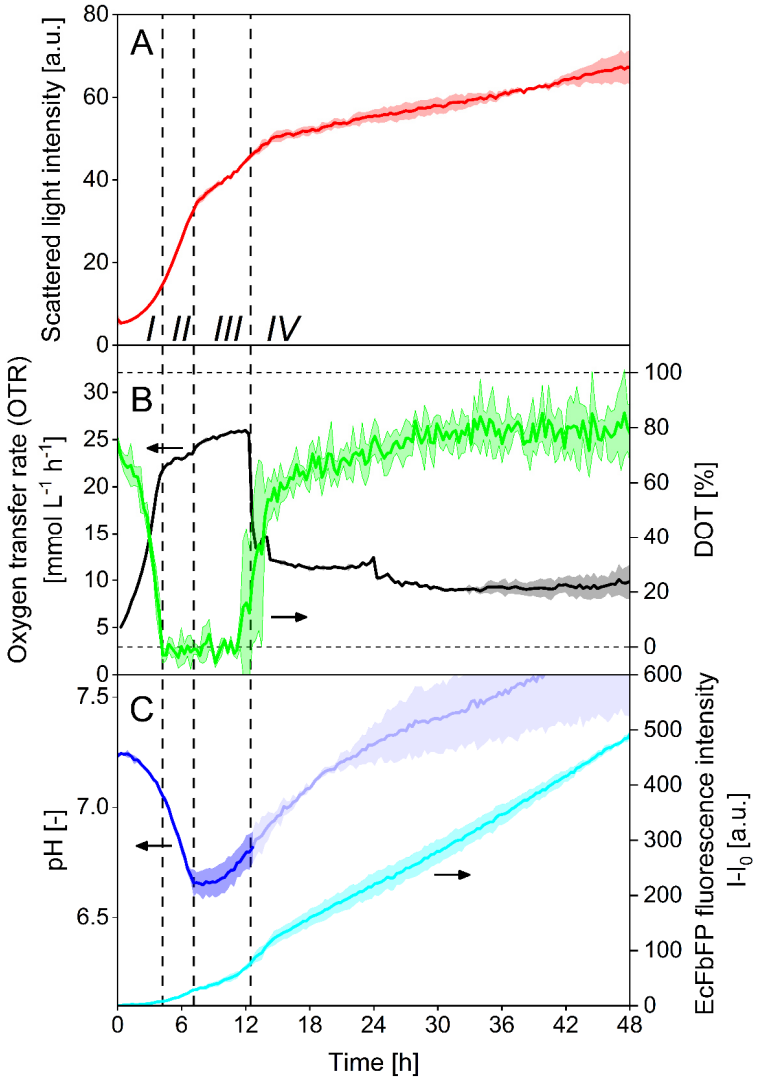

Figure 4.7: Fed-batch cultivation of *E. coli* BL21 (DE3) in wells with polymer ring. (A) Scattered light intensity, (B) DOT, oxygen transfer rate, (C) pH and EcFbFP fluorescence intensity over time. Oxygen transfer rates were measured in a parallel experiment with a µRAMOS device [n = 2]. After approximately 12 h, the pH course is faded out due to measurement interferences with EcFbFP fluorescence. The polymer ring had an outer diameter of 12 mm and inner diameter of 8 mm. Glucose release was realized by using the standard release polymer matrix. Roman numbers divide the cultivation into four distinct phases: *I* unlimited growth on glucose, *II* oxygen limited growth on glucose, *III* oxygen and glucose limited growth on overflow metabolites, *IV* glucose limited growth. Cultivations were done in triplicates [n = 3], shadows symbolize the standard deviation. Adjusted measurement position for biomass and fluorescence (x = 4.5 mm, y = 0 mm). Culture medium: Wilms-MOPS medium, 0 g L^{-1} glucose, 0.2 M MOPS, OD_{600} = 0.5. Cultivation conditions: 48-well round- deep-well microtiter plate with optodes, n = 1000 rpm, d_0 = 3 mm, V_{Broth} = 1.2 mL, T = 30 °C.

In phase *III*, the cultures are still oxygen-limited, but the pH switch into an upwards direction indicates the depletion of the previously accumulated glucose (Figure 4.7C). Usually, glucose depletion is accompanied with a distinct drop of the OTR (Bähr et al., 2012; Philip et al., 2017, 2018). At the same time, the DOT should abruptly increase (Funke, Buchenauer, Mokwa, et al.,

2010; Toeroek et al., 2015). However, the OTR as well as the DOT indicate a still persisting oxygen limitation (Figure 4.7B). Under glucose-limited conditions, *E. coli* BL21 (DE3) switches metabolism and starts to consume the previously accumulated overflow metabolites in parallel to the released glucose (Riesenberg et al., 1991). In presence of a glucose feed, for example, acetate consumption is three times faster compared to glucose starvation conditions (Xu, Jahic, & Enfors, 1999). Due to this fast metabolic switch towards parallel acetate consumption, a distinct drop of the OTR and DOT is not visible within this experiment (Figure 4.7B). Consequently, this phase is characterized by oxygen- and glucose-limited growth with overflow metabolites in excess. When compared to the oxygen-limited conditions in phase *II*, these conditions result in a reduced growth, visible from the slope of the linearly increasing scattered light intensity (Figure 4.7A).

In phase *IV*, the OTR drops sharply, whereas the DOT increases likewise (Figure 4.7A, B). At this point, overflow metabolites are depleted and the cultures are solely glucose-limited. In this phase, both the OTR and DOT exhibit a nearly constant plateau that is defined by the constant glucose release rate of 0.37 mg h^{-1} from the polymer ring. The scattered light intensity increases constantly and linearly. This linear increase is the result of a constant feeding rate under carbon-limited conditions (Bower, Lee, Ram, & Prather, 2012; Funke et al., 2010; Panula-Perälä et al., 2008; Wilming, Bähr, Kamerke, & Büchs, 2014; Xu et al., 1999). The slope of the scattered light intensity of phase *IV* indicates that under glucose-limited conditions, growth slows down when compared to phase *II* and *III*. Nevertheless, the EcFbFP fluorescence intensity constantly and linearly increases under glucose limited-conditions (Figure 4.7C). This highlights the de-repressive effect of glucose-limited conditions for EcFbFP synthesis with the applied *E. coli* BL21 (DE3) strain, without the necessity of online sampling (Bähr et al., 2012; Philip et al., 2017). As already mentioned above, EcFbFP fluorescence interferes with the pH signal from the fluorescent optode (Kunze et al., 2014). Due to the high EcFbFP intensities achieved under glucose-limited conditions, the online pH signal is faded out in phase *IV* (Figure 4.7C).

The data presented in Figure 4.7 demonstrate that the polymer ring enables fed-batch operation with parallel online measurement of scattered light, DOT, pH and fluorescence with the BioLector. The acquired online data reflect typical fed-batch growth phases. Without these online signals, the determination of the time points of transition from one growth phase to another would require frequent offline sampling. The time points of transition were in

accordance with the online OTR. Since the OTR was measured in parallel cultures using the µRAMOS device, the OTR measurement represents an opportunity to independently validate the online data measured with the BioLector.

To reveal the robustness of online monitoring in wells with polymer ring, further fed-batch cultivations with varied initial culture conditions were conducted. On basis of the acquired online data, quantitative relations of *E. coli* BL21 (DE3) fed-batch cultivations with different initial biomass concentration are shown (Appendix 19).

4.3.6 Comparison of batch and fed-batch cultivations with polymer ring

The polymer ring enables fed-batch operation with parallel online monitoring. Consequently, batch and fed-batch mode can directly be compared based on online signals. Thus, time-, labor- and cost-intensive offline sampling can completely be avoided. Figure 4.8 shows the course of scattered light, OTR, DOT, pH and EcFbFP fluorescence of parallel *E. coli* BL21 (DE3) batch and fed-batch cultivations. The individual phases of the batch and fed-batch cultivation were already described in detail in Chapter 4.3.5. In this section, the focus is on comparing the outcome of batch and fed-batch cultivations on basis of the acquired online signals.

After 48 h of cultivation, 25.2 and 26 mg of glucose (corresponding to 21 and 21.7 g L^{-1}) were consumed within the batch and fed-batch cultivation, respectively. The corresponding biomass yield ($Y_{X/S_{Glu}}$) (scattered light [a.u.] / consumed glucose [mg]) shows a 1.7-fold increase when fed-batch is related to batch. The EcFbFP yield ($Y_{P_{FbFP}/S_{Glu}}$) is 2.4-fold increased.

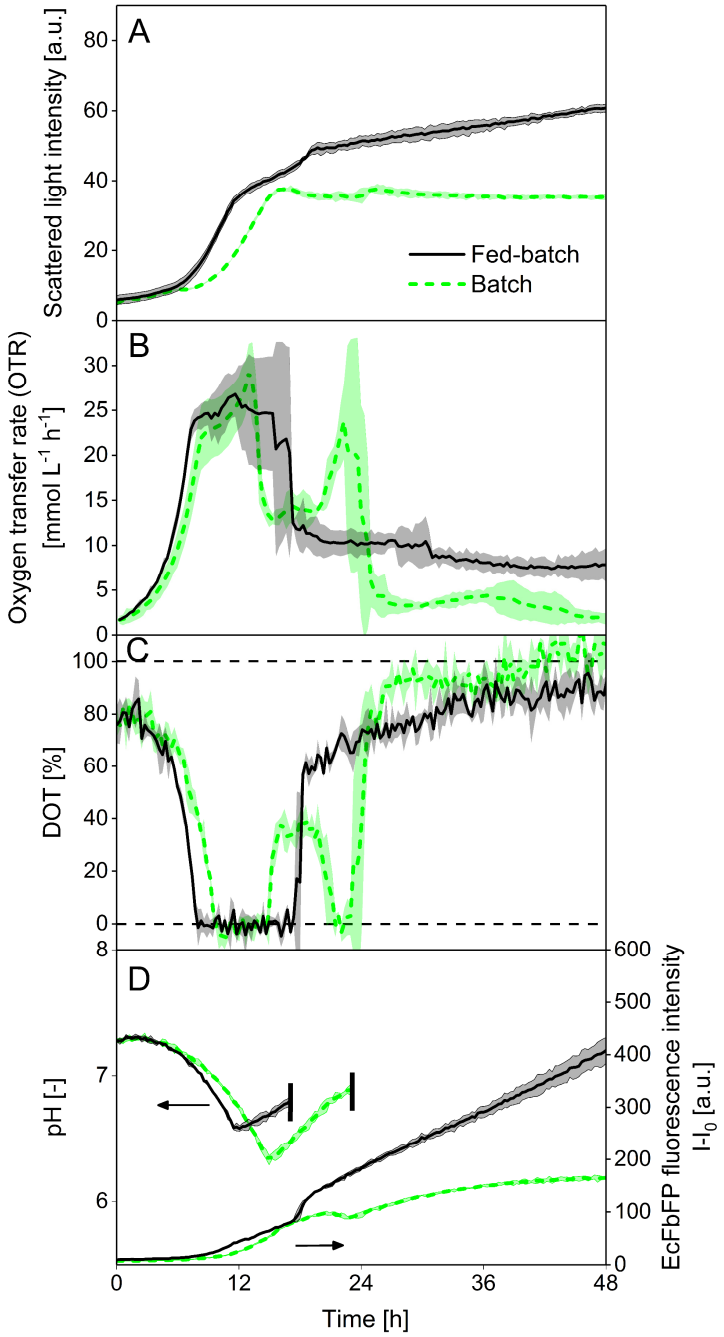

Figure 4.8: Comparison of batch and fed-batch cultivations of *E. coli* BL21 (DE3) in wells with polymer ring. (A) Scattered light intensity, (B) oxygen transfer rate, (C) DOT, (D) pH and EcFbFP fluorescence intensity over time. The oxygen transfer rate was measured in a parallel experiment with a µRAMOS device [n = 2]. The pH course is only shown up to 17 and 23 h, respectively. Polymer rings had an outer diameter of 12 mm and inner diameter of 8 mm. For fed-batch cultivations, glucose release was realized by using the standard release polymer matrix. For batch cultivations, the slow release polymer matrix that releases negligible amounts of glucose was used. Cultivations were done in triplicates [n = 3], shadows symbolize the standard deviation. Adjusted measurement position for biomass and fluorescence (x = 4.5 mm, y = 0 mm). Culture medium: Wilms-MOPS medium, 0 g L^{-1} glucose for fed-batch/20 g L^{-1} glucose for batch, 0.2 M MOPS, OD_{600} = 0.1. Cultivation conditions: 48-well round- deep-well microtiter plate with optodes, n = 1000 rpm, d_0 = 3 mm, V_{Broth} = 1.2 mL, T = 30 °C.

It is generally known that *E. coli* fed-batch processes outperform batch processes in terms of biomass and product yields (Huang, Lin, & Yang, 2012; Shiloach & Fass, 2005). This is mainly due to the reduction of glucose overflow metabolism that causes the formation and secretion of various overflow metabolites, such as acetate, that have a negative effect on cell growth and protein production. The secondary OTR and DOT peak indicates overflow metabolite consumption in batch cultivations (Figure 4.8B, C). Under glucose-limited conditions, overflow metabolites are consumed instead of being produced (Riesenberg et al., 1991). The reduced accumulation of overflow metabolites is also apparent from the pH that drops to 6.3 in batch and to 6.6 in fed-batch (Figure 4.8D). Since growth is highly dependent on pH (Davey, 1994), the increased acidification in batch mode may result in suboptimal growth conditions. Furthermore, glucose-limited conditions cause a de-repression of the catabolite repression in *E.coli* (Görke & Stülke, 2008). Since within the used *E. coli* BL21 (DE3) strain EcFbFP synthesis is catabolite controlled, the positive effect of glucose-limited conditions is evident from the 2.4-fold increased yield ($Y_{P_{FbFP}/S_{Glu}}$) when compared to batch.

4.4 Summary

In this chapter, a glucose-containing polymer matrix was used to manufacture polymer rings that were placed at the bottom of a 48-well microtiter plate. Thereby, the liquid content of the well became accessible for optical measurement with the BioLector device. Reflections caused by the polymer ring were minimized by adjusting the scattered light measurement position. Influences on the measurement of the DOT and pH could be avoided by choosing appropriate polymer ring geometries. These adjustments enabled parallel online measurement of scattered light, fluorescence, DOT and pH of *Escherichia coli* BL21 (DE3) fed-batch cultivations. The online monitoring and fed-batch operation capabilities of the here presented fed-batch microtiter plate finds optimal application in screenings and initial bioprocess development.

Chapter 5

Conclusion and Outlook

Small-scale shaken bioreactors are the most frequently used reaction vessels for optimal strain and medium screening programs as well as for initial bioprocess development (Klöckner & Büchs, 2012). Experiments in small-scale shaken bioreactors are usually performed in batch mode without online monitoring. In contrast, the predominant mode in industrial production processes is substrate-limited fed-batch. Fed-batch mode is applied in order to overcome adverse effects like overflow metabolism, substrate inhibition, osmotic inhibition, oxygen limitation and catabolite repression. To mimic the physiological conditions relevant for fed-batch production processes already during screening and initial bioprocess development, small-scale shaken bioreactors operated in fed-batch mode with parallel online monitoring were investigated and developed.

In Chapter 2, membrane-based fed-batch shake flasks were used to introduce a variety of defined substrate-limited fed-batch conditions at small scale. The investigation of substrate limitations plays an important role for the understanding and optimization of protease expression using *Bacillus licheniformis*. In batch mode, a high initial glucose concentration clearly showed a repressing effect on protease activity. After glucose depletion, the protease activity increased. However, the resulting glucose starvation conditions are completely undefined in terms of nutrient availability. Thus, glucose- and NH_4^+-limited fed-batch conditions were introduced to examine the reaction of *B. licheniformis*. In a fed-batch cultivation with a constant and continuous glucose release rate, the protease activity started to increase as soon as

glucose became the growth limiting substrate. However, when the glucose release rate was increased under the applied experimental conditions, NH_4^+ depleted and the process switched from glucose to NH_4^+ limitation. Since elevated concentrations of NH_4^+ also exhibited inhibiting effects on *B. licheniformis*, glucose and NH_4^+ were fed simultaneously into the culture broth. As a result, substrate inhibition was reduced and nitrogen depletion was prevented. In fact, NH_4^+-limited fed-batch cultivations reached final relative protease activities comparable to glucose-limited cultivations. Under NH_4^+-limited conditions, however, growth ceased and production of overflow metabolites continued. Finally, glucose and NH_4^+-limited fed-batch cultivations with different release rates were compared based on the protease yield. Interestingly, the obtained protease yields ($Y_{P/S_{Glu}}$) differ under glucose and NH_4^+-limitation, but were independent of the release rate. This suggests that for the investigated *B. licheniformis* strain, the general need of a defined substrate-limited fed-batch operation mode is more decisive than the degree of limitation, in other words the feeding rate.

The scale-up of the 250 mL to the 500 mL membrane-based fed-batch shake flask demonstrated the scalability of the underlying operating principle. With a constant volumetric glucose release rate, both systems exhibited similar results in terms of online and offline data. The main advantage of having membrane-based fed-batch shake flask systems of various scales can be attributed to the filling volume. With an increased filling volume, more product can be harvested. This can be advantageous in applications that otherwise would require time and cost intensive stirred tank reactor cultivations. Since currently no limits concerning the scalability are known, future projects could deal with the design and construction of membrane-based fed-batch shake flask systems with a nominal volume of 1 to 5 L.

Independent from scale, membrane-based fed-batch shake flasks proved to be versatile, easy to use, reliable and robust. Nevertheless, to standardize and simplify use, the further development towards a single-use product is required. Since the manual application of the membrane onto the diffusion tip is the most time-consuming step, special emphasis should be placed on developing a ready to use and disposable diffusion tip where the membrane is already fixed. Besides the diffusion tip with feed reservoir, no peripheral equipment is neccesary to realize feeding. This characteristic allows a parallelized application, which is neccesary for screening and initial bioprocess development. Furthermore, the membrane-based fed-batch

shake flask is not limited in the spectrum of feedable nutrients. Various defined substrate limitations can be introduced to get deeper insights into the regulatory elements of recombinant protein production with various promoters and host strains. With knowledge of the control mechanisms of product biosynthesis, production can be optimized by designing fed-batch strategies in stirred tank reactors that are individually tailored to the used production host.

The 250 mL as well as 500 mL membrane-based fed-batch shake flasks are compatible with the RAMOS device. Based on the OTR course over time, the fed batch cultivations can be clearly divided into batch and fed-batch phase without time-consuming sampling and offline analysis. Further, the OTR gives a direct feedback on the release kinetics and makes the detection of unknown secondary substrate limitations possible. Since a high comparability between the glucose- ($Y_{P/S_{Glu}}$) and oxygen-based yield (Y_{P/O_2}) was found for the applied *B. licheniformis* culture, the OTR proved to be an adequate parameter to deduce the oxygen-based yield (Y_{P/O_2}) as process performance indicator.

In Chapter 3, polymer-based controlled-release microtiter plates were successfully used for glucose-limited fed-batch cultivations of a protease producing *B. licheniformis* strain. Reproducibility was shown by means of cultivation experiments using five individual polymer-based controlled-release fed-batch microtiter plates from two different production lots. µRAMOS-based online OTR monitoring provided the basis to visualize the effect of changing initial cultivation conditions, such as biomass concentration, filling volume and osmotic pressure. The initial biomass concentration has a direct influence on glucose accumulation, and thus, on the extend of the batch phase. The filling volume enables changing the volumetric release rate, whereas the osmotic pressure physically influences the release rate. It was further shown that an increasing osmotic pressure negatively influences growth and protease yield. These results provide the basis for future designs of high-throughput strain and media screening experiments with *B. licheniformis* using the polymer-based controlled-release fed-batch microtiter plate.

Fed-batch cultivations with a similar volumetric glucose release rate were highly comparable in polymer-based controlled-release microtiter plates and 250 mL membrane-based shake flasks. A good comparability was also achieved between the 250 and 500 mL membrane-based fed-batch shake flasks and between 250 mL membrane-based fed-batch shake flasks and

laboratory stirred tank reactors (Müller et al., 2019; Philip et al., 2017). Being able to introduce fed-batch conditions at each scale during development projects, paves the way to obtain consistent and transferable conditions. For instance, after a primary screening in polymer-based controlled-release fed-batch microtiter plates, the versatile membrane-based fed-batch shake flasks could be applied to evaluate various substrate-limited fed-batch modes before continuing with process optimization in stirred tank reactors.

Combining small-scale shaken bioreactors operated in fed-batch mode with online monitoring devices, such as the µRAMOS device, significantly increased information content. This enables creating and validating mathematical models in early development stages, which improves process understanding. The established model can be used to determine the maximum oxygen transfer capacity (OTR_{max}) and the length of the batch phase as a function of the initial biomass concentration. On this basis, extended batch phases with possible oxygen limitations can be avoided. Hence, the model enables defining optimal cultivation conditions for screening processes with the polymer-based controlled-release fed-batch microtiter plate.

In Chapter 4, a polymer-based glucose release microtiter plate enabling online monitoring with the BioLector device was presented. Fed-batch mode with parallel online monitoring of scattered light, DOT, pH and fluorescence was realized by introducing a glucose-releasing polymer ring to the bottom of each well. Depending on the measurement position, the polymer ring caused reflections. Reflections could be minimized by choosing an adapted measuring position. It was further shown that the ring geometry influenced the DOT and pH measurement. A polymer ring with an inner diameter of 6 or 7 mm covered a part of the fluorescent optodes on the bottom of the microtiter plate and hampered correct measurements. An accurate measurement of DOT and pH was possible using a polymer ring with an inner diameter of 8 mm. Based on these adjustments, scattered light, DOT, pH and EcFbFP fluorescence was comparable in wells without and with polymer ring.

The presented microtiter plate uses the polymer-based controlled-release system to introduce fed-batch conditions (Chapter 3). Glucose is released continuously from the polymer matrix and was described to be stable and reproducible (Keil et al., 2019). However, due to the manual manufacturing of the polymer rings, the cut surface of the polymer ring caused a strong and abrupt initial glucose release. This glucose release characteristic resulted in oxygen-limited

conditions, which do not occur in fed-batch cultivations with controlled stirred tank reactors. To avoid the strong and abrupt initial glucose release, future polymer rings should be manufactured by using molds so that the entire surface of the ring is polymerized. Thus, the robust release characteristics of the polymer matrix find optimal application for strain screening under physiological conditions relevant for fed-batch production processes. Due to the unrestrained possibilities for online monitoring with the BioLector device, process relevant data are already obtained during screening. Based on the acquired online data, valuable information for the initial bioprocess development are gained. Thus, the here presented fed-batch microtiter plate is not only an efficient tool for the secured selection of optimal production strains, but also for accelerating initial bioprocess development.

In this thesis, small-scale shaken bioreactors were operated in fed-batch mode with parallel online monitoring. In shake flasks, fed-batch mode was realized by applying a membrane-based release system while in microtiter plates fed-batch mode was achieved with a polymer-based release system. Besides enabling a continuous substrate release at small scale, special emphasis was placed on parallel online monitoring. Shake flasks were designed to be compatible with the RAMOS device while the polymer-based controlled-release fed-batch microtiter plate was online monitored with the µRAMOS device. Further process parameters, such as scattered light (biomass), fluorescence (fluorescent proteins or metabolites), dissolved oxygen tension (DOT) and pH, became accessible with the BioLector device by developing a fed-batch microtiter plate with a polymer ring on the bottom of each well. Finally, the presented small-scale shaken bioreactors allow fed-batch operation with parallel online monitoring of the most important process parameters. This allows to mimic the physiological conditions relevant for fed-batch production processes already during initial bioprocess development and paves the way for a consistent and accelerated bioprocess development.

Bibliography

Anderlei, T., & Büchs, J. (2001). Device for sterile online measurement of the oxygen transfer rate in shaking flasks. *Biochemical Engineering Journal*, *7*(2), 157–162. http://doi.org/10.1016/S1369-703X(00)00116-9

Anderlei, T., Zang, W., Papaspyrou, M., & Büchs, J. (2004). Online respiration activity measurement (OTR, CTR, RQ) in shake flasks. *Biochemical Engineering Journal*, *17*(3), 187–194. http://doi.org/10.1016/S1369-703X(03)00181-5

Arain, S., John, G. T., Krause, C., Gerlach, J., Wolfbeis, O. S., & Klimant, I. (2006). Characterization of microtiterplates with integrated optical sensors for oxygen and pH, and their applications to enzyme activity screening, respirometry, and toxicological assays. *Sensors and Actuators, B: Chemical*, *113*(2), 639–648. http://doi.org/10.1016/j.snb.2005.07.056

Bähr, C. (2013). Small-scale bioreactors for efficient bioprocess development (Doctoral thesis). RWTH Aachen University.

Bähr, C., Leuchtle, B., Lehmann, C., Becker, J., Jeude, M., Peinemann, F., … Büchs, J. (2012). Dialysis shake flask for effective screening in fed-batch mode. *Biochemical Engineering Journal*, *69*, 182–195. http://doi.org/10.1016/j.bej.2012.08.012

Bareither, R., & Pollard, D. (2011). A review of advanced small-scale parallel bioreactor technology for accelerated process development: Current state and future need. *Biotechnology Progress*, *27*(1), 2–14. http://doi.org/10.1002/btpr.522

Bettin, H., Emmerich, A., Frank, S., & Hans, T. (1998). Density data for aqueous solutions of glucose. *Sugar Industry*, *123*(5), 341–348.

Bower, D. M., Lee, K. S., Ram, R. J., & Prather, K. L. J. (2012). Fed-batch microbioreactor platform for scale down and analysis of a plasmid DNA production process. *Biotechnology*

and Bioengineering, *109*(8), 1976–1986. http://doi.org/10.1002/bit.24498

Bruder, S., Reifenrath, M., Thomik, T., Boles, E., & Herzog, K. (2016). Parallelised online biomass monitoring in shake flasks enables efficient strain and carbon source dependent growth characterisation of *Saccharomyces cerevisiae*. *Microbial Cell Factories*, *15*(1), 127. http://doi.org/10.1186/s12934-016-0526-3

Büchs, J. (2001). Introduction to advantages and problems of shaken cultures. *Biochemical Engineering Journal*, *7*(2), 91–98. http://doi.org/10.1016/S1369-703X(00)00106-6

Büchs, J., Lotter, S., & Milbradt, C. (2001). Out-of-phase operating conditions, a hitherto unknown phenomenon in shaking bioreactors. *Biochemical Engineering Journal*, *7*(2), 135–141. http://doi.org/10.1016/S1369-703X(00)00113-3

Çalık, P., Bilir, E., Çalık, G., & Özdamar, T. H. (2002). Influence of pH conditions on metabolic regulations in serine alkaline protease production by *Bacillus licheniformis*. *Enzyme and Microbial Technology*, *31*(5), 685–697. http://doi.org/10.1016/S0141-0229(02)00162-X

Çalık, P., Çalık, G., & Özdamar, T. H. (2000). Oxygen-transfer strategy and its regulation effects in serine alkaline protease production by *Bacillus licheniformis*. *Biotechnology and Bioengineering*, *69*(3), 301–311. http://doi.org/10.1002/1097-0290(20000805)69:3<301::AID-BIT8>3.0.CO;2-4

Chen, P. T., Shaw, J.-F., Chao, Y.-P., Ho, T.-H. D., & Yu, S.-M. (2010). Construction of chromosomally located T7 expression system for production of heterologous secreted proteins in *Bacillus subtilis*. *Journal of Agricultural and Food Chemistry*, *58*(9), 5392–5399. http://doi.org/10.1021/jf100445a

Cui, W., Han, L., Suo, F., Liu, Z., Zhou, L., & Zhou, Z. (2018). Exploitation of *Bacillus subtilis* as a robust workhorse for production of heterologous proteins and beyond. *World Journal of Microbiology and Biotechnology*, *34*(10), 145. http://doi.org/10.1007/s11274-018-2531-7

Davey, K. R. (1994). Modelling the combined effect of temperature and pH on the rate coefficient for bacterial growth. *International Journal of Food Microbiology*, *23*(3–4), 295–303. http://doi.org/10.1016/0168-1605(94)90158-9

DelMar, E. G., Largman, C., Brodrick, J. W., & Geokas, M. C. (1979). A sensitive new substrate for chymotrypsin. *Analytical Biochemistry*, *99*(2), 316–320. http://doi.org/10.1016/S0003-2697(79)80013-5

Drepper, T., Eggert, T., Circolone, F., Heck, A., Krauß, U., Guterl, J.-K., … Jaeger, K.-E. (2007). Reporter proteins for in vivo fluorescence without oxygen. *Nature Biotechnology*, *25*(4), 443–445. http://doi.org/10.1038/nbt1293

Drepper, T., Huber, R., Heck, A., Circolone, F., Hillmer, A.-K., Büchs, J., & Jaeger, K.-E. (2010). Flavin mononucleotide-based fluorescent reporter proteins outperform green fluorescent protein-like proteins as quantitative in vivo real-time reporters. *Applied and Environmental Microbiology*, *76*(17), 5990–5994. http://doi.org/10.1128/AEM.00701-10

Duetz, W. A. (2007). Microtiter plates as mini-bioreactors: Miniaturization of fermentation methods. *Trends in Microbiology*, *15*(10), 469–475. http://doi.org/10.1016/J.TIM.2007.09.004

Eiteman, M. A., & Altman, E. (2006). Overcoming acetate in *Escherichia coli* recombinant protein fermentations. *Trends in Biotechnology*, *24*(11), 530–536. http://doi.org/10.1016/J.TIBTECH.2006.09.001

Emmerich, W., Battino, R., & Wilcock, R. J. (1976). Low-pressure solubility of gases in liquid water. *Chemical Reviews*, *77*(2), 219–262.

Flitsch, D., Krabbe, S., Ladner, T., Beckers, M., Schilling, J., Mahr, S., … Büchs, J. (2016). Respiration activity monitoring system for any individual well of a 48-well microtiter plate. *Journal of Biological Engineering*, *10*(1), 14. http://doi.org/10.1186/s13036-016-0034-3

Frankena, J., Koningstein, G. M., van Verseveld, H. W., & Stouthamer, A. H. (1986). Effect of different limitations in chemostat cultures on growth and production of exocellular protease by *Bacillus licheniformis*. *Applied Microbiology and Biotechnology*, *24*(2), 106–112. http://doi.org/10.1007/BF00938779

Frankena, J., van Verseveld, H. W., & Stouthamer, A. H. (1985). A continuous culture study of the bioenergetic aspects of growth and production of exocellular protease in *Bacillus licheniformis*. *Applied Microbiology and Biotechnology*, *22*(3), 169–176. http://doi.org/10.1007/BF00253604

Fujita, Y. (2009). Carbon catabolite control of the metabolic network in *Bacillus subtilis*. *Bioscience, Biotechnology, and Biochemistry*, *73*(2), 245–59. http://doi.org/10.1271/bbb.80479

Funke, M., Buchenauer, A., Mokwa, W., Kluge, S., Hein, L., Müller, C., … Büchs, J. (2010). Bioprocess Control in Microscale: Scalable Fermentations in Disposable and User-Friendly Microfluidic Systems. *Microbial Cell Factories*, *9*(1), 86. http://doi.org/10.1186/1475-2859-9-86

Funke, M., Buchenauer, A., Schnakenberg, U., Mokwa, W., Diederichs, S., Mertens, A., … Büchs, J. (2010). Microfluidic biolector-microfluidic bioprocess control in microtiter plates. *Biotechnology and Bioengineering*, *107*(3), 497–505. http://doi.org/10.1002/bit.22825

Gebhard, S., Popp, P., Höfler, C., Mascher, T., Fritz, G., Fritsch, A., & Heckmann, J. (2016). Cannibalism stress response in *Bacillus subtilis*. *Microbiology*, *162*(1), 164–176. http://doi.org/10.1099/mic.0.000176

Giesecke, U., Bierbaum, G., Rudde, H., Spohn, U., & Wandrey, C. (1991). Production of alkaline protease with *Bacillus licheniformis* in a controlled fed-batch process. *Applied Microbiology and Biotechnology*, *35*(6), 720–724. http://doi.org/10.1007/BF00169884

Gonzalez-Pastor, J. E., Hobbs, E. C., & Losick, R. (2003). Cannibalism by sporulating bacteria.

Science, *301*(5632), 510–513. http://doi.org/10.1126/science.1086462

Görke, B., & Stülke, J. (2008). Carbon catabolite repression in bacteria: Many ways to make the most out of nutrients. *Nature Reviews Microbiology*, *6*(8), 613–624. http://doi.org/10.1038/nrmicro1932

Grimm, T., Grimm, M., Klat, R., Neubauer, A., Palela, M., & Neubauer, P. (2012). Enzyme-based glucose delivery as a high content screening tool in yeast-based whole-cell biocatalysis. *Applied Microbiology and Biotechnology*, *94*(4), 931–937. http://doi.org/10.1007/s00253-011-3850-x

Gupta, R., Beg, Q., & Lorenz, P. (2002). Bacterial alkaline proteases: Molecular approaches and industrial applications. *Applied Microbiology and Biotechnology*, *59*(1), 15–32. http://doi.org/10.1007/s00253-002-0975-y

Gupta, R., Gigras, P., Mohapatra, H., Goswami, V. K., & Chauhan, B. (2003). Microbial α-amylases: A biotechnological perspective. *Process Biochemistry*, *38*(11), 1599–1616. http://doi.org/10.1016/S0032-9592(03)00053-0

Hanlon, G. W., Hodges, N. A., & Russell, A. D. (1982). The influence of glucose, ammonium and magnesium availability on the production of protease and bacitracin by *Bacillus licheniformis*. *Microbiology*, *128*(4), 845–851. http://doi.org/10.1099/00221287-128-4-845

Hansen, S., Kensy, F., Käser, A., & Büchs, J. (2011). Potential errors in conventional DOT measurement techniques in shake flasks and verification using a rotating flexitube optical sensor. *BMC Biotechnology*, *11*, 49. http://doi.org/10.1186/1472-6750-11-49

Huang, C.-J., Lin, H., & Yang, X. (2012). Industrial production of recombinant therapeutics in *Escherichia coli* and its recent advancements. *Journal of Industrial Microbiology & Biotechnology*, *39*(3), 383–399. http://doi.org/10.1007/s10295-011-1082-9

Huber, R., Ritter, D., Hering, T., Hillmer, A.-K., Kensy, F., Müller, C., … Büchs, J. (2009).

Robo-Lector – a novel platform for automated high-throughput cultivations in microtiter plates with high information content. *Microbial Cell Factories*, *8*(1), 42. http://doi.org/10.1186/1475-2859-8-42

Huber, R., Scheidle, M., Dittrich, B., Klee, D., & Büchs, J. (2009). Equalizing growth in high-throughput small scale cultivations via precultures operated in fed-batch mode. *Biotechnology and Bioengineering*, *103*(6), 1095–1102. http://doi.org/10.1002/bit.22349

Hubmann, G., Thevelein, J. M., & Nevoigt, E. (2014). Natural and modified promoters for tailored metabolic engineering of the yeast *Saccharomyces cerevisiae*. New York, NY: Humana Press. http://doi.org/10.1007/978-1-4939-0563-8_2

Iwai, Y., & Omura, S. (1982). Culture conditions for screening of new antibiotics. *The Journal of Antibiotics*, *35*(2), 123–141.

Jeude, M., Dittrich, B., Niederschulte, H., Anderlei, T., Knocke, C., Klee, D., & Büchs, J. (2006). Fed-batch mode in shake flasks by slow-release technique. *Biotechnology and Bioengineering*, *95*(3), 433–445. http://doi.org/10.1002/bit.21012

John, G. T., & Heinzle, E. (2001). Quantitative screening method for hydrolases in microplates using pH indicators: Determination of kinetic parameters by dynamic pH monitoring. *Biotechnology and Bioengineering*, *72*(6), 620–627. http://doi.org/10.1002/1097-0290(20010320)72:6<620::AID-BIT1027>3.0.CO;2-W

John, G. T., Klimant, I., Wittmann, C., & Heinzle, E. (2003). Integrated optical sensing of dissolved oxygen in microtiter plates: A novel tool for microbial cultivation. *Biotechnology and Bioengineering*, *81*(7), 829–836. http://doi.org/10.1002/bit.10534

Juturu, V., & Wu, J. C. (2018). Heterologous protein expression in *Pichia pastoris* : Latest research progress and applications. *ChemBioChem*, *19*(1), 7–21. http://doi.org/10.1002/cbic.201700460

Keil, T., Dittrich, B., Lattermann, C., Habicher, T., & Büchs, J. (2019). Polymer-based

controlled-release fed-batch microtiter plate – diminishing the gap between early process development and production conditions. *Journal of Biological Engineering*, *13*(1), 18. http://doi.org/10.1186/s13036-019-0147-6

Kensy, F., Zang, E., Faulhammer, C., Tan, R.-K., & Büchs, J. (2009). Validation of a high-throughput fermentation system based on online monitoring of biomass and fluorescence in continuously shaken microtiter plates. *Microbial Cell Factories*, *8*(1), 31. http://doi.org/10.1186/1475-2859-8-31

Klöckner, W., & Büchs, J. (2012). Advances in shaking technologies. *Trends in Biotechnology*, *30*(6), 307–314. http://doi.org/10.1016/j.tibtech.2012.03.001

Kluge, J., Terfehr, D., & Kück, U. (2018). Inducible promoters and functional genomic approaches for the genetic engineering of filamentous fungi. *Applied Microbiology and Biotechnology*, *102*(15), 6357–6372. http://doi.org/10.1007/s00253-018-9115-1

Korz, D. J., Rinas, U., Hellmuth, K., Sanders, E. A., & Deckwer, W.-D. (1995). Simple fed-batch technique for high cell density cultivation of *Escherichia coli*. *Journal of Biotechnology*, *39*(1), 59–65. http://doi.org/10.1016/0168-1656(94)00143-Z

Krause, M., Ukkonen, K., Haataja, T., Ruottinen, M., Glumoff, T., Neubauer, A., … Vasala, A. (2010). A novel fed-batch based cultivation method provides high cell-density and improves yield of soluble recombinant proteins in shaken cultures. *Microbial Cell Factories*, *9*, 1–11. http://doi.org/10.1186/1475-2859-9-11

Kunze, M., Roth, S., Gartz, E., & Büchs, J. (2014). Pitfalls in optical on-line monitoring for high-throughput screening of microbial systems. *Microbial Cell Factories*, *13*(1), 53. http://doi.org/10.1186/1475-2859-13-53

Ladner, T., Beckers, M., Hitzmann, B., & Büchs, J. (2016). Parallel online multi-wavelength (2D) fluorescence spectroscopy in each well of a continuously shaken microtiter plate. *Biotechnology Journal*, *11*(12), 1605–1616. http://doi.org/10.1002/biot.201600515

Ladner, T., Held, M., Flitsch, D., Beckers, M., & Büchs, J. (2016). Quasi-continuous parallel online scattered light, fluorescence and dissolved oxygen tension measurement combined with monitoring of the oxygen transfer rate in each well of a shaken microtiter plate. *Microbial Cell Factories*, *15*(1), 1–15. http://doi.org/10.1186/s12934-016-0608-2

Laishley, E. J., & Bernlohr, R. W. (1968). Regulation of arginine and proline catabolism in *Bacillus licheniformis*. *Journal of Bacteriology*, *96*(2), 322–329.

Lattermann, C., & Büchs, J. (2015). Microscale and miniscale fermentation and screening. *Current Opinion in Biotechnology*, *35*, 1–6. http://doi.org/10.1016/J.COPBIO.2014.12.005

Liu, L., Liu, Y., Shin, H., Chen, R. R., Wang, N. S., Li, J., … Chen, J. (2013). Developing *Bacillus* spp. as a cell factory for production of microbial enzymes and industrially important biochemicals in the context of systems and synthetic biology. *Applied Microbiology and Biotechnology*, *97*(14), 6113–6127. http://doi.org/10.1007/s00253-013-4960-4

Losen, M., Frölich, B., Pohl, M., & Büchs, J. (2004). Effect of oxygen limitation and medium composition on *Escherichia coli* fermentation in shake flask cultures. *Biotechnology Progress*, *20*(4), 1062–1068. http://doi.org/10.1021/bp034282t

Mao, W., Pan, R., & Freedman, D. (1992). High production of alkaline protease by *Bacillus licheniformis* in a fed-batch fermentation using a synthetic medium. *Journal of Industrial Microbiology*, *11*(1), 1–6. http://doi.org/10.1007/BF01583724

Martin, J. F., & Demain, A. L. (1980). Control of antibiotic biosynthesis. *Microbiological Reviews*, *44*(2), 230–51.

Maurer, K.-H. (2004). Detergent proteases. *Current Opinion in Biotechnology*, *15*(4), 330–334. http://doi.org/10.1016/j.copbio.2004.06.005

Mears, L., Stocks, S. M., Sin, G., & Gernaey, K. V. (2017). A review of control strategies for

manipulating the feed rate in fed-batch fermentation processes. *Journal of Biotechnology*, *245*, 34–46. http://doi.org/10.1016/J.JBIOTEC.2017.01.008

Meier, K., Klöckner, W., Bonhage, B., Antonov, E., Regestein, L., & Büchs, J. (2016). Correlation for the maximum oxygen transfer capacity in shake flasks for a wide range of operating conditions and for different culture media. *Biochemical Engineering Journal*, *109*, 228–235. http://doi.org/10.1016/j.bej.2016.01.014

Meissner, L., Kauffmann, K., Wengeler, T., Mitsunaga, H., Fukusaki, E., & Büchs, J. (2015). Influence of nitrogen source and pH value on undesired poly(γ-glutamic acid) formation of a protease producing *Bacillus licheniformis* strain. *Journal of Industrial Microbiology & Biotechnology*, *42*(9), 1203–1215. http://doi.org/10.1007/s10295-015-1640-7

Mendoza-Vega, O., Sabatié, J., & Brown, S. W. (1994). Industrial production of heterologous proteins by fed-batch cultures of the yeast *Saccharomyces cerevisiae*. *FEMS Microbiology Reviews*, *15*(4), 369–410. http://doi.org/10.1016/0168-6445(94)90070-1

Minihane, B. J., & Brown, D. E. (1986). Fed-batch culture technology. *Biotechnology Advances*, *4*(2), 207–218. http://doi.org/10.1016/0734-9750(86)90309-5

Mühlmann, M. J., Forsten, E., Noack, S., & Büchs, J. (2018). Prediction of recombinant protein production by *Escherichia coli* derived online from indicators of metabolic burden. *Biotechnology Progress*, *34*(6), 1543-1552. http://doi.org/10.1002/btpr.2704

Müller, J., Hütterott, A., Habicher, T., Mußmann, N., & Büchs, J. (2019). Validation of the transferability of membrane-based fed-batch shake flask cultivations to stirred-tank reactor using three different protease producing *Bacillus* strains. *Journal of Bioscience and Bioengineering*, *128*(5), 599–605. https://doi.org/10.1016/j.jbiosc.2019.05.003

Nathan, S., & Nair, M. (2013). Engineering a repression-free catabolite-enhanced expression system for a thermophilic alpha-amylase from *Bacillus licheniformis* MSG. *Journal of Biotechnology*, *168*(4), 394–402. http://doi.org/10.1016/j.jbiotec.2013.09.016

Neubauer, P., Cruz, N., Glauche, F., Junne, S., Knepper, A., & Raven, M. (2013). Consistent development of bioprocesses from microliter cultures to the industrial scale. *Engineering in Life Sciences*, *13*(3), 224–238. http://doi.org/10.1002/elsc.201200021

Novotny, P., & Söhnel, O. (1988). Densities of binary aqueous solutions of 306 inorganic substances. *Journal of Chemical and Engineering Data*, *33*(1), 49–55. http://doi.org/10.1002/bbpc.19850890633

Öztürk, S., Çalık, P., & Özdamar, T. H. (2016). Fed-batch biomolecule production by *Bacillus subtilis* : A state of the art review. *Trends in Biotechnology*, *34*(4), 329–345. http://doi.org/10.1016/j.tibtech.2015.12.008

Panula-Perälä, J., Šiurkus, J., Vasala, A., Wilmanowski, R., Casteleijn, M. G., & Neubauer, P. (2008). Enzyme controlled glucose auto-delivery for high cell density cultivations in microplates and shake flasks. *Microbial Cell Factories*, *7*(31), 1–12. http://doi.org/10.1186/1475-2859-7-31

Panula-Perälä, J., Vasala, A., Karhunen, J., Ojamo, H., Neubauer, P., & Mursula, A. (2014). Small-scale slow glucose feed cultivation of *Pichia pastoris* without repression of AOX1 promoter: Towards high throughput cultivations. *Bioprocess and Biosystems Engineering*, *37*(7), 1261–1269. http://doi.org/10.1007/s00449-013-1098-9

Paul, S., Aggarwal, C., Thakur, J. K., Bandeppa, G. S., Khan, M. A., Pearson, L. M., … Joachimiak, A. (2015). Induction of osmoadaptive mechanisms and modulation of cellular physiology help *Bacillus licheniformis* strain SSA 61 adapt to salt stress. *Current Microbiology*, *70*(4), 610–7. http://doi.org/10.1007/s00284-014-0761-y

Phan, T. T. P., Nguyen, H. D., & Schumann, W. (2012). Development of a strong intracellular expression system for *Bacillus subtilis* by optimizing promoter elements. *Journal of Biotechnology*, *157*(1), 167–172. http://doi.org/10.1016/J.JBIOTEC.2011.10.006

Philip, P., Kern, D., Goldmanns, J., Seiler, F., Schulte, A., Habicher, T., & Büchs, J. (2018). Parallel substrate supply and pH stabilization for optimal screening of *E. coli* with the

membrane-based fed-batch shake flask. *Microbial Cell Factories*, *17*(1), 1–17. http://doi.org/10.1186/s12934-018-0917-8

Philip, P., Meier, K., Kern, D., Goldmanns, J., Stockmeier, F., Bähr, C., & Büchs, J. (2017). Systematic evaluation of characteristics of the membrane-based fed-batch shake flask. *Microbial Cell Factories*, *16*(1), 122. http://doi.org/10.1186/s12934-017-0741-6

Priest, F. G. (1977). Extracellular enzyme synthesis in the genus *Bacillus*. *Bacteriological Reviews*, *41*(3), 711–753.

Rao, M. B., Tanksale, A. M., Ghatge, M. S., & Deshpande, V. V. (1998). Molecular and biotechnological aspects of microbial proteases. *Microbiology and Molecular Biology Reviews*, *62*(3), 597–635.

Riesenberg, D., Schulz, V., Knorre, W. A., Pohl, H.-D., Korz, D., Sanders, E. A., … Deckwer, W.-D. (1991). High cell density cultivation of *Escherichia coli* at controlled specific growth rate. *Journal of Biotechnology*, *20*(1), 17–27. http://doi.org/10.1016/0168-1656(91)90032-Q

Rischbieter, E., Schumpe, A., & Wunder, V. (1996). Gas solubilities in aqueous solutions of organic substances. *Journal of Chemical and Engineering Data*, *41*(4), 809–812. http://doi.org/10.1021/je960039c

Ruiz, B., Chávez, A., Forero, A., García-Huante, Y., Romero, A., Sánchez, M., … Langley, E. (2010). Production of microbial secondary metabolites: Regulation by the carbon source. *Critical Reviews in Microbiology*, *36*(2), 146–167. http://doi.org/10.3109/10408410903489576

Russell, J. B., & Cook, G. M. (1995). Energetics of bacterial growth: Balance of anabolic and catabolic reactions. *Microbiological Reviews*, *59*(1), 48–62. http://doi.org/10.1.1.321.8181

Samorski, M., Müller-Newen, G., & Büchs, J. (2005). Quasi-continuous combined scattered

light and fluorescence measurements: A novel measurement technique for shaken microtiter plates. *Biotechnology and Bioengineering*, *92*(1), 61–68. http://doi.org/10.1002/bit.20573

Sánchez, S., Chávez, A., Forero, A., García-Huante, Y., Romero, A., Sánchez, M., … Ruiz, B. (2010). Carbon source regulation of antibiotic production. *Journal of Antibiotics*, *63*(8), 442–459. http://doi.org/10.1038/ja.2010.78

Sauer, U., Hatzimanikatis, V., Hohmann, H. P., Manneberg, M., van Loon, A. P. G. M., & Bailey, J. E. (1996). Physiology and metabolic fluxes of wild-type and riboflavin-producing *Bacillus subtilis*. *Applied and Environmental Microbiology*, *62*(10), 3687–3696.

Schallmey, M., Singh, A., & Ward, O. P. (2004). Developments in the use of *Bacillus* species for industrial production. *Canadian Journal of Microbiology*, *50*(1), 1–17. http://doi.org/10.1139/W03-076

Scheidle, M., Jeude, M., Dittrich, B., Denter, S., Kensy, F., Suckow, M., … Büchs, J. (2010). High-throughput screening of *Hansenula polymorpha* clones in the batch compared with the controlled-release fed-batch mode on a small scale. *FEMS Yeast Research*, *10*(1), 83–92. http://doi.org/10.1111/j.1567-1364.2009.00586.x

Schroeter, R., Hoffmann, T., Voigt, B., Meyer, H., Bleisteiner, M., Muntel, J., … Bremer, E. (2013). Stress responses of the industrial workhorse *Bacillus licheniformis* to osmotic challenges. *PloS One*, *8*(11), 1–22. http://doi.org/10.1371/journal.pone.0080956

Shiloach, J., & Fass, R. (2005). Growing *E. coli* to high cell density - A historical perspective on method development. *Biotechnology Advances*, *23*(5), 345–357. http://doi.org/10.1016/j.biotechadv.2005.04.004

Singh, K. D., Schmalisch, M. H., Stülke, J., & Görke, B. (2008). Carbon catabolite repression in *Bacillus subtilis*: Quantitative analysis of repression exerted by different carbon sources. *Journal of Bacteriology*, *190*(21), 7275–7284. http://doi.org/10.1128/JB.00848-08

Sonenshein, A. L. (2007). Control of key metabolic intersections in *Bacillus subtilis*. *Nature Reviews Microbiology*, *5*(12), 917–927. http://doi.org/10.1038/nrmicro1772

Stöckmann, C., Maier, U., Anderlei, T., Knocke, C., Gellissen, G., & Büchs, J. (2003). The oxygen transfer rate as key parameter for the characterization of *Hansenula polymorpha* screening cultures. *Journal of Industrial Microbiology & Biotechnology*, *30*(10), 613–622. http://doi.org/10.1007/s10295-003-0090-9

Stöckmann, C., Scheidle, M., Klee, D., Dittrich, B., Merckelbach, A., Hehmann, G., … Gellissen, G. (2009). Process development in *Hansenula polymorpha* and *Arxula adeninivorans*, a re-assessment. *Microbial Cell Factories*, *8*(1), 22. http://doi.org/10.1186/1475-2859-8-22

Sundarram, A., & Murthy, T. P. K. (2014). α-amylase production and applications: A review. *Journal of Applied & Environmental Microbiology*, *2*(4), 166–175. http://doi.org/10.12691/JAEM-2-4-10

Tännler, S., Decasper, S., & Sauer, U. (2008). Maintenance metabolism and carbon fluxes in *Bacillus* species. *Microbial Cell Factories*, *7*(1), 19. http://doi.org/10.1186/1475-2859-7-19

Toeroek, C., Cserjan-Puschmann, M., Bayer, K., & Striedner, G. (2015). Fed-batch like cultivation in a micro-bioreactor: Screening conditions relevant for *Escherichia coli* based production processes. *SpringerPlus*, *4*(1), 490. http://doi.org/10.1186/s40064-015-1313-z

Van der Bruggen, B., Schaep, J., Wilms, D., & Vandecasteele, C. (1999). Influence of molecular size, polarity and charge on the retention of organic molecules by nanofiltration. *Journal of Membrane Science*, *156*(1), 29–41. http://doi.org/10.1016/S0376-7388(98)00326-3

Voigt, B., Albrecht, D., Sievers, S., Becher, D., Bongaerts, J., Evers, S., … Hecker, M. (2015). High-resolution proteome maps of *Bacillus licheniformis* cells growing in minimal medium. *Proteomics*, *15*(15), 2629–2633. http://doi.org/10.1002/pmic.201400504

Voigt, B., Hoi, L. T., Jürgen, B., Albrecht, D., Ehrenreich, A., Veith, B., … Schweder, T. (2007). The glucose and nitrogen starvation response of *Bacillus licheniformis*. *Proteomics*, *7*(3), 413–23. http://doi.org/10.1002/pmic.200600556

Voigt, B., Schweder, T., Sibbald, M. J. J. B., Albrecht, D., Ehrenreich, A., Bernhardt, J., … Hecker, M. (2006). The extracellular proteome of *Bacillus licheniformis* grown in different media and under different nutrient starvation conditions. *Proteomics*, *6*(1), 268–81. http://doi.org/10.1002/pmic.200500091

Weisenberger, S., & Schumpe, A. (1996). Estimation of gas solublility in salt solution at temperatures from 273 to 363 K. *AIChE Journal*, *42*(1), 298–300.

Wewetzer, S. J., Kunze, M., Ladner, T., Luchterhand, B., Roth, S., Rahmen, N., … Büchs, J. (2015). Parallel use of shake flask and microtiter plate online measuring devices (RAMOS and BioLector) reduces the number of experiments in laboratory-scale stirred tank bioreactors. *Journal of Biological Engineering*, *9*(1), 0–18. http://doi.org/10.1186/s13036-015-0005-0

Wiegand, S., Voigt, B., Albrecht, D., Bongaerts, J., Evers, S., Hecker, M., … Liesegang, H. (2013). Fermentation stage-dependent adaptations of *Bacillus licheniformis* during enzyme production. *Microbial Cell Factories*, *12*, 120. http://doi.org/10.1186/1475-2859-12-120

Wilming, A. (2012). Metabolic studies of *Bacillus licheniformis* using small scale batch , fed-batch and continuous cultivations (Doctoral thesis). RWTH Aachen University.

Wilming, A., Bähr, C., Kamerke, C., & Büchs, J. (2014). Fed-batch operation in special microtiter plates: A new method for screening under production conditions. *Journal of Industrial Microbiology and Biotechnology*, *41*(3), 513–525. http://doi.org/10.1007/s10295-013-1396-x

Wilming, A., Begemann, J., Kuhne, S., Regestein, L., Bongaerts, J., Evers, S., … Büchs, J. (2013). Metabolic studies of γ-polyglutamic acid production in *Bacillus licheniformis* by

small-scale continuous cultivations. *Biochemical Engineering Journal*, *73*, 29–37. http://doi.org/10.1016/j.bej.2013.01.008

Wilms, B., Hauck, A., Reuss, M., Syldatk, C., Mattes, R., Siemann, M., & Altenbuchner, J. (2001). High-cell-density fermentation for production of L-N-carbamoylase using an expression system based on the *Escherichia coli* rhaBAD promoter. *Biotechnology and Bioengineering*, *73*(2), 95–103. http://doi.org/10.1002/bit.1041

Xu, B., Jahic, M., Blomsten, G., & Enfors, S.-O. (1999). Glucose overflow metabolism and mixed-acid fermentation in aerobic large-scale fed-batch processes with *Escherichia coli*. *Applied Microbiology and Biotechnology*, *51*(5), 564–571. http://doi.org/10.1007/s002530051433

Xu, B., Jahic, M., & Enfors, S.-O. (1999). Modeling of overflow metabolism in batch and fed-batch cultures of *Escherichia coli*. *Biotechnology Progress*, *15*(1), 81–90. http://doi.org/10.1021/bp9801087

Zimmermann, H. F., Anderlei, T., Büchs, J., & Binder, M. (2006). Oxygen limitation is a pitfall during screening for industrial strains. *Applied Microbiology and Biotechnology*, *72*(6), 1157–1160. http://doi.org/10.1007/s00253-006-0414-6

Appendix

Appendices for Chapter 2

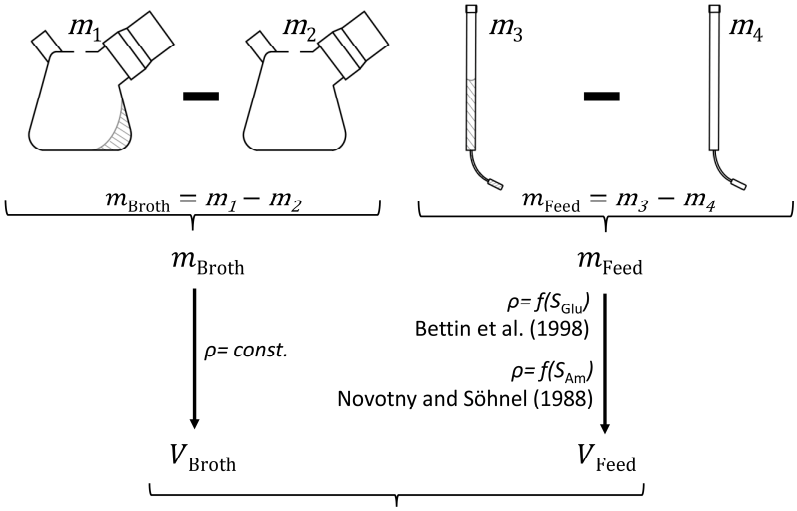

$$m_{\text{Glucose, consumed}} = m_{\text{Glucose, } t_0} - m_{\text{Glucose}}$$

with

$$m_{\text{Glucose}} = S_{\text{Glu, Feed}} \cdot V_{\text{Feed}} + S_{\text{Glu, Broth}} \cdot V_{\text{Broth}}$$

$$m_{\text{Glucose, } t_0} = S_{\text{Glu, Feed, } t_0} \cdot V_{\text{Feed, } t_0} + S_{\text{Glu, Broth, } t_0} \cdot V_{\text{Broth, } t_0}$$

$$m_{\text{Glucose, released}} = m_{\text{Glucose, Feed, } t_0} - m_{\text{Glucose, Feed}}$$

with

$$m_{\text{Glucose, Feed}} = S_{\text{Glu, Feed}} \cdot V_{\text{Feed}}$$

$$m_{\text{Glucose, Feed, } t_0} = S_{\text{Glu, Feed, } t_0} \cdot V_{\text{Feed, } t_0}$$

Appendix 1: Procedure to determine substrate consumption and release in membrane-based fed-batch shake flasks. Weights of the empty shake flask and feed reservoir as well as of the filled shake flask and feed reservoir were measured. To convert the mass into volume, the density of the culture broth was assumed to be constant, whereas the density of the feed solution was calculated based on the glucose (glucose-limited fed-batch, Figure 2.10) and ammonium (ammonium-limited fed-batch, Figure 2.13) concentration. For the two component glucose and ammonium feed (glucose-limited fed-batch, Figure 2.11), the density was calculated based on the glucose concentration without considering ammonium. With known volumes and concentrations of the culture broth and the feed reservoir at the beginning of the cultivation (t_0), the amount of consumed glucose ($m_{\text{Glucose,consumed}}$) can be determined. If the culture is glucose limited at the end of cultivation, the consumed glucose is equal to the released glucose ($m_{\text{Glucose,consumed}} = m_{\text{Glucose,released}}$). If not, the released glucose can be calculated on basis of glucose mass differences within the feed reservoir at the beginning and at the end of cultivation. This procedure shows the determination of glucose consumption and release, however, the procedure is identical to determine consumption and release of ammonium.

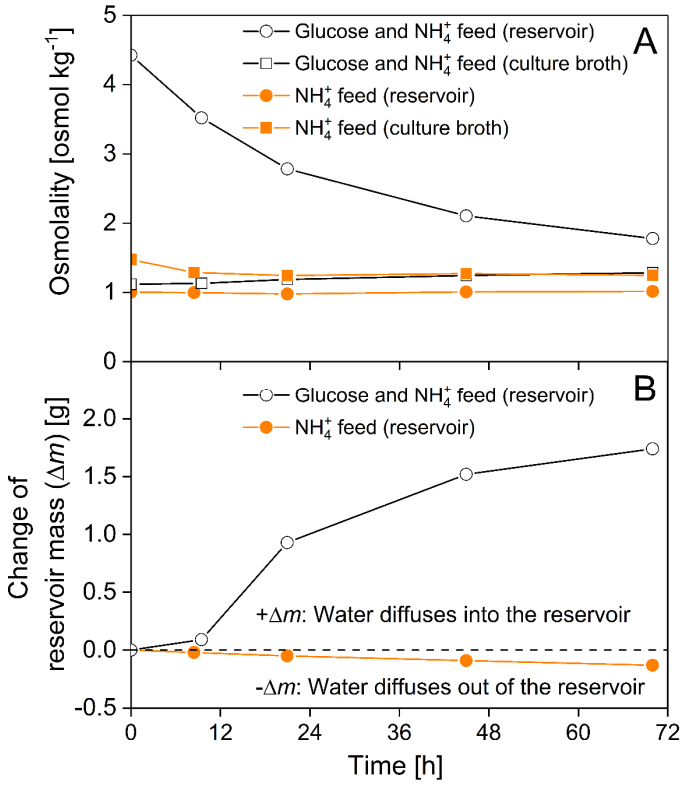

Appendix 2: Water flux into and out of the feed reservoir depending on the osmolality difference between the culture broth and reservoir within the 250 mL membrane-based fed-batch shake flasks. (A, B) Data are shown for 250 mL membrane-based fed-batch shake flask experiments with the highest (two-component glucose and ammonium feed, according to Figure 2.2B and Figure 2.11) and lowest (ammonium feed, according to Figure 2.2C and Figure 2.13) osmolality within the feed reservoir. (A) Osmolality within culture broth and reservoir over time. The osmolality within the feed reservoir of the two component feed experiment (open symbols) has an elevated osmolality when compared to the culture broth. In the experiment with the ammonium feed (closed symbols) the osmolality of the culture broth is higher than the osmolality within the feed reservoir. (B) Change of reservoir mass over time in relation to the beginning of the cultivation. Due to the osmotic effect, water diffuses over the cellulose membrane from the compartment with the lower osmolality into the compartment with the higher osmolality. Consequently, in the two component feed experiment (open symbols) water diffuses into the feed reservoir and increases its mass. For the experiment with the ammonium feed (closed symbols) the water flow is reversed, thereby decreasing the mass of the reservoir.

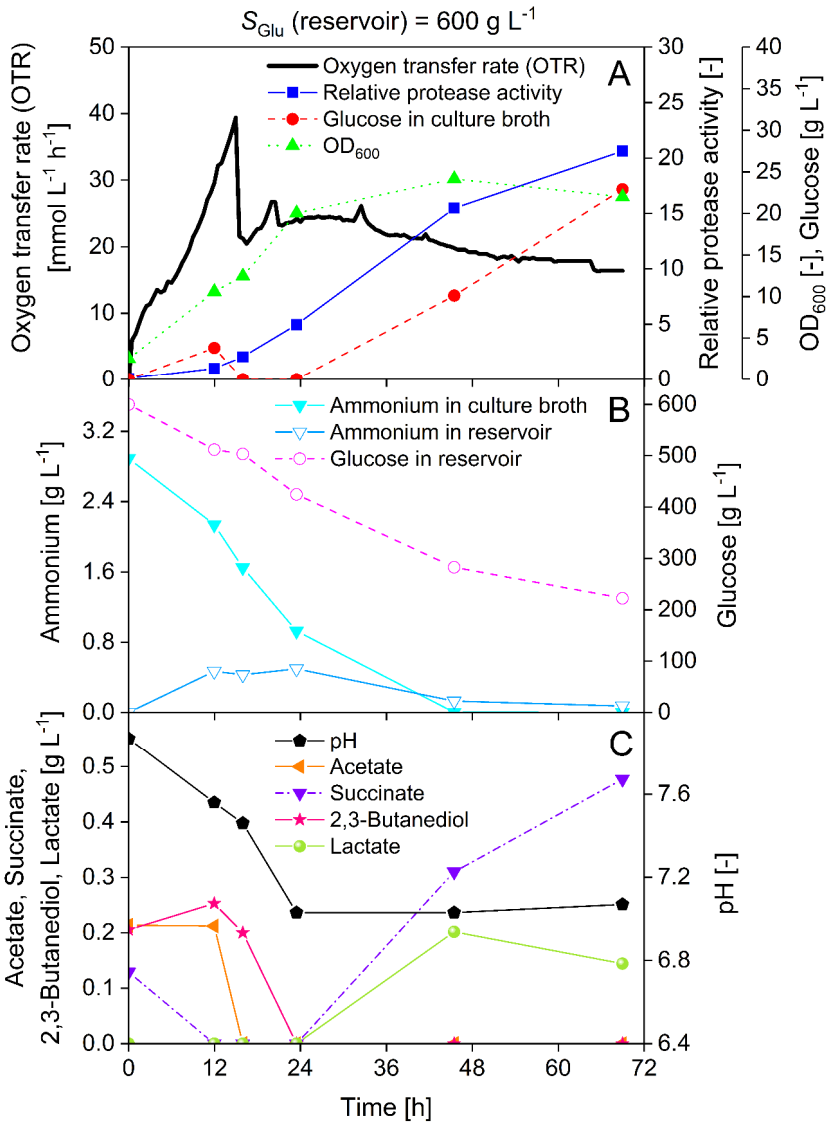

Appendix 3: Carbon (C)-limited fed-batch cultivations of *Bacillus licheniformis* with elevated glucose concentration within the feed reservoir according to Figure 2.2A. (A-C) Glucose concentration of 600 g L^{-1} within the feed reservoir. (A) Oxygen transfer rate (OTR), relative protease activity, glucose concentration and optical density (OD$_{600}$). Protease activities were set in relation to the measured protease activity directly after glucose depletion at 11.5 h within the batch experiment shown in Figure 2.9. (B) Ammonium concentration within culture broth and ammonium and glucose concentration within the feed reservoir. (C) pH value, acetate, succinate, 2,3-butanediol and lactate concentrations. Initial values (culture broth): OD$_{600}$ = 2.5, pH = 7.9, 0 g L^{-1} glucose, 2.9 g L^{-1} ammonium, 0.4 M MOPS buffer, V3 medium. Initial values (reservoir): V_{Feed} = 3 mL, active membrane diameter = 4.8 mm. Membrane: type = RCT-NatureFlex-NP, material = regenerated cellulose, thickness = 42 µm, cut-off = 10–20 kDa. Cultivation parameters: T = 30 °C, 250 mL membrane-based fed-batch shake flask, V_{Broth} = 10 mL, n = 350 rpm, d_0 = 50 mm.

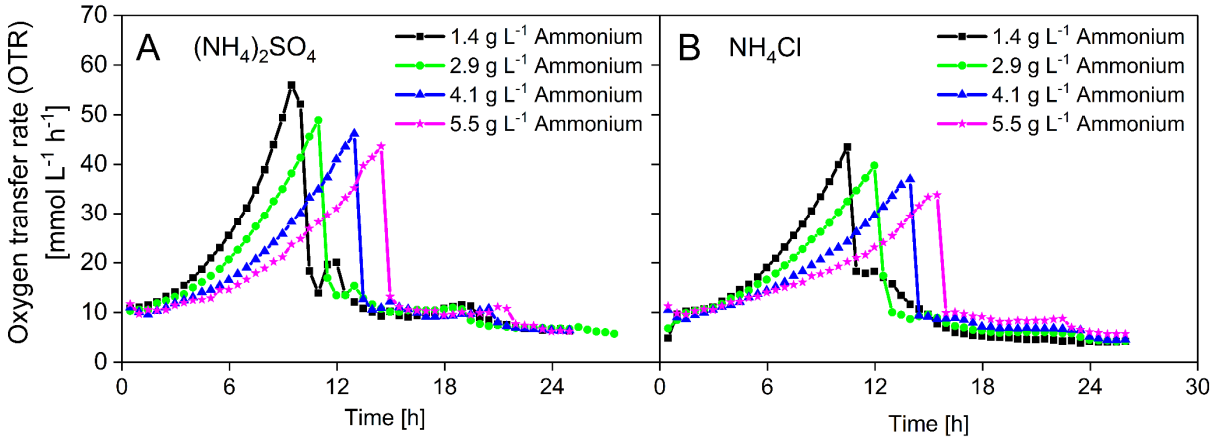

Appendix 4: Influence of ammonium on cultivations with *Bacillus licheniformis.* (A, B) Oxygen transfer rates (OTRs) are shown for batch cultivations with different initial (t = 0) ammonium concentrations. A concentrated sodium chloride solution was added to the 1.4, 2.9 and 4.1 g L^{-1} ammonium experiments to match the osmolality within the 5.5 g L^{-1} experiments. (A) Ammonium sulphate ($(NH_4)_2SO_4$) was used as ammonium source. Initial values: OD_{600} = 2.5, pH = 7.7, 20 g L^{-1} glucose, osmolality 1.03 – 1.09 osmol kg^{-1}, 0.2 M MOPS buffer, V3 medium. (B) Ammonium chloride (NH_4Cl) was used as ammonium source to investigate a hypothetical negative effect of SO_4^{2-} ions. Initial values: OD_{600} = 2.5, pH = 7.6, 20 g L^{-1} glucose, 0.2 M MOPS buffer, osmolality 1.3 - 1.49 osmol kg^{-1}. Despite using the same ammonium concentrations for $(NH_4)_2SO_4$ and NH_4Cl, the inhibiting effect was more pronounced for NH_4Cl. This can be explained by the overall higher osmolality, since $(NH_4)_2SO_4$ contains two moles of NH_4^+ per mole of SO_4^{2-}, whereas NH_4Cl one mole of NH_4^+ per mole of Cl^-. Still not excluded is the question whether Cl^- influences growth, although no literature was found that reported independently of the osmolality about the negative impact of Cl^- -ions on *Bacillus* species. Cultivation conditions: T = 30 °C, 250 mL shake flasks, V_{Broth} = 10 mL, n = 350 rpm, d_0 = 50 mm.

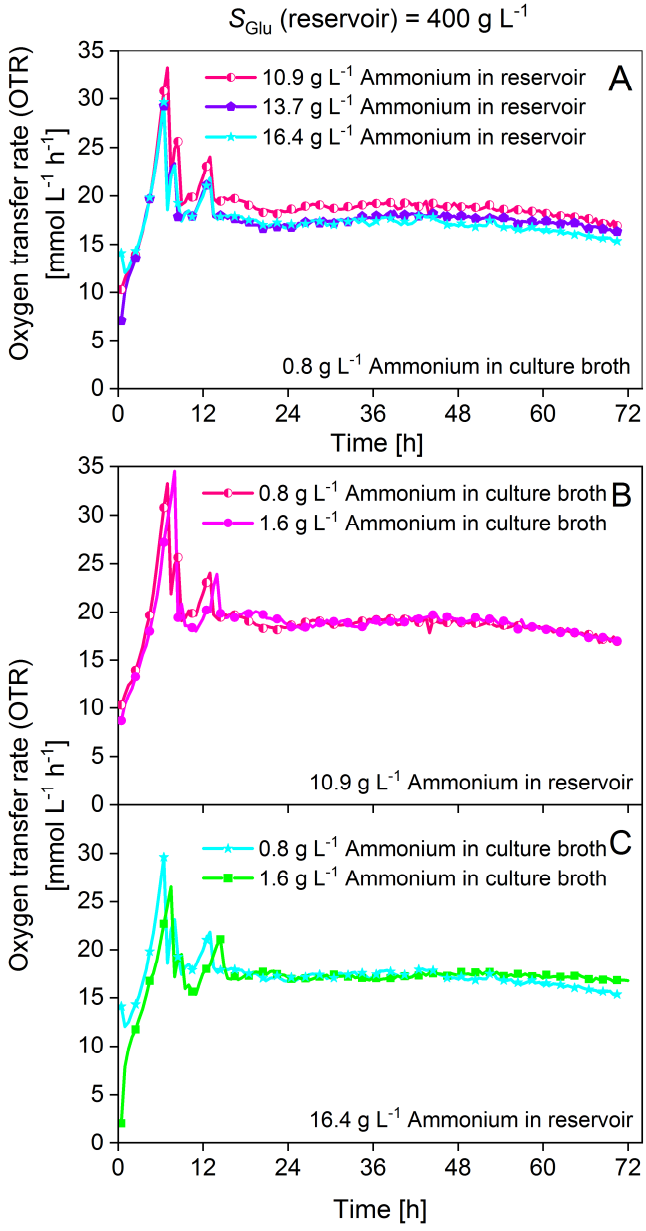

Appendix 5: Carbon (C)-limited fed-batch cultivation of *Bacillus licheniformis* with 400 g L^{-1} glucose and varying ammonium concentrations within the feed reservoir and culture broth according to Figure 2.2B. (A-C) Oxygen transfer rates (OTRs) with varying ammonium concentrations within the feed reservoir and culture broth. (A) Ammonium concentration was kept constant at 0.8 g L^{-1} within the culture broth and varied between 10.9, 13.7 and 16.4 g L^{-1} within the feed reservoir. (B) Ammonium concentration was kept constant at 10.9 g L^{-1} within the reservoir and varied between 0.8 and 1.6 g L^{-1} within the culture broth. (C) Ammonium concentration was kept constant at 16.4 g L^{-1} within the feed reservoir and varied between 0.8 and 1.6 g L^{-1} within the culture broth. Initial values (culture broth): OD_{600} = 2.5, pH = 7.9, 0 g L^{-1} glucose, 0.4 M MOPS buffer, V3 medium. Initial values (reservoir): V_{Feed} = 3 mL, active membrane diameter = 4.8 mm. Membrane: type = RCT-NatureFlex-NP, material = regenerated cellulose, thickness = 42 µm, cut-off = 10–20 kDa. Cultivation parameters: T = 30 °C, 250 mL membrane-based fed-batch shake flask, V_{Broth} = 10 mL, n = 350 rpm, d_0 = 50 mm.

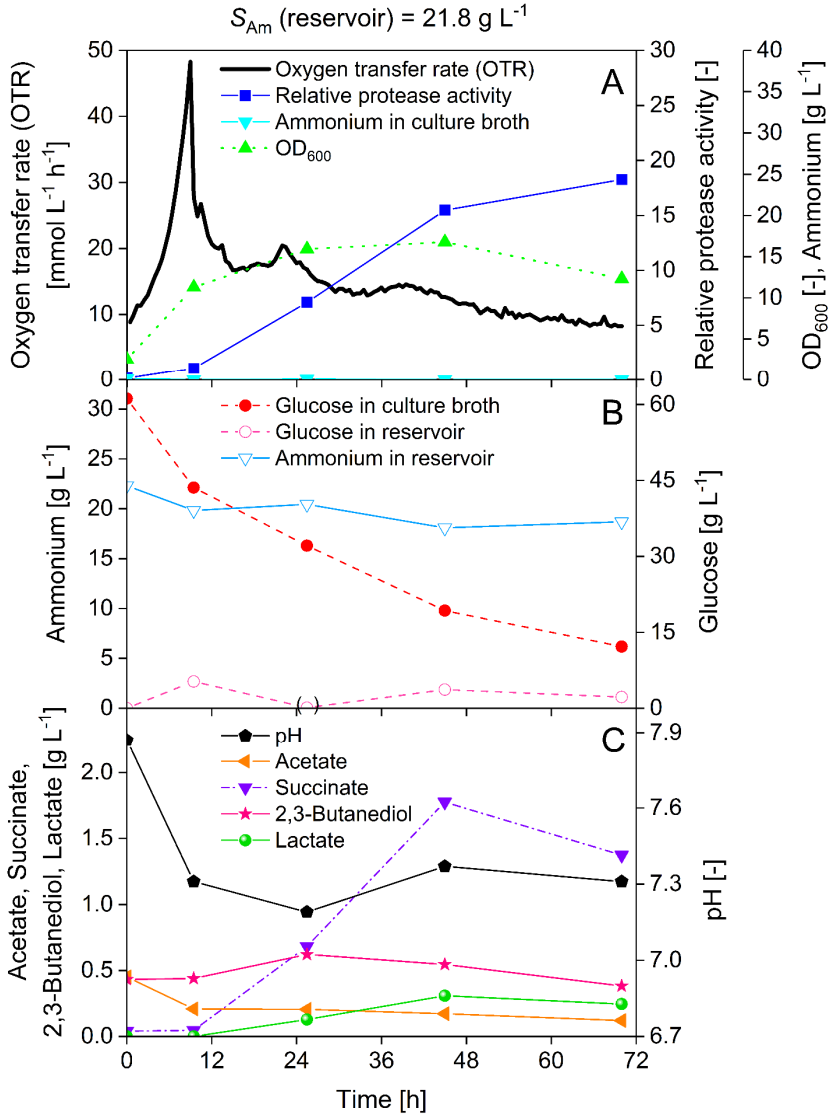

Appendix 6: Nitrogen (N)-limited fed-batch cultivation of *Bacillus licheniformis* with ammonium within the feed reservoir according to Figure 2.2C. (A-C) Ammonium concentration of 21.8 g L^{-1} within the feed reservoir. (A) Oxygen transfer rate (OTR), relative protease activity, ammonium concentration and optical density (OD$_{600}$). Protease activities were set in relation to the measured protease activity directly after glucose depletion at 11.5 h within the batch experiment shown in Figure 2.9. (B) Glucose concentration within the feed reservoir and culture broth and ammonium concentration within the feed reservoir. (C) pH value, acetate, succinate, 2,3-butanediol and lactate concentrations. Initial values (culture broth): OD$_{600}$ = 2.5, pH = 7.9, 60 g L^{-1} glucose, 0 g L^{-1} ammonium, 0.4 M MOPS buffer, V3 medium. Initial values (reservoir): V_{Feed} = 3 mL, active membrane diameter = 4.8 mm. Membrane: type = RCT-NatureFlex-NP, thickness = 42 µm, cut-off = 10–20 kDa. Cultivation parameters: T = 30 °C, 250 mL membrane-based fed-batch shake flask, V_{Broth} = 10 mL, n = 350 rpm, d_0 = 50 mm.

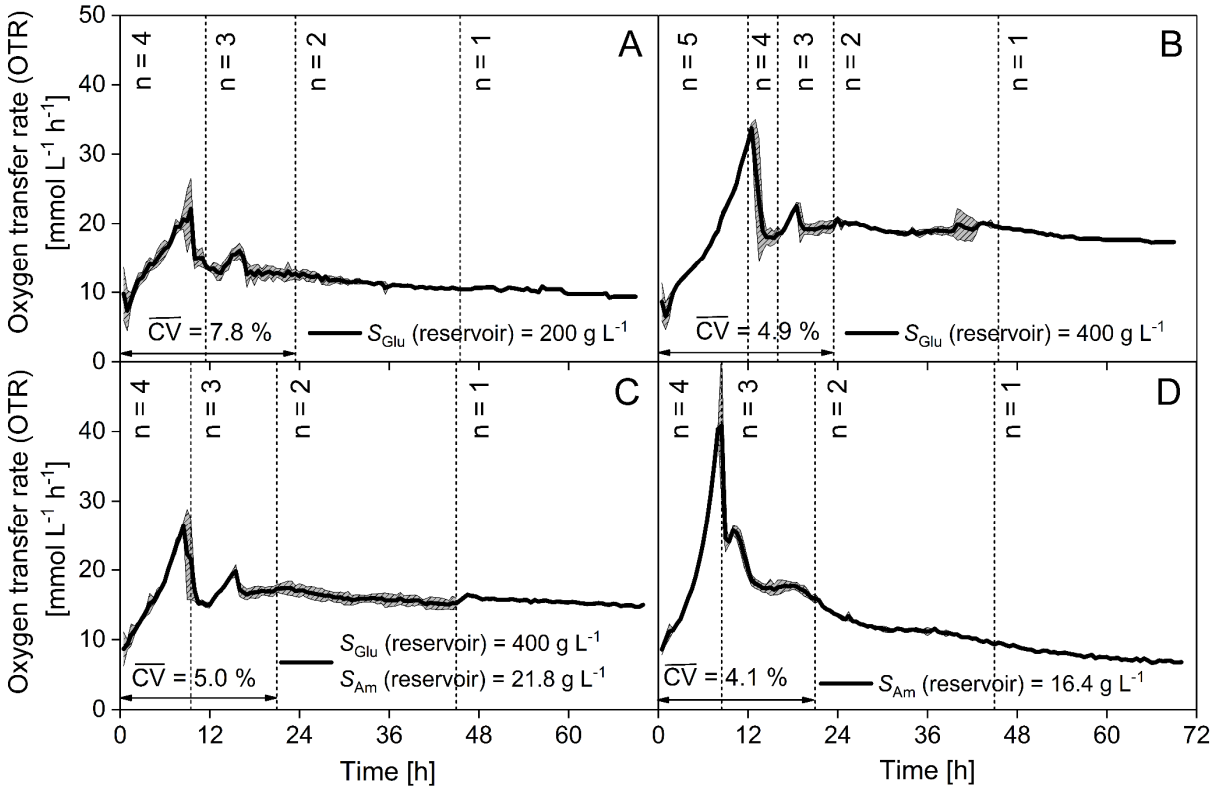

Appendix 7: Reproducibility of fed-batch experiments with different experimental set-ups using the 250 mL membrane-based fed-batch shake flasks. (A-D) Mean oxygen transfer rate (OTR) (line) with standard deviation (hatched area) over time. Dashed lines represent the time point when a membrane-based fed-batch shake flask was harvested for sampling. Harvested shake flasks were not put back on the shaker. Thus, each sampling point represents a replicate. With increasing process time, the mean oxygen transfer rate (OTR) and the standard deviation were calculated based on a decreasing number of membrane-based fed-batch shake flasks (n = number of flasks). The mean coefficient of variation ($\overline{CV}$) was calculated with n ≥ 3 parallel flasks and is shown for each experimental set-up. The $\overline{CV}$ of all experimental set-ups (n ≥ 3 parallel flasks) is 5.5 %. (A) Mean oxygen transfer rate with standard deviation of single component glucose feed resulting in carbon-limited fed-batch process according to Figure 2.2A and Figure 2.10A-C. (B) Mean oxygen transfer rate with standard deviation of single component glucose feed resulting in carbon- and nitrogen-limited fed-batch process according to Figure 2.2A and Figure 2.10D-F. (C) Mean oxygen transfer rate with standard deviation of two component glucose and ammonium feed resulting in carbon-limited fed-batch process according to Figure 2.2B and Figure 2.11. (D) Mean oxygen transfer rate with standard deviation of single component ammonium feed resulting in nitrogen-limited fed-batch process according to Figure 2.2C and Figure 2.13. Initial value (reservoir): V_{Feed} = 3 mL, active membrane diameter = 4.8 mm. Membrane: type = RCT-NatureFlex-NP, material = regenerated cellulose, thickness = 42 µm, cut-off = 10–20 kDa. Cultivation parameters: T = 30 °C, 250 mL membrane-based fed-batch shake flask, V_{Broth} = 10 mL, n = 350 rpm, d_0 = 50 mm.

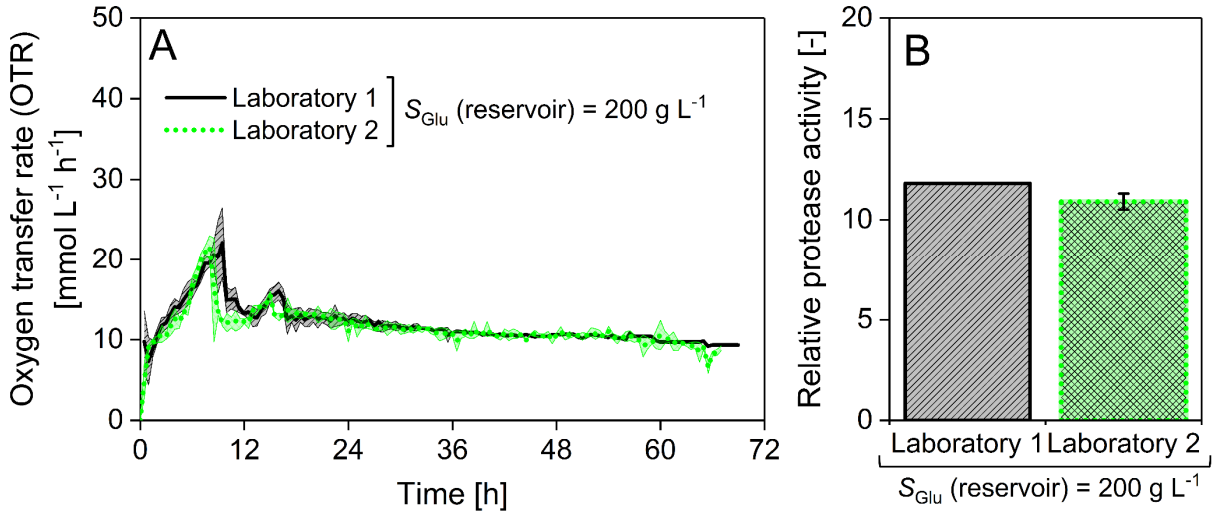

Appendix 8: Reproducibility of a single fed-batch experiment in two different laboratories using the 250 mL membrane-based fed-batch shake flasks. (A) Mean oxygen transfer rates (OTR) with standard deviation (hatched area) over time. The performed experiment is characterized by a single component glucose feed, resulting in a carbon-limited fed-batch process according to Figure 2.2A and Figure 2.10A-C. The experiment of Laboratory 1 is the same as shown in Figure 2.10A and Appendix 7A. The mean coefficient of variation ($\overline{CV}$) was calculated with n ≥ 3 parallel flasks and was 7.8 %. This experiment was repeated in another laboratory (Laboratory 2) with three membrane-based fed-batch shake flasks (n = 3), resulting in a $\overline{CV}$ of 5 %. (B) Relative protease activities at the end of cultivation. The activity measured in Laboratory 1 (n =1) is in the same range as the activity of the experiment performed and evaluated in Laboratory 2 (n = 3). Initial values (culture broth): OD_{600} = 2.5, pH ~ 7.9, 0 g L^{-1} glucose, 2.9 g L^{-1} ammonium, 0.4 M MOPS buffer, V3 medium. Initial value (reservoir): V_{Feed} = 3 mL, active membrane diameter = 4.8 mm. Membrane: type = RCT-NatureFlex-NP, material = regenerated cellulose, thickness = 42 µm, cut-off = 10–20 kDa. Cultivation parameters: T = 30 °C, 250 mL membrane-based fed-batch shake flask, V_{Broth} = 10 mL, n = 350 rpm, d_0 = 50 mm.

Appendix 9: Glucose- and oxygen-based protease yields of fed-batch cultivations in comparison to batch.

	Final relative protease activity	Total consumed glucose	Relative protease activity per consumed glucose ($Y_{P/S_{Glu}}$)	Relative protease activity per consumed glucose related to batch	Total consumed oxygen	Relative protease activity per consumed oxygen (Y_{P/O_2})	Relative protease activity per consumed oxygen related to batch	Reference
	[-]	[g]	[g^{-1}]	[-]	[mol L^{-1}]	[L mol^{-1}]	[-]	
Batch	3.6	0.20	18.1	1.0	0.406	8.9	1.0	Figure 2.9
Fed-Batch C-limited (S_{Glu} (reservoir) = 200 g L^{-1})	11.8	0.41	29.4	1.6	0.791	14.9	1.7	Figure 2.2A, Figure 2.10A-C
Fed-Batch C/N-limited (S_{Glu} (reservoir) = 400 g L^{-1})	17.4	0.52	33.4	1.8	1.297	13.4	1.5	Figure 2.2A, Figure 2.10D-F
Fed-Batch C-limited (S_{Glu} (reservoir) = 400 g L^{-1} S_{Am} (reservoir) = 21.8 g L^{-1})	15.7	0.58	26.9	1.5 [a]	1.153	13.6	1.5 [a]	Figure 2.2B, Figure 2.11
Fed-Batch N-limited (S_{Am} (reservoir) = 16.4 g L^{-1})	15.9	0.43	37.2	2.1 [b]	0.882	18.0	2.0 [b]	Figure 2.2C, Figure 2.13

[a] For statistical relevance eight C-limited fed-batch cultivations with 400 g L^{-1} glucose within the reservoir and varying ammonium concentrations within reservoir and culture broth (according to Figure 2.2B) have been investigated (n = 8). The relative protease activity per consumed glucose related to batch was 1.5 ± 0.1 and the relative protease activity per consumed oxygen related to batch was 1.5 ± 0.1 too.

[b] The N-limited fed batch process was additionally performed with 21.8 g L^{-1} ammonium within the feed reservoir (Appendix 6). The relative protease activity per consumed glucose related to batch was 2.0 and the relative protease activity per consumed oxygen related to batch was 2.0 too.

Appendix 10: Experimental set-up of carbon (C)-limited fed-batch cultivation using 250 and 500 mL membrane-based fed-batch shake flasks.

	Active diffusion area	**Shake flask filling volume (V_{Broth})**	**Feed reservoir filling volume (V_{Feed})**	**Feed reservoir glucose amount (concentration)**
	[mm^2]	**[mL]**	**[mL]**	**[g] ([g L^{-1}])**
250 mL membrane-based-fed-batch shake flask	18.1	10	3	0.6 (200)
	↓ 3x	**↓ 3x**	**↓ 3x**	**↓ 3x**
500 mL membrane-based fed-batch shake flask	54.1	30	9	1.8 (200)

Appendices for Chapter 3

Appendix 11: Model parameters for the fed-batch model.

Parameter	Value	Unit	Reference
$\mu_{\max}$	0.16[a]	[h^{-1}]	Figure 2.9
$K_{S_{Glu}}$	0.001	[g L^{-1}]	(Wilming, 2012)
A	0.0151	-	-
B	0.0012	-	-
C	-0.0148	-	-
D	-0.0163	-	-
$Y_{X/S_{Glu}}$	0.44[a]	[g g^{-1}]	Figure 2.9
$Y_{X/O2}$	34[a]	[g mol^{-1}]	Figure 2.9
$k_L a$	245-477 [b]	[h^{-1}]	(Ladner, Held, et al., 2016)
L_{O2}	0.001[c]	[mol $L^{-1} bar^{-1}$]	(Emmerich, Battino, & Wilcock, 1976; Rischbieter, Schumpe, & Wunder, 1996; Weisenberger & Schumpe, 1996)
p_{amb}	1	[bar]	-
y_{O2}	0.2095	%	-

[a] determination based on batch experiments in shake flasks with similar cultivation conditions.

[b] range given for filling volumes from 1.0 to 0.5 mL. $k_L a$ for 0.5 mL was extrapolated based on the data from Ladner et al. (2016) with the rational function $(V_{Broth}\, a + b)/(V_{Broth} + c)$ were a, b and c are fitting parameter.

[c] empirical correlations concerning the influence of boric acid and molybdenum on the oxygen solubility are not described in literature and therefore these medium components were excluded from the calculation.

Appendix 12: Glucose- and oxygen-based protease yields of shake flask- and microtiter plate-based fed-batch cultivations in comparison to batch

	Relative protease activity [-]	Consumed glucose [g L^{-1}]	Relative protease activity per consumed glucose ($Y_{P/S}$) [e] [L g^{-1}]	Relative protease activity per consumed glucose related to batch [-]	Consumed oxygen [mol L^{-1}]	Relative protease activity per consumed oxygen (Y_{P/O_2}) [L mol^{-1}]	Relative protease activity per consumed oxygen related to batch [-]	References
Batch SF (OD_{600} = 2.5, V_{Broth} = 10 mL)	3.6	20	0.18	1.0	0.406	8.9	1.0	Figure 2.9
Fed-batch SF (OD_{600} = 2.5, V_{Broth} = 10 mL, S_{Glu} (reservoir) = 200 g L^{-1})	11.8	41	0.29	1.6	0.791	14.9	1.7	Figure 2.10 (A-C)
Fed-batch SF (OD_{600} = 2.5, V_{Broth} = 10 mL, S_{Glu} (reservoir) = 400 g L^{-1}, S_{Am} (reservoir) = 21.8 g L^{-1})	15.7	58	0.27	1.5	1.153	13.6	1.5	Figure 2.11
Fed-batch MTP (OD_{600} = 0.1, V_{Broth} = 0.5 mL)	5.4	26 ± 1 [a]	0.21	1.2	0.544	10.0	1.1	Figure 3.4
Fed-batch MTP (OD_{600} = 0.5, V_{Broth} = 0.5 mL)	6.7 ± 0.2	26 ± 1 [a]	0.26 ± 0.01	1.4 ± 0.0	0.516	13.0 ± 0.3	1.5 ± 0.0	Figure 3.4
Fed-batch MTP (OD_{600} = 1.0, V_{Broth} = 0.5 mL)	7.6 ± 0.4	26 ± 1 [a]	0.30 ± 0.02	1.6 ± 0.1	0.551	13.8 ± 0.7	1.5 ± 0.1	Figure 3.4
Fed-batch MTP (OD_{600} = 1.5, V_{Broth} = 0.5 mL)	7.1 ± 0.2	26 ± 1 [a]	0.28 ± 0.01	1.5 ± 0.0	0.590	12.0 ± 0.4	1.3 ± 0.0	Figure 3.4
Fed-batch MTP (OD_{600} = 2.5, V_{Broth} = 0.5 mL)	6.9 ± 0.1	26 ± 1 [a]	0.27 ± 0.01	1.5 ± 0.0	0.589	11.8 ± 0.3	1.3 ± 0.0	Figure 3.4
Fed-batch MTP (OD_{600} = 0.5, V_{Broth} = 0.5 mL)	7.3 ± 0.9	26 ± 1 [a]	0.29 ± 0.04	1.6 ± 0.2	0.588	12.4 ± 1.5	1.4 ± 0.2	Figure 3.5
Fed-batch MTP (OD_{600} = 0.5, V_{Broth} = 0.8 mL)	5.3 ± 0.5	16 ± 1 [b]	0.33 ± 0.03	1.8 ± 0.2	0.394	13.5 ± 1.2	1.5 ± 0.1	Figure 3.5
Fed-batch MTP (OD_{600} = 0.5, V_{Broth} = 1.0 mL)	3.8 ± 0.2	13 ± 1 [b]	0.29 ± 0.01	1.6 ± 0.1	0.267	14.1 ± 0.7	1.6 ± 0.1	Figure 3.5
Fed-batch MTP (OD_{600} = 0.5, V_{Broth} = 0.5 mL, 0.63 osmol kg^{-1})	7.3 ± 0.1	26 ± 1 [a]	0.29 ± 0.00	1.6 ± 0.0	0.496	14.8 ± 0.2	1.7 ± 0.0	Figure 3.6
Fed-batch MTP (OD_{600} = 0.5, V_{Broth} = 0.5 mL, 1.09 osmol kg^{-1})	4.3 ± 0.2	17 ± 0 [c]	0.25 ± 0.01	1.4 ± 0.1	0.355	12.2 ± 0.6	1.4 ± 0.1	Figure 3.6
Fed-batch MTP (OD_{600} = 0.5, V_{Broth} = 0.5 mL, 1.72 osmol kg^{-1})	1.1 ± 0.4	8 ± 0 [c]	0.14 ± 0.04	0.8 ± 0.2	0.212	5.4 ± 1.7	0.6 ± 0.2	Figure 3.6
Fed-batch MTP (OD_{600} = 0.5, V_{Broth} = 0.5 mL)	6.7 ± 0.2	26 ± 1 [a]	0.26 ± 0.01	1.4 ± 0.0	0.516	13.0 ± 0.3	1.5 ± 0.0	Figure 3.7
Fed-batch SF (OD_{600} = 1.0, V_{Broth} = 16 mL, S_{Glu} (reservoir) = 200 g L^{-1})	6.6	25 [d]	0.26	1.4	0.511	12.8	1.4	Figure 3.7
Fed-batch MTP (OD_{600} = 1.5, V_{Broth} = 0.5 mL, 0 g L^{-1} glucose)	7.1 ± 0.2	26 ± 1 [a]	0.28 ± 0.01	1.5 ± 0.0	0.589	12.0 ± 0.4	1.3 ± 0.0	Appendix 14
Fed-batch MTP (OD_{600} = 1.5, V_{Broth} = 0.5 mL, + 2.5 g L^{-1} S_{Glu})	7.8 ± 0.3	28 ± 1	0.28 ± 0.01	1.5 ± 0.1	0.677	11.5 ± 0.5	1.3 ± 0.1	Appendix 14
Fed-batch MTP (OD_{600} = 1.5, V_{Broth} = 0.5 mL, + 5.0 g L^{-1} S_{Glu})	8.4 ± 0.2	31 ± 1	0.28 ± 0.01	1.5 ± 0.0	0.704	12.0 ± 0.3	1.3 ± 0.0	Appendix 14

SF = shake flask, MTP = microtiter plate, Fed-batch = glucose-limited fed-batch conditions

[a] mean amount of glucose consumed after 70 ± 1.5 h, determined under cultivation conditions without biomass in 9 wells [n = 9] of 4 individual plates [m = 4].
[b] mean amount of glucose consumed after 70 ± 1.5 h, calculated with the corresponding dilution factor (V_{Broth}) on basis of [1].
[c] mean amount of glucose consumed after 70.5 h, determined under cultivation conditions without biomass in 3 wells [n = 3].
[d] amount of glucose consumed after 70 h of cultivation, calculated with the corresponding dilution factor (V_{Broth}) on basis of Fed-batch SF (OD_{600} = 2.5, V_{Broth} = 10 mL, S_{Glu} (reservoir) = 200 g L^{-1}).
[e] since the error of the relative protease activity already reflects differences in consumed glucose, calculation is done without taking the error of the consumed glucose into account.

Appendix 13: Glucose- based biomass yields and protease productivities of shake flask- and microtiter plate-based fed-batch cultivations in comparison to batch

	Optical density (OD_{600}) [-]	Consumed glucose [g L^{-1}]	Optical density per consumed glucose ($Y_{X/S}$) [e] [L g^{-1}]	Optical density per consumed glucose related to batch [-]	Relative protease activity [-]	Cultivation time [h]	Relative protease activity per cultivation time [h^{-1}]	Relative protease activity per cultivation time related to batch [-]	References
Batch SF (OD_{600} = 2.5, V_{Broth} = 10 mL)	11.8	20	0.59	1.0	3.6	27.5	0.13	1.0	Figure 2.9
Fed-batch SF (OD_{600} = 2.5, V_{Broth} = 10 mL, S_{Glu} (reservoir) = 200 g L^{-1})	19.4	41	0.48	0.8	11.8	69.0	0.17	1.3	Figure 2.10 (A-C)
Fed-batch SF (OD_{600} = 2.5, V_{Broth} = 10 mL, S_{Glu} (reservoir) = 400 g L^{-1}, S_{Am} (reservoir) = 21.8 g L^{-1})	28.0	58	0.48	0.8	15.7	70.0	0.22	1.7	Figure 2.11
Fed-batch MTP (OD_{600} = 0.1, V_{Broth} = 0.5 mL)	9.1	26 ± 1 [a]	0.36	0.6	5.4	70.0	0.08	0.6	Figure 3.4
Fed-batch MTP (OD_{600} = 0.5, V_{Broth} = 0.5 mL)	9.8 ± 0.0	26 ± 1 [a]	0.38 ± 0.00	0.7 ± 0.0	6.7 ± 0.2	70.0	0.10 ± 0.00	0.7 ± 0.0	Figure 3.4
Fed-batch MTP (OD_{600} = 1.0, V_{Broth} = 0.5 mL)	8.8 ± 0.1	26 ± 1 [a]	0.34 ± 0.01	0.6 ± 0.0	7.6 ± 0.4	70.0	0.11 ± 0.01	0.8 ± 0.0	Figure 3.4
Fed-batch MTP (OD_{600} = 1.5, V_{Broth} = 0.5 mL)	9.4 ± 0.5	26 ± 1 [a]	0.37 ± 0.02	0.6 ± 0.0	7.1 ± 0.2	70.0	0.10 ± 0.00	0.8 ± 0.0	Figure 3.4
Fed-batch MTP (OD_{600} = 2.5, V_{Broth} = 0.5 mL)	9.8 ± 0.2	26 ± 1 [a]	0.38 ± 0.01	0.6 ± 0.0	6.9 ± 0.1	70.0	0.10 ± 0.00	0.7 ± 0.0	Figure 3.4
Fed-batch MTP (OD_{600} = 0.5, V_{Broth} = 0.5 mL)	8.4 ± 0.8	26 ± 1 [a]	0.33 ± 0.03	0.6 ± 0.1	7.3 ± 0.9	71.3	0.10 ± 0.01	0.8 ± 0.1	Figure 3.5
Fed-batch MTP (OD_{600} = 0.5, V_{Broth} = 0.8 mL)	4.8 ± 0.3	16 ± 1 [b]	0.30 ± 0.02	0.5 ± 0.0	5.3 ± 0.5	71.3	0.07 ± 0.01	0.6 ± 0.0	Figure 3.5
Fed-batch MTP (OD_{600} = 0.5, V_{Broth} = 1.0 mL)	3.8 ± 0.0	13 ± 1 [b]	0.29 ± 0.00	0.5 ± 0.0	3.8 ± 0.2	71.3	0.05 ± 0.00	0.4 ± 0.0	Figure 3.5
Fed-batch MTP (OD_{600} = 0.5, V_{Broth} = 0.5 mL, 0.63 osmol kg^{-1})	10.7 ± 0.4	26 ± 1 [a]	0.42 ± 0.01	0.7 ± 0.0	7.3 ± 0.1	70.5	0.10 ± 0.00	0.8 ± 0.0	Figure 3.6
Fed-batch MTP (OD_{600} = 0.5, V_{Broth} = 0.5 mL, 1.09 osmol kg^{-1})	7.0 ± 0.4	17 ± 0 [c]	0.40 ± 0.02	0.7 ± 0.0	4.3 ± 0.2	70.5	0.06 ± 0.00	0.5 ± 0.0	Figure 3.6
Fed-batch MTP (OD_{600} = 0.5, V_{Broth} = 0.5 mL, 1.72 osmol kg^{-1})	4.8 ± 0.1	8 ± 0 [c]	0.58 ± 0.02	1.0 ± 0.0	1.1 ± 0.4	70.5	0.02 ± 0.01	0.1 ± 0.0	Figure 3.6
Fed-batch MTP (OD_{600} = 0.5, V_{Broth} = 0.5 mL)	9.8 ± 0.0	26 ± 1 [a]	0.38 ± 0.00	0.7 ± 0.0	6.7 ± 0.2	70.0	0.10 ± 0.00	0.7 ± 0.0	Figure 3.7
Fed-batch SF (OD_{600} = 1.0, V_{Broth} = 16 mL, S_{Glu} (reservoir) = 200 g L^{-1})	10.9	25 [d]	0.43	0.7	6.6	70.0	0.09	0.7	Figure 3.7
Fed-batch MTP (OD_{600} = 1.5, V_{Broth} = 0.5 mL, + 0 g L^{-1} S_{Glu})	9.5 ± 0.3	26 ± 1 [a]	0.37 ± 0.01	0.6 ± 0.0	7.1 ± 0.2	70.0	0.10 ± 0.00	0.8 ± 0.0	Appendix 14
Fed-batch MTP (OD_{600} = 1.5, V_{Broth} = 0.5 mL, + 2.5 g L^{-1} S_{Glu})	10.7 ± 0.1	28 ± 1	0.38 ± 0.00	0.6 ± 0.0	7.8 ± 0.3	70.0	0.11 ± 0.00	0.8 ± 0.0	Appendix 14
Fed-batch MTP (OD_{600} = 1.5, V_{Broth} = 0.5 mL, + 5.0 g L^{-1} S_{Glu})	11.2 ± 0.1	31 ± 1	0.37 ± 0.00	0.6 ± 0.0	8.4 ± 0.2	70.0	0.12 ± 0.00	0.9 ± 0.0	Appendix 14

SF = shake flask, MTP = microtiter plate, Fed-batch = glucose-limited fed-batch conditions

[a] mean amount of glucose consumed after 70 ± 1.5 h, determined under cultivation conditions without biomass in 9 wells [n = 9] of 4 individual plates [m = 4].

[b] mean amount of glucose consumed after 70 ± 1.5 h, calculated with the corresponding dilution factor (V_{Broth}) on basis of [1].

[c] mean amount of glucose consumed after 70.5 h, determined under cultivation conditions without biomass in 3 wells [n = 3].

[d] amount of glucose consumed after 70h of cultivation, calculated with the corresponding dilution factor (V_{Broth}) on basis of Fed-batch SF (OD_{600} = 2.5, V_{Broth} = 10 mL, S_{Glu} (reservoir) = 200 g L^{-1}).

[e] since the error of the optical density already reflects differences in consumed glucose, calculation is done without taking the error of the consumed glucose into account.

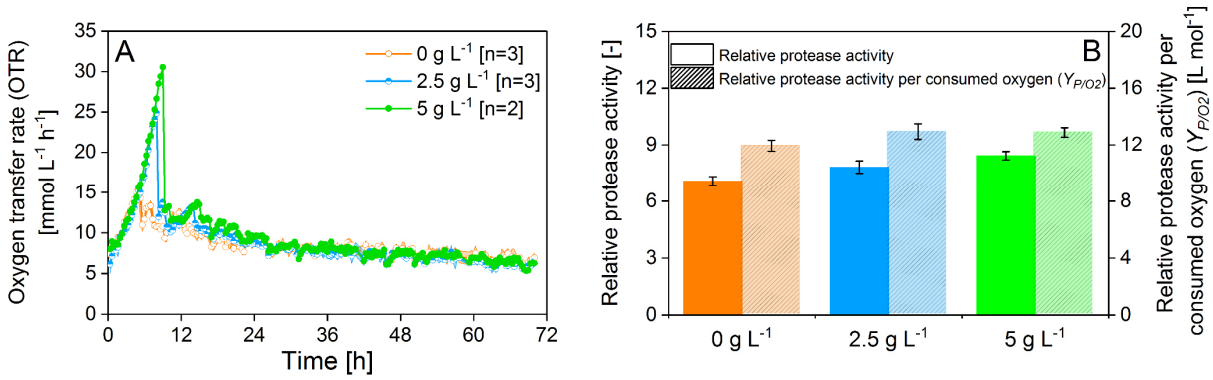

Appendix 14: Fed-batch cultivations of *Bacillus licheniformis* with initially provided glucose using the polymer-based controlled-release fed-batch microtiter plate. (A) Mean oxygen transfer rate (OTR) over time. The experiment with 0 g L^{-1} initial glucose is similar to the experiment with an initial OD_{600} of 1.5 depicted in Figure 3.4. Each experiment was conducted in triplicates. However, wells that could not be sealed tightly by the measurement device or had a noisy p_{O_2} signal were excluded. Shadows symbolize the standard deviation (for n > 2). (B) Mean relative protease activity (filled bars) and relative protease activity per consumed oxygen (Y_{P/O_2}) (dashed bars) at the end of the cultivation. Error bars symbolize the standard deviation [n = 3]. Protease activities were set in relation to the measured protease activity directly after glucose depletion at 11.5 h within the batch experiment, shown in Figure 2.9. Cultivation conditions: polymer-based controlled-release fed-batch microtiter plate (48-well round- and deep-well), OD_{600} = 1.5, V_{Broth} = 0.5 mL, n = 1000 rpm, d_0 = 3 mm, T = 30 °C.

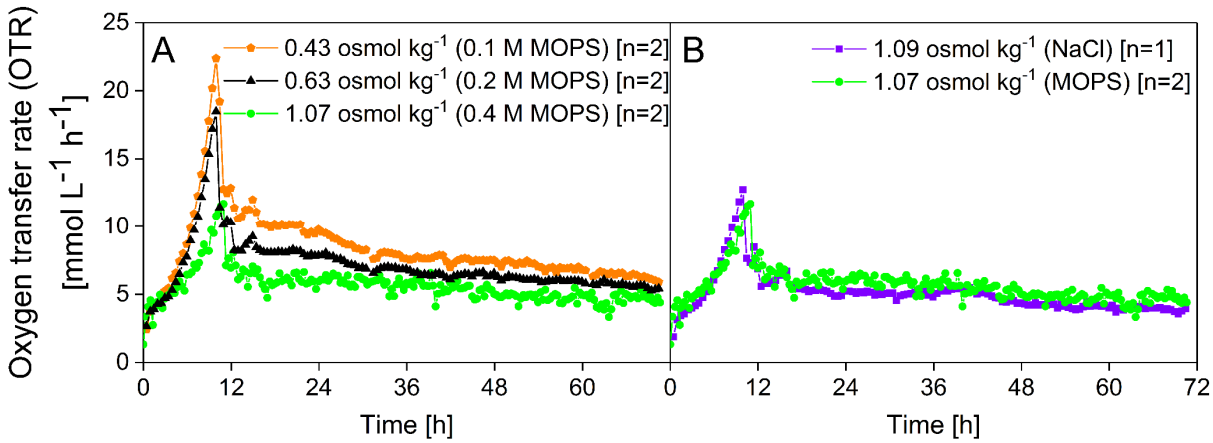

Appendix 15: Influence of MOPS buffer concentration on fed-batch cultivations of *Bacillus licheniformis* in the polymer-based controlled-release fed-batch microtiter plate. (A, B) The respective osmolalities are depicted in the figure legend. (A) Mean oxygen transfer rate (OTR) over time. Each experiment was conducted in triplicates, however wells that could not be sealed tightly by the measurement device or had a noisy p_{O_2} signal were excluded. (B) Mean oxygen transfer rate of cultivations with a similar osmolality of 1.09 and 1.07 osmol kg^{-1} caused by the addition of sodium chloride (NaCl) and MOPS buffer. Cultivation conditions: polymer-based controlled-release fed-batch microtiter plate (48-well round- and deep-well), OD_{600} = 0.5, V_{Broth} = 0.5 mL, n = 1000 rpm, d_0 = 3 mm, T = 30 °C.

Appendices for Chapter 4

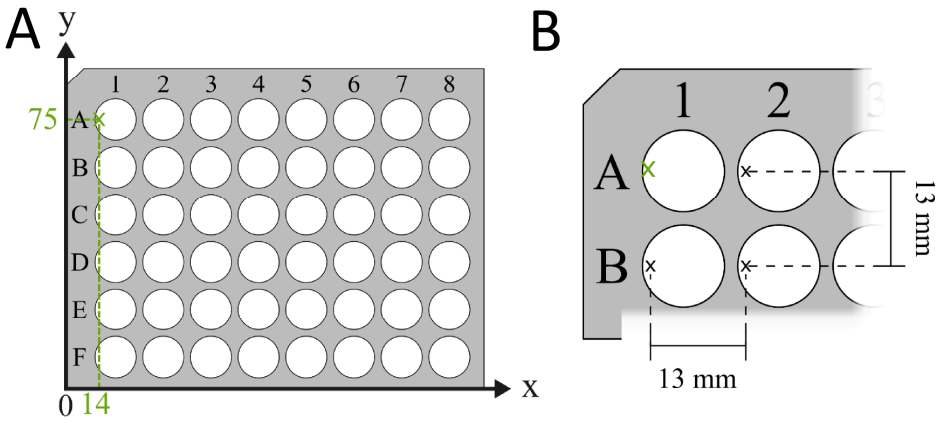

Appendix 16: Coordinate sytem of the x-y-positioning device within the BioLector software. (A) The software uses the 48-well microtiter plate (MTP-R48- series) as basis for the internal coordinate system for the x-y-positioning device. The left corner of the plate represents the origin of the coordinate system. The default measurement position for well A1 is indicated with x_1 = 14 mm and y_1= 75 mm. (B) Starting from the default measurement position, the x-y-positioning device moves 13 mm in x- and y-direction in order to measure at the same relative positon within each well of the microtiter plate.

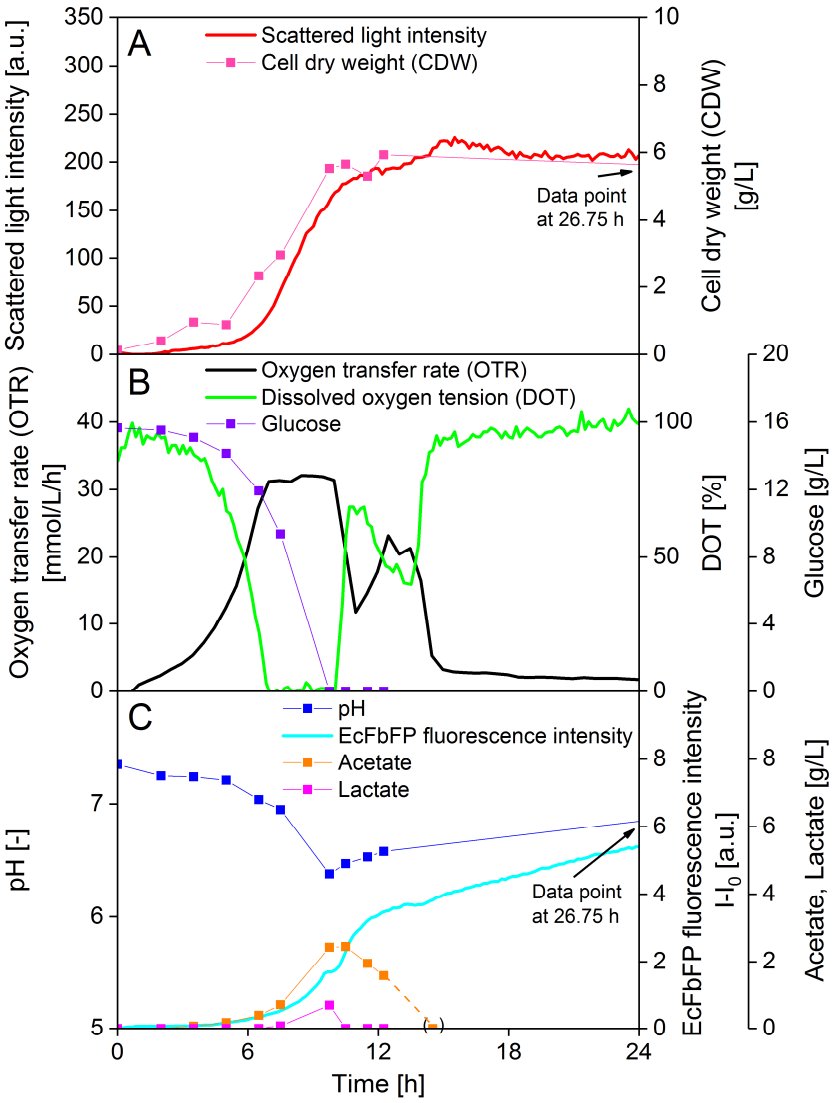

Appendix 17: Online and offline data of parallel cultivations of *E. coli* BL21 (DE3) with microtiter plates and shake flasks, adapted from Wewetzer et al. (2015). (A-C) Online data are depicted as lines and offline data as points with lines. The online oxygen transfer rate (OTR) was measured in shake flasks with the RAMOS device. The online scattered light intensity, dissolved oxygen tension (DOT) and EcFbFP fluorescence intensity were measured in microtiter plates with the BioLector device. Offline samples were taken from shake flasks. (A) Scattered light intensity, cell dry weight (CDW), (B) oxygen transfer rate (OTR), dissolved oxygen tension (DOT), glucose, (C) pH, EcFbFP fluorescence intensity, acetate and lactate over time. Culture medium and strain: Wilms-MOPS medium, 15 g/L glucose, 0.2 M MOPS, *E. coli* BL21 (DE3) pRhotHi- 2-EcFbFP-His6. Cultivation conditions with microtiter plates and shake flasks were adjusted to obtain a similar maximum oxygen transfer capacity (OTR_{max}) (Wewetzer et al., 2015).Cultivation conditions for shake flasks (RAMOS): 250 mL RAMOS shake flask, n = 350 rpm, d_0 = 50 mm, V_{Broth} = 25 mL, T = 37 °C. Cultivation conditions for microtiter plates (BioLector): 48-well Flowerplate, n = 800 rpm, d_0 = 3 mm, V_{Broth} = 1 mL, T = 37 °C.

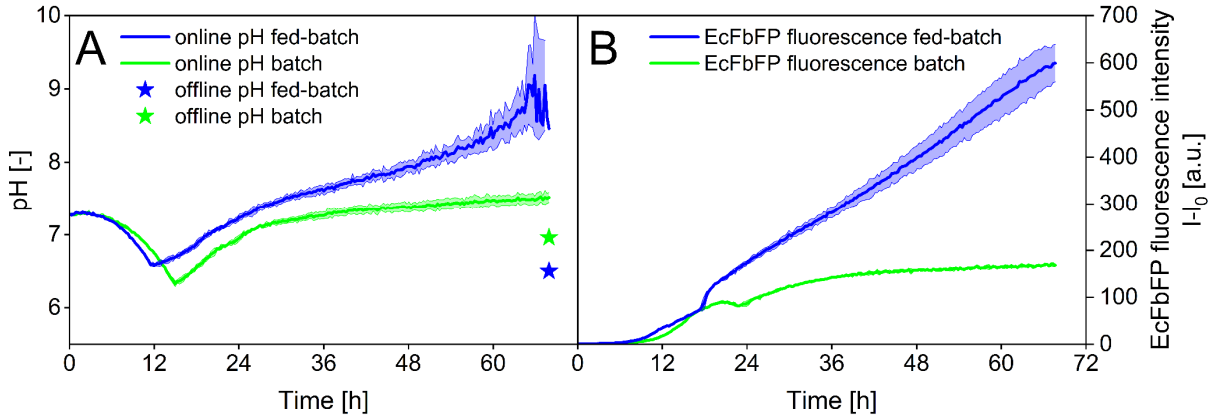

Appendix 18: Comparison of online and offline pH measurement in batch and fed-batch cultivations. (A) Online and offline pH and (B) EcFbFP fluorescence intensity of batch and fed-batch cultivations of *E. coli* BL21 (DE3). Polymer rings had an outer diameter of 12 mm and inner diameter of 8 mm. For batch cultivations, the slow release polymer matrix that releases negligible amounts of glucose was used. For fed-batch cultivations, glucose release was realized by using a standard release polymer matrix. Due to measurement interferences between pH optodes and EcFbFP, which was already reported by Kunze et al. (2014), the online pH value differs from the offline value. Correction of the online measured pH value on basis of the online measured EcFbFP fluorescence intensity is possible with the following linear approximation: ΔpH = 0.0035 * EcFbFP fluorescence intensity. On basis of ΔpH, the correct offline pH can be calculated with: $pH_{offline} = pH_{online} - \Delta pH$. Cultivations were done in triplicates [n = 3], shadows symbolize the standard deviation. Culture medium: Wilms-MOPS medium, 20 g L^{-1} glucose for batch and 0 g L^{-1} glucose for fed-batch, 0.2 M MOPS, OD_{600} = 0.1. Cultivation conditions: 48-well round- deep-well microtiter plate with optodes, n = 1000 rpm, d_0 = 3 mm, V_{Broth} = 1.2 mL, T = 30 °C.

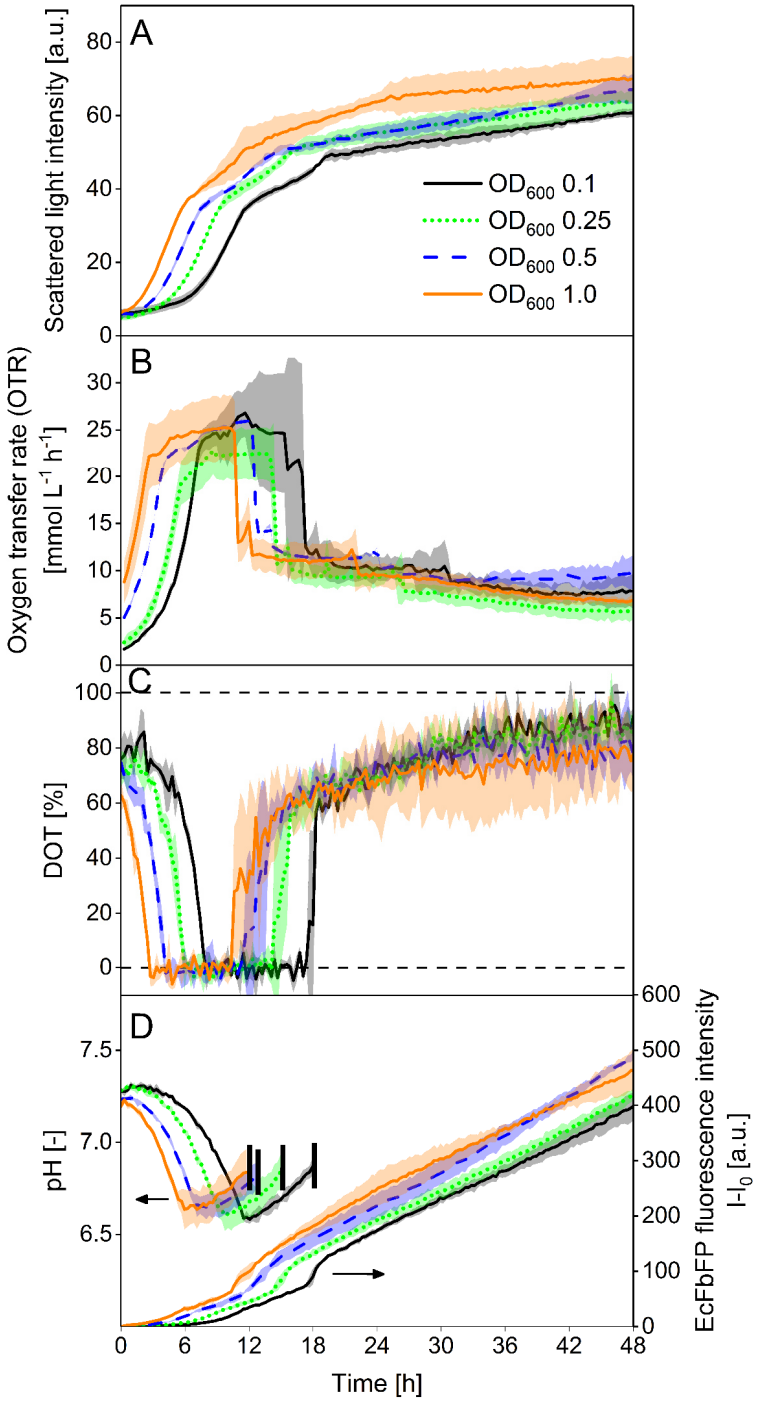

Appendix 19: Fed-batch cultivation of *E. coli* with varying initial biomass concentrations in wells with polymer ring. (A) Scattered light intensity, (B) oxygen transfer rate, (C) DOT, (D) pH and EcFbFP fluorescence intensity over time. The oxygen transfer rate was measured in a parallel experiment with a µRAMOS device [n = 2]. Due to measurement interferences between pH and EcFbFP, the pH course is only shown within the initial cultivation phase. Glucose release was realized by using the standard release polymer matrix. Polymer rings had an outer diameter of 12 mm and inner diameter of 8 mm. Cultivations were done in triplicates [n = 3], shadows symbolize the standard deviation. Adjusted measurement position for biomass and fluorescence (x = 4.5 mm, y = 0 mm). Culture medium: Wilms-MOPS medium, 0 g L^{-1} glucose, 0.2 M MOPS. Cultivation conditions: 48-well round- deep-well microtiter plate with optodes, n = 1000 rpm, d_0 = 3 mm, V_{Broth} = 1.2 mL, T = 30 °C.